Mathematical Studies Of Oxygen Transport To Tissue.

MATHEMATICAL STUDIES OF OXYGEN TRANSPORT TO TISSUE

by

Tseng-Chan Wang

A Dissertation

Presented to the Graduate Committee

of Lehigh University

in Candidacy for the Degree of

Doctor of Philosophy

in

Applied Mathematics

Lehigh University

1978

CERTIFICATE OF APPROVAL

This dissertation by Mr. Tseng-Chan Wang is approved and recommended for acceptance in partial fulfillment of the requirements for the degree of Doctor of Philosophy.

9/15/78
(Date)

Eric P. Salathé
Thesis Advisor:
Professor E. P. Salathé

Accepted 9/15/78
(Date)

Special committee directing the doctoral work of Mr. Tseng-Chan Wang

Eric P. Salathé
Professor E. P. Salathé
Chairman

Kenneth N. Sawyers
Professor K. N. Sawyers

Stephen W. Schaffer
Professor S. W. Schaffer

R. Venkataraman
Professor R. Venkataraman

ACKNOWLEDGEMENTS

I would like to thank my thesis advisor, Professor Eric P. Salathé, for his guidance, advice and encouragement with my studies and research. The helpful discussions and encouragement of Professor R. Venkataraman are gratefully acknowledged. I thank Professors K. N. Sawyers and S. W. Schaffer for acting as members of my Ph.D. committee. Sincere appreciation is also extended to Mrs. Fern Sotzing and Mrs. Lois Nakata for their assistance with the preparation of the manuscript.

The financial support of a Fellowship from Lehigh University is deeply appreciated. Partial support from Program Project Grant P01 HL-14721 is also acknowledged.

TABLE OF CONTENTS

LIST OF TABLES

LIST OF FIGURES

Figure 14. Normalized blood oxygen concentration as a function of distance, for example (1) in table I. (I) ———— without axial diffusion, (II) ———— with axial diffusion, (III) — — — — arterial boundary layer solution, (IV) — — — — venous boundary layer solution, (V) ····· composite solution.

Figure 15. Normalized tissue oxygen concentration midway between the capillary wall and the outer edge of the tissue as a function of axial position, for example (1) in table I. (I) ———— without axial diffusion, (II) ———— with axial diffusion, (III) — — — — arterial boundary layer solution, (IV) — — — — venous boundary layer solution, (V) ····· composite solution.

Figure 16. Normalized tissue oxygen concentration at the outer edge of the tissue as a function of axial position, for example (1) in table I. (I) ———— without axial diffusion, (II) ———— with axial diffusion, (III) — — — — arterial boundary layer solution, (IV) — — — —venous boundary layer solution, (V) ····· composite solution.

Figure 17. Normalized blood oxygen concentration as a function of distance, for example (2) of table I. (I) ———— without axial diffusion, (II) ———— with axial diffusion, (III) — — — —arterial boundary layer solution, (IV) — — — — venous boundary layer solution, (V) ····· composite solution.

Figure 18. Normalized tissue oxygen concentration midway between the capillary wall and the outer edge of the tissue as a function of axial position, for example (2) in table I. (I) ———— without axial diffusion, (II) ———— with axial diffusion, (III) — — — — arterial boundary layer solution, (IV) — — — — venous boundary layer solution, (V) ····· composite solution.

Figure 19. Normalized tissue oxygen concentration at the outer edge of the tissue as a function of axial position, for example (2) in table I. (I) ———— without axial diffusion, (II) ———— with axial diffusion, (III) — — — —arterial boundary layer solution, (IV) — — — —venous boundary layer solution, (V) ····· composite solution.

Figure 25. Normalized tissue oxygen concentration at the outer edge of the tissue as a function of axial position, for example (2) in table I. ———— composite solution, — — — — exact solution.

Figure 26. Slope of oxyhemoglobin dissociation curves as a function of blood oxygen concentration for various $S^*(C_b)$ which are shown in figure 2.

Figure 27. Normalized blood oxygen concentration as a function of axial position z, for the 1st set of data in table III. (I) ———— without axial diffusion, (II) ———— with axial diffusion, (III) ····· boundary layer solution, (IV) — — — — — composite solution.

Figure 28. Normalized tissue oxygen concentration midway between the capillary wall and the outer edge of the tissue as a function of axial position z, for the 1st set of data in table III. (I) ———— without axial diffusion, (II) ———— with axial diffusion, (III) ····· boundary layer solution, (IV) — — — — — composite solution.

Figure 29. Normalized tissue oxygen concentration at the outer edge of the tissue as a function of axial position z , for the 1st set of data in table III. (I) ———— without axial diffusion, (II) ———— with axial diffusion, (III) ····· boundary layer solution (IV) — — — — composite solution.

Figure 30. Normalized blood oxygen concentration as a function of axial position z , for the 2nd set of data in table III. (I) ———— without axial diffusion, (II) ———— with axial diffusion, (III) ····· boundary layer solution, (IV) — — — — composite solution.

Figure 31. Normalized tissue oxygen concentration midway between the capillary wall and the outer edge of the tissue as a function of axial position z , for the 2nd set of data in table III. (I) ———— without axial diffusion, (II) ———— with axial diffusion, — — — — — boundary layer solution.

Figure 32. Normalized tissue oxygen concentration at the outer edge of the tissue as a function of axial position z , for the 2nd set of data in table III. (I) ———— without

Figure 44. Normalized blood oxygen concentration as a function of axial position, for C_A=0.003 cm^3O_2/cm^3 blood, the values in the 3rd set of data of table III, and various oxyhemoglobin dissociation curves shown in figure 2. (a) Curve (II), (b) Curve (III), (c) Curve (I). ———— with axial diffusion, — — — — without axial diffusion.

Figure 45. Normalized blood oxygen concentration as a function of axial position, for the outflux Krogh model with $f_1=f_2=0.03M_oL$, and the 1st set of data in table III. (I) ———— without axial diffusion, (II) ———— with axial diffusion, ····· boundary layer solution, — — — — composite solution.

Figure 46. Normalized tissue oxygen concentration midway between the capillary wall and the outer edge of the tissue as a function of axial position, for the outflux Krogh model with $f_1=f_2=0.03M_oL$, and the 1st set of data in table III. (I) ———— without axial diffusion, (II) ———— with axial diffusion, ····· boundary layer solution, — — — — composite solution.

Figure 47. Normalized tissue oxygen concentration at the outer edge of the tissue as a function of axial position, for the outflux Krogh model with $f_1=f_2=0.03M_oL$, and the 1st set of data in table III. (I) ———— without axial diffusion, (II) ———— with axial diffusion, ····· boundary layer solution, — — — — composite solution.

Figure 48. Normalized blood oxygen concentration as a function of axial position, for the outflux Krogh model with $f_1=f_2=0.05M_oL$, and the 3rd set of data in table III. (I) ———— without axial diffusion, (II) ———— with axial diffusion, — — — — composite solution.

Figure 49. Normalized tissue oxygen concentration midway between the capillary wall and the outer edge of the tissue as a function of axial position, for the outflux Krogh model with $f_1=f_2=0.05M_oL$, and the 3rd set of data in table III. (I) ———— without axial diffusion, (II) ———— with axial diffusion, — — — — composite solution.

Figure 50. Normalized tissue oxygen concentration at the outer edge of the tissue as a function of

axial position, for the outflux Krogh model with $f_1=f_2=0.05M_oL$, and the 3rd set of data in table III. (I) ———— without axial diffusion, (II) ———— with axial diffusion, — — — — composite solution.

ABSTRACT

A mathematical analysis of oxygen transport to tissue is presented. A conceptual model is used that consists of a single capillary surrounded by a concentric cylinder of tissue. Due to the non-linearity of the relationship governing the dissociation of oxygen from hemoglobin, a non-linear system of coupled equations results. These equations describe the convection of oxygen by the blood in the capillary and its diffusion in the surrounding tissue. An analysis of these equations for steady state conditions, using the techniques of matched asymptotic expansions, is presented. The solutions obtained in this way are applicable when the mean capillary spacing is small compared to the capillary length. A corresponding linear problem has been solved exactly and the solution used to examine the accuracy of the perturbation solution. This linear problem was analyzed previously by Blum (1960). It is shown that Blum's method of solution is incorrect, and the correct analysis of the problem is presented.

1. INTRODUCTION

Oxygen transport is one of the most vital processes in the living body. The transport mechanisms for oxygen in the microcirculation and tissue are important physiologically and essential to normal life functioning. Oxygen enters all parts of the body with exchange occurring through capillaries. When oxygen dissociates from the blood, it diffuses out into the surrounding tissue (Guyton 1976), and supplies each cell with oxygen for normal life function. Although the recent experimental results by Duling and Berne (1970), and Sejrsen and Tonneson (1972) indicate that some oxygen loss occurs from the arterioles, the capillaries are still the primary exchange site.

The conceptual model of a single capillary surrounded by a concentric cylinder of tissue has played a central role in the mathematical study of oxygen transport to tissue. It was originally introduced by Krogh (1919) for the study of oxygen distribution in the highly regular capillary beds of skeletal muscle. The idea is that oxygen delivered to tissue by a capillary is consumed only in the tissue immediately surrounding the capillary. Conversely, the tissue in the immediate vicinity of a capillary receives its oxygen requirements from that capillary. Krogh proposed that this conceptual

model could be treated as a functional unit for the entire capillary bed. Although not all tissues show the geometric regularity of skeletal muscle, the Krogh cylinder has been used in studies of oxygen transport in several organs (for example, Knisely et al. 1969, Middleman 1972, Guilbeau et al. 1973, and Reneau et al. 1974). It has also been applied to such irregular capillary beds as cerebral gray matter of the brain (Opitz and Schneider 1950, Thews 1960, Reneau et al. 1967, 1969, 1970, and Reneau et al. 1977). In Krogh's initial work only a rather elementary mathematical analysis of the model was presented. Since that time, however, considerable attention has been given to the development of more elaborate analyses. Summary of some of these works can be found in Reneau et al. (1967), Middleman (1972), Lightfoot (1974), Davis et al. (1974), Leonard and Jorgensen (1974), Reisdrof (1975), Lih (1975), Fletcher (1975), and the proceedings of recent symposiums on oxygen transport to tissue (Bruley and Bicher, eds. 1973, Grote et al., eds. 1976) contain numerous accounts of mathematical studies of the Krogh cylinder, as this model is now known. The very complex nature of the governing equations has always resulted in significant simplications being made at the outset, so that the mathematics become tractable. Therefore,

the analytical treatment is still far from complete. There are a number of numerical analyses which deal with the full equations (for example, Reneau et al. 1967, 1969, 1970, Hyman et al. 1975, Fletcher 1973, 1975, 1976, Artigue and Hyman 1976, and Hyman and Artigue 1977), but such studies are inherently of limited value.

Mathematical studies of oxygen distribution in a Krogh cylinder are presented in this thesis. The full equations are considered, including axial diffusion in the tissue and the blood, and an arbitrary oxyhemoglobin dissociation relationship is used. A detailed formulation of this problem is presented in the next section.

In section 3, some of the previous studies are briefly reviewed and discussed. An analysis, given by Blum (1960), of a model with finite permeability at the capillary wall is shown to be incorrect. The correct analysis is presented in section 4. Several numerical examples of the solution for substrate concentrations are given for various values of permeability and tissue diffusivity.

The problem of determining the steady state oxygen distribution when a linear oxyhemoglobin dissociation relationship is used and axial diffusion in the capillary is neglected can be considered as a special limiting case of the model considered by Blum (1960), by taking the

permeability of the capillary to be infinite. This case is also presented in section 4.

In section 5, a nonlinear oxyhemoglobin dissociation relationship is used. The methods of asymptotic analysis are used to obtain solutions applicable when the diameter of the Krogh cylinder is small compared to its length. A perturbation solution for the region bounded away from the ends of the Krogh cylinder, and boundary layer solutions at both ends are presented in sections 5.1, 5.2 and 5.3, respectively. The solutions are obtained in the form of an infinite series involving infinite eigenvalues. The accuracy of this expansion is examined in section 5.4. A uniformly valid composite solution is given in section 5.5. An exact numerical solution is given in section 5.6. The analysis of a modification of the Krogh model is presented in section 5.7.

Numerical examples are presented in section 6. Using the linear theory in section 6.1, it is shown that the perturbation method is a good approximation to the exact solution. In section 6.2, the effect of axial diffusion is studied, and it is ascertained when this effect can be neglected and when it must be taken into account. Several numerical examples are presented. In section 6.3, numerical examples of the modified Krogh

model with outflux of oxygen through the ends of the Krogh cylinder are presented. The results are compared with the corresponding results of the isolated Krogh model shown in section 6.2.

2. FORMULATION OF THE PROBLEM

The physical model, which is illustrated in fig. 1, consists of a single capillary of length L and radius R_c surrounded by a concentric cylinder of tissue having radius R_t. The tissue cylinder is bounded at the arterial and venous ends by planes normal to the capillary, so that its length is also L. The mathematical simplification of axial symmetry is assumed, so that only two space dimensions are considered. Let $\bar{z}$ denote the distance along the capillary axis $(0 \leq \bar{z} \leq L)$ and $\bar{r}$ the distance normal to the axis $(0 \leq \bar{r} \leq R_t)$.

Oxygen is transported in the blood dissolved in the plasma and chemically bound to hemoglobin molecules. The rate of dissociation of oxygen from hemoglobin is negligible in comparison to the time required for diffusion in the plasma (Thews 1960), so the degree of saturation of hemoglobin is assumed to be in chemical equilibrium with respect to the oxygen dissolved in the plasma. The amount of oxygen bound to hemoglobin is a function of the concentration of oxygen dissolved in the plasma, but also depends on the pH, carbon dioxide concentration and temperature of the blood. Here, the dissolved oxygen, C_b, is defined as the amount of oxygen physically dissolved in plasma per unit volume of blood. The oxygen bound to the hemoglobin per unit volume

of blood is given by $\bar{Q}S^*$, where $\bar{Q}$ is the oxygen capacity of the blood at 100% saturation, and S^* is the degree of saturation. As noted, S^* is a function of C_b , and may be approximated by the empirical formula (Reneau et al. 1967, 1969, 1970, Hyman 1973, Hyman et al. 1975)

$$S^*(C_b) = \frac{KC_b^x}{1+KC_b^x} \qquad (2.1)$$

for a suitable choice of the constants K and x . These constants depend on the pH, carbon dioxide concentration, and temperature of the blood. Typical oxyhemoglobin dissociation relationships are shown in fig. 2 for various values of K and x . The characteristic shape of these curves have important physiological significance. At higher blood oxygen concentrations, the shape of $S^*(C_b)$ is rather flat so that only a small amount of oxygen is released from hemoglobin even for a large drop in blood oxygen concentration. At lower blood oxygen concentrations, small changes in blood oxygen concentration causes large amounts of oxygen to dissociate from hemoglobin. Therefore, in this region large quantities of oxygen can be supplied to the tissue with only a small drop in the concentration, C_b .

The oxygen concentration, C_b , varies with both

radial and axial location within the capillary. However, the radial variation may be neglected, as it is insignificant. A number of previous studies (e.g. Reneau et al. 1967, 1969, 1970, Davis et al. 1974) have considerably complicated the problem by attempting to consider a radial variation in oxygen concentration based on the assumption of laminar homogeneous flow within the capillary. The passage of red blood cells single file through the capillary, separated from each other by a bolus of fluid (Prothero and Burton 1961), precludes such an assumption. In addition, the recirculating flow within each bolus results in convective mixing (Bugliarello and Hsau 1970, Gross and Aroesty 1972), so that a uniform radial oxygen distribution is a more reasonable assumption (Hyman et al. 1975). Keller and Friedlander (1966) and Spaeth (1970) have demonstrated that oxyhemoglobin diffusion is negligible. Therefore, when oxygen is convected in the capillary by blood only dissolved oxygen diffuses across the capillary wall into the surrounding tissue. The governing equation for oxygen concentration within the capillary is

$$\pi R_c^2 \frac{\partial}{\partial \tau} [C_b + \bar{Q} S^*(C_b)] + q \frac{\partial}{\partial \bar{z}} [C_b + \bar{Q} S^*(C_b)]$$
$$= -2\pi R_c J + \pi R_c^2 D_b \frac{\partial^2 C_b}{\partial \bar{z}^2}, \quad \tau > 0, \quad 0 \leq z \leq L, \qquad (2.2)$$

where $C_b = C_b(\tau, \bar{z})$ ($cm^3 O_2/cm^3$ blood), since the oxygen

concentration is radially independent, and τ is time (sec.). This equation states that the oxygen in any small volume of blood moving through the capillary changes as a result of axial diffusion within the capillary and radial diffusion into the surrounding tissue. Here q is the volume blood flow rate ($\mu m^3/sec$), $\bar{Q}$ is the oxygen capacity of the blood at 100% saturation (cm^3O_2/cm^3 blood) and is proportional to the hematocrit, J is the oxygen flux across the capillary wall into the tissue (cm^3O_2/cm^2 capillary wall - sec), and D_b is the oxygen diffusivity of blood ($\mu m^2/sec$), which is assumed to be constant. The oxyhemoglobin dissociation relationship, $S^*(C_b)$, is given by eqn. (2.1). The particular form of this relationship makes no difference to the present analysis, and eqn. (2.1) may be replaced by a tabular or graphical representation if desired.

The initial condition for blood oxygen concentration is given by

$$C_b(0,\bar{z}) = C_s(\bar{z}) , \quad 0 \leq \bar{z} \leq L , \tag{2.3}$$

where $C_s(\bar{z})$ is a known steady state solution.

The blood oxygen concentration at the arterial end is prescribed by

$$C_b(\tau,0) = C_A(\tau) , \quad \text{for all } \tau . \tag{2.4}$$

It is assumed that tissue oxygen consumption is uniformly distributed throughout the tissue cylinder. Oxygen diffuses from the capillary into the tissue, where it is consumed. The consumption rate is a function of tissue oxygen concentration. Michaelis-Menten Kinetics is generally used to describe the dependence of oxygen consumption rate on tissue oxygen concentration c_t . This leads to the formula

$$M(c_t) = \frac{Ac_t}{B+c_t} \qquad (2.5)$$

where A and B are constants that depend on physiological conditions. For $c_t \to 0$, $M(c_t) \sim \frac{A}{B} c_t$, which is referred to as first order kinetics. For $c_t \to \infty$, $M(c_t) \sim A$, and is independent of tissue oxygen concentration. Fig. 3 shows a typical form for the relationship $M(c_t)$, taken from Guyton (1976). At normal tissue oxygen concentration the tissue oxygen consumption rate is fairly constant, but at very low tissue oxygen concentration the tissue oxygen consumption rate decreases rapidly to zero as tissue oxygen concentration drops to zero (Forster 1964, Duling and Pittman 1975, Reneau et al. 1977).

Inside the tissue, oxygen is transported by radial and axial diffusion (Blum 1960, Thews 1960), with no convection (Krogh 1919). Therefore, the governing

equation for tissue oxygen concentration, c_t, is

$$\frac{\partial c_t}{\partial \tau} = D_r \frac{1}{\bar{r}} \frac{\partial}{\partial \bar{r}} \bar{r} \frac{\partial c_t}{\partial \bar{r}} + D_z \frac{\partial^2 c_t}{\partial \bar{z}^2} - M(c_t) , \quad \tau>0 , \quad R_c \leq \bar{r} \leq R_t , \quad 0 \leq \bar{z} \leq L , \quad (2.6)$$

where $c_t = c_t(\tau, \bar{r}, \bar{z})$ ($cm^3 O_2/cm^3$ tissue). This states that the time change of tissue oxygen concentration is due to diffusion and consumption of oxygen. Since the tissue may be anisotropic (Blum 1960), radial and axial oxygen diffusivities are not necessarily equal, and these two constants are denoted by D_r and D_z ($\mu m^2/sec$), respectively.

The initial condition for the tissue oxygen concentration is given by

$$c_t(0, \bar{r}, \bar{z}) = c_s(\bar{r}, \bar{z}) , \quad R_c \leq \bar{r} \leq R_t , \quad 0 \leq \bar{z} \leq L , \quad (2.7)$$

where $c_s(\bar{r}, \bar{z})$ is a known steady state solution.

By definition of the isolated Krogh cylinder, no oxygen diffuses across the tissue boundary, so that

$$\left.\frac{\partial c_t}{\partial \bar{r}}\right|_{\bar{r}=R_t} = 0 , \quad 0 \leq \bar{z} \leq L , \quad \tau>0 , \quad (2.8)$$

$$\left.\frac{\partial c_t}{\partial \bar{z}}\right|_{\bar{z}=0} = 0 , \quad R_c \leq \bar{r} \leq R_t , \quad \tau>0 , \quad (2.9)$$

$$\left.\frac{\partial c_t}{\partial \bar{z}}\right|_{\bar{z}=L} = 0 , \quad R_c \leq \bar{r} \leq R_t , \quad \tau>0 . \quad (2.10)$$

The capillary wall consists of endothelial cells which are highly permeable to small molecules such as oxygen (Krogh 1930), and no resistance to the diffusion of oxygen at the capillary wall occurs (Blum 1960). Therefore, the oxygen concentration of the blood and the tissue are equal at the capillary wall,

$$c_t = C_b \ , \quad \bar{r} = R_c \ , \quad 0 \leq \bar{z} \leq L \ , \quad \tau > 0 \ . \qquad (2.11)$$

The oxygen that crosses the capillary wall is convected away from the capillary by the radial gradient of the tissue oxygen concentration. Therefore,

$$J = - D_r \left. \frac{\partial c_t}{\partial \bar{r}} \right|_{\bar{r}=R_c} . \qquad (2.12)$$

Substituting eqn. (2.12) into eqn. (2.2), the governing equation for oxygen concentration within the capillary becomes

$$\pi R_c^2 \frac{\partial}{\partial \tau} [C_b + \bar{Q} S^*(C_b)] + q \frac{\partial}{\partial \bar{z}} [C_b + \bar{Q} S^*(C_b)]$$

$$= 2\pi R_c D_r \left. \frac{\partial c_t}{\partial \bar{r}} \right|_{r=R_c} + \pi R_c^2 D_b \frac{\partial^2 C_b}{\partial \bar{z}^2} \ , \quad 0 \leq z \leq 1 \ , \quad \tau > 0. \qquad (2.13)$$

This completes the formulation of the mathematical problem of oxygen transport to tissue.

3. HISTORICAL REVIEW

The number of works on mathematical studies of oxygen transport to tissue has grown considerably in recent years, and in this section, some of these will be briefly discussed.

In 1919, Krogh studied steady state oxygen transport, considering only radial diffusion and constant oxygen consumption, M_o, in the tissue. His elementary mathematical model can be obtained from eqns. (2.6), (2.8) and (2.11):

$$D_r \frac{1}{\bar{r}} \frac{\partial}{\partial \bar{r}} \bar{r} \frac{\partial c_t}{\partial \bar{r}} = M_o \,, \tag{3.1}$$

$$\left. \frac{\partial c_t}{\partial \bar{r}} \right|_{\bar{r}=R_t} = 0 \,, \tag{3.2}$$

$$c_t = C_b \,, \text{ at } \bar{r} = R_c \,, \tag{3.3}$$

where the oxygen concentration, C_b, at the capillary wall is given. Krogh ignored all aspects of oxygen carried by blood in the capillary and axial diffusion in the tissue.

Bloch (1943) modified Krogh's model by assuming a finite permeability to oxygen at the capillary wall. The oxygen concentration at the tissue side of the capillary boundary is therefore related to that in the blood by

$$-D_r \frac{\partial c_t}{\partial \bar{r}} = H(C_b - c_t) \ , \ \text{at} \ \ \bar{r} = R_c \ , \qquad (3.4)$$

where H is a mass transfer coefficient (permeability) (μm/sec).

Bloch accounted for both dissolved oxygen in plasma and bound oxygen with hemoglobin. These two forms of oxygen are convected by the blood flow, q , and balanced by the amount of dissolved oxygen diffusing across the capillary wall into the tissue. The blood phase equation is

$$-q \frac{d}{d\bar{z}}(C_b + \bar{Q}S^*) = 2\pi R_c H[C_b - c_t\Big|_{\bar{r}=R_c}] \ , \quad 0 \leq \bar{z} \leq L \ , \ (3.5)$$

where the variable S* represents the fractional saturation of oxyhemoglobin. Combining eqns. (3.4) and (3.5) gives the same equation as (2.13) for steady state and without axial diffusion. Bloch did not solve these simultaneous partial differential equations because of their mathematical complexity.

Opitz and Schneider (1950), Kety (1957), and Thews (1960) developed the necessary equation for taking into account axial diffusion in the tissue. Through application of the equation, Thews (1960) indicated that axial diffusion did have a significant effect on the results. Kety assumed a linear axial oxygen concentration profile in the blood, with fixed arterial and venous oxygen

concentration, C_A and C_V, respectively. The equation was

$$C_A - C_b = (C_A - C_V)\,\bar{z}/L\,, \quad 0 \leq \bar{z} \leq L\,. \tag{3.6}$$

This analysis is questionable, since the analysis should permit one to predict the venous oxygen concentration.

Blum (1960) extended the works of Krogh, Bloch, Kety and Thews and agreed with the appropriateness of using infinite permeability of the capillary wall for oxygen transport to tissue. For large molecular diffusion, such as glucose, lactic acid, etc., the capillary wall offers finite resistance. Blum followed Bloch's format for the capillary equation, but he failed to include a major function in oxygen distribution, the production of oxygen in the blood from dissociation of oxyhemoglobin. In the capillary, the equation, confined to the steady state, for the substrate without chemical reaction with blood is

$$-q\,\frac{d}{d\bar{z}}\,C_b = 2\pi R_c H\left[C_b - c_t\Big|_{r=R_c}\right]\,, \quad 0 \leq \bar{z} \leq L\,. \tag{3.7}$$

The substrate coming in at the arterial end was prescribed

$$C_b = C_A\,, \text{ at } \bar{z} = 0\,. \tag{3.8}$$

Eqn. (3.4) was also prescribed at the capillary wall. For oxygen transport, the permeability H becomes

infinite and eqns. (3.7) and (3.4) become

$$q \frac{d}{d\bar{z}} C_b = 2\pi R_c \left. \frac{\partial c_t}{\partial \bar{r}} \right|_{\bar{r}=R_c} , \quad 0 \leq \bar{z} \leq L , \tag{3.9}$$

$$c_t = C_b , \quad \bar{r} = R_c , \quad 0 \leq \bar{z} \leq L . \tag{3.10}$$

Blum considered that oxygen might be transported by the radial and axial diffusion in an anisotropic tissue. Confining his analysis to the steady state, Blum attempted to solve eqn. (2.6) for zero order kinetics, $M(c_t) = M_o$, and by neglecting axial diffusion, for first order kinetics, $M(c_t) = M_1 c_t$. The equations were

(i) zero order kinetics,

$$D_r \frac{1}{\bar{r}} \frac{\partial}{\partial \bar{r}} \bar{r} \frac{\partial c_t}{\partial \bar{r}} + D_z \frac{\partial^2 c_t}{\partial \bar{z}^2} = M_o , \tag{3.11}$$

with zero flux boundary conditions, eqns. (2.8), (2.9) and (2.10),

(ii) first order kinetics,

$$D_r \frac{1}{\bar{r}} \frac{\partial}{\partial \bar{r}} \bar{r} \frac{\partial c_t}{\partial \bar{r}} = M_1 c_t , \tag{3.12}$$

with eqn. (2.8).

Unfortunately, his method of solution for zero order kinetics (constant tissue oxygen consumption rate) was incorrect, and he failed to obtain meaningful results. The correct analysis will be presented in the next

section.

Reneau et al. (1967,1969,1970) presented numerical solutions to the steady state and unsteady state problem of oxygen supply to the brain. In their works, the Krogh cylinder model was used. The capillary equation included the nonlinear oxyhemoglobin dissociation relationship, $S^*(C_b)$, in the capillary equation. They assumed both plug and Poiseuille blood flow, and allowed radial gradients in the capillary due to radial diffusion. Therefore, they replaced eqn. (2.2) by

$$\frac{\partial}{\partial\tau}[C_b+\bar{Q}S^*(C_b)] + v\,\frac{\partial}{\partial\bar{z}}[C_b+\bar{Q}S^*(C_b)]$$

$$= D_b\left[\frac{1}{\bar{r}}\,\frac{\partial}{\partial\bar{r}}\,\bar{r}\,\frac{\partial C_b}{\partial\bar{r}} + \frac{\partial^2 C_b}{\partial\bar{z}^2}\right] , \quad t>0,\ 0\le\bar{r}\le R\ ,\ 0\le\bar{z}\le L\ , \quad (3.13)$$

where $C_b = C_b(\tau,\bar{r},\bar{z})$, and v is the velocity of blood flow.

The symmetry property at the capillary axis was prescribed

$$\left.\frac{\partial C_b}{\partial\bar{r}}\right|_{\bar{r}=0} = 0\ . \quad (3.14)$$

An isotropic tissue with constant tissue oxygen consumption was assumed. Eqn. (2.6) becomes

$$\frac{\partial c_t}{\partial\tau} = D_t\left[\frac{1}{\bar{r}}\,\frac{\partial}{\partial\bar{r}}\,\bar{r}\,\frac{\partial c_t}{\partial\bar{r}} + \frac{\partial^2 c_t}{\partial\bar{z}^2}\right] - M_o\ ,$$

$$\tau>0,\ R\le\bar{r}\le R_t,\ 0\le\bar{z}\le L, \quad (3.15)$$

where D_t is an isotropic tissue oxygen diffusivity.

The boundary conditions eqns. (2.8) and (2.9) were used. A finite, nonzero flux tissue boundary condition at $\bar{z} = L$ was assumed. This finite value was chosen to fit arterial oxygen concentrations and the corresponding venous oxygen concentrations of the experimental data of Opitz and Schneider (1950). This data dependent flux is questionable on mathematical grounds. At the capillary wall, eqn. (2.11) was used and an additional condition was prescribed

$$D_b \left.\frac{\partial C_b}{\partial \bar{r}}\right|_{\bar{r}=R_c} = D_t \left.\frac{\partial c_t}{\partial \bar{r}}\right|_{\bar{r}=R_c} . \qquad (3.16)$$

The numerical works of Reneau et al. required a large amount of computer time not only for the final results but also for checking the stability and convergence properties of the numerical method. Any change in the parameters required repeating the computations, so that it is inconvenient and too time consuming to examine the significance of the various parameters. The radial gradient which Reneau et al. considered inside the capillary not only unnecessarily complicates the problem but also gives computational difficulty at the arterial end where the oxygen concentration is flat. Therefore, they were forced to assume a shape for the incoming arterial oxygen concentration similar to what they would expect

to find some distance from the arterial end.

After the numerical works of Reneau et al., many investigators attempted to solve this problem analytically. Stewart and Morrazzi (1973) approximated the slope of oxyhemoglobin dissociation curve by a simple exponential function. They solved the steady state problem without axial diffusion in the capillary and the tissue, and obtained approximate analytical solutions for tissue oxygen concentration and the space averaged blood oxygen concentration. This problem can be solved exactly (Hyman 1973, also see section 5) without approximating the nonlinear oxyhemoglobin relationship. Davis et al. (1974) followed the format of Reneau et al. (1967) and attempted to solve the steady-state problem analytically by neglecting axial diffusion in the blood and linearizing the oxyhemoglobin dissociation relationship. They pointed out that the errors resulting from the linearization causes the oxygen profiles to fall more slowly with distance over the first part of the capillary and more rapidly further along, as compared to the results of Reneau et al. (1967). They also studied the difference between plug flow and Poiseuille flow to the overall transport process and concluded that the mathematical model of the blood flow has rather little effect on the results. A unidirectional blood flow with a constant average

velocity is a reasonable assumption. A linear solution, similar to the work of Davis et al., for the well mixed blood phase model will be presented in the next section.

Fletcher (1973,1975,1976), Hyman (1973), and Hyman et al. (1975) used a well mixed capillary model which assumes no radial oxygen gradient. Hyman et al. (1975) strongly defended their use of this model. Fletcher (1973,1975,1976) formulated a more complicated mathematical model in the capillary by considering nonequilibrium kinetics of oxyhemoglobin dissociation. The equations in the capillary were

$$\frac{\partial}{\partial \tau} S^*(C_b^{(e)}) + \frac{q}{\pi R_c^2} \frac{\partial}{\partial \bar{z}} S^*(C_b^{(e)}) = -\beta[C_b^{(e)} - C_b^{(N)}] \ , \tag{3.17}$$

$$\pi R_c^2 \frac{\partial C_b^{(N)}}{\partial \tau} + q \frac{\partial C_b^{(N)}}{\partial \bar{z}} = 2\pi R_c D_r \left.\frac{\partial c_t}{\partial \bar{r}}\right|_{\bar{r}=R_c} + \pi R_c^2 \bar{Q} \beta [C_b^{(e)} - C_b^{(N)}] \ , \tag{3.18}$$

where $C_b^{(e)}$ and $C_b^{(N)}$ are equilibrium and nonequilibrium blood oxygen concentration, respectively, and β is the release frequency of oxyhemoglobin (sec^{-1}) . When the equilibrium kinetics of oxyhemoglobin is assumed, $\beta \to \infty$ $(C_b^{(e)} = C_b^{(N)} = C_b)$, and eqns. (3.17) and (3.18) become eqn. (2.13) with $D_b = 0$.

Fletcher studied eqn. (2.6) and used three forms for tissue oxygen consumption rate, $M(c_t)$,

$$M(c_t) = \begin{cases} M_o \text{ , zero order kinetics} \\ M_1 c_t \text{ , first order kinetics} \\ \dfrac{Ac_t}{B+c_t} \text{ , Michaelis-Menton kinetics.} \end{cases} \quad (3.19)$$

Due to the mathematical complexity, Fletcher solved this problem numerically for a linearized oxyhemoglobin dissociation relationship. The equilibrium kinetics of oxyhemoglobin dissociation ($\beta \to \infty$) is a reasonable assumption compared to the normal blood with nonequilibrium kinetics (β=5000/sec, based on the data of Staub et al. 1961) over most of the blood flow range, as indicated in Fletcher (1976). Fletcher (1976) also studied the effect on oxygen transport of shifts in the oxyhemoglobin dissociation curve.

Hyman et al. (1975) studied the oxygen transport in skeletal muscle subject to periodic occlusion. The production and transport of lactic acid was included in their mathematical model. Eqn. (2.13) with $D_b=0$, and eqn. (2.6) with constant tissue oxygen consumption rate, M_o , were used. Boundary condition were prescribed as in the previous section. The concept of the oxygen debt was formulated and included in the model in terms of the mechanism of lactic acid production and removal. In the absence of oxygen, lactic acid is produced according to the following equation

$$\frac{dC_{LA}}{d\tau} = M_L \ , \quad C_b = 0$$

$$= 0 \ , \quad C_b > 0 \ , \qquad (3.20)$$

where C_{LA} is the lactic acid concentration, and M_L is constant lactic acid production rate. They solved their problem numerically and demonstrated the significance of a local oxygen debt as a factor in recovery from the ischemic condition. In contrast to the works of Hill (1928), and Reneau and Lafitte (1973), Hyman et al. did not allow local lactic acid to diffuse through the tissue or out into the bloodstream.

No analytical solutions have been obtained for the model which includes axial diffusion and the nonlinear oxyhemoglobin dissociation relationship. All studies of this type have been done numerically (Reneau et al. 1967, 1969, 1970, Hyman et al. 1975, Fletcher 1973, 1975, 1976). Only a few investigators (Blum 1960, Davis et al. 1974) attempted to obtain analytical solutions by neglecting or linearizing the oxyhemoglobin dissociation relationship.

4. LINEAR PROBLEM

In this section, steady state oxygen transport with a linear oxyhemoglobin dissociation relationship is studied. The linear oxyhemoglobin dissociation relationship is taken to be of the form

$$S^*(C_b) = S_1^* C_b + S_o^* \quad , \tag{4.1}$$

where S_1^* and S_o^* are known constants. Axial oxygen diffusion in the capillary is neglected, $D_b=0$, and a constant tissue oxygen consumption rate, M_o , is used. Therefore, the governing equations (2.6), (2.8)-(2.11), (2.13) and (2.4) reduce to

$$D_r \frac{1}{\bar{r}} \frac{\partial}{\partial \bar{r}} \bar{r} \frac{\partial c_t}{\partial \bar{r}} + D_z \frac{\partial^2 c_t}{\partial \bar{z}^2} = M_o \quad , \quad R_c \leq \bar{r} \leq R_t \quad , \quad 0 \leq \bar{z} \leq L \quad , \tag{4.2}$$

$$\left. \frac{\partial c_t}{\partial \bar{r}} \right|_{\bar{r}=R_c} = 0 \quad , \quad 0 \leq \bar{z} \leq L \quad , \tag{4.3}$$

$$\left. \frac{\partial c_t}{\partial \bar{z}} \right|_{\bar{z}=0} = 0 \quad , \quad R_c \leq \bar{r} \leq R_t \quad , \tag{4.4}$$

$$\left. \frac{\partial c_t}{\partial \bar{z}} \right|_{\bar{z}=L} = 0 \quad , \quad R_c \leq \bar{r} \leq R_t \quad , \tag{4.5}$$

$$c_t = C_b \quad , \quad \bar{r} = R_c \quad , \quad 0 \leq \bar{z} \leq L \quad , \tag{4.6}$$

$$q \frac{d}{d\bar{z}} [C_b + \bar{Q} S^*(C_b)] = 2\pi R_c D_r \left. \frac{\partial c_t}{\partial \bar{r}} \right|_{\bar{r}=R_c} \quad , \quad 0 \leq \bar{z} \leq L, \tag{4.7}$$

$$C_b = C_A \ , \quad \bar{z} = 0 \ , \tag{4.8}$$

where $c_t = c_t(\bar{r},\bar{z})$, $C_b = C_b(\bar{z})$ and C_A is the known arterial oxygen concentration.

Substituting eqn. (4.1) into eqn. (4.7), we have

$$q^* \frac{dC_b}{d\bar{z}} = 2\pi R_c D_r \left.\frac{\partial c_t}{\partial \bar{r}}\right|_{\bar{r}=R_c} \ , \quad 0 \leq \bar{z} \leq L \ , \tag{4.9}$$

where

$$q^* = q(1+\bar{Q}S_1^*) \ . \tag{4.10}$$

This linear model, which includes eqns. (4.2)-(4.6), (4.9) and (4.8), can be considered as a special case of Blum's model (1960) with infinite permeability of the capillary wall ($H \to \infty$, as described in section 3).

Since Blum was interested in the concentration profiles of substrates which experience a finite resistance at the capillary wall, he considered a finite capillary permeability, H . In this case eqn. (4.6) is replaced by

$$D_r \left.\frac{\partial c_t}{\partial \bar{r}}\right|_{\bar{r}=R_c} = -H[C_b - c_t(R_c,\bar{z})] \ , \quad 0 \leq \bar{z} \leq L \ . \tag{4.11}$$

Blum did not take the oxyhemoglobin dissociation (chemical reaction with red blood cells) into account in his model, so the capillary equation was

$$q \frac{dC_b}{d\bar{z}} = 2\pi R_c D_r \left. \frac{\partial c_t}{\partial \bar{r}} \right|_{\bar{r}=R_c}, \quad 0 \leq \bar{z} \leq L . \qquad (4.12)$$

Eqn. (4.9) differs from eqn. (4.12) only in the use of q^* instead of q .

Therefore the analyses of the linear oxygen transport model and Blum's model are similar, and the solution for an infinitely permeable capillary can be obtained from Blum's solution as a special limiting case. Unfortunately, Blum's solution is incorrect, and his results are not meaningful. The error in Blum's analysis has never been realized, and the paper is widely quoted in the literature, including a number of textbooks on microcirculatory physiology (Middleman 1972, Lih 1975, for example). Lih (1975) devoted an appendix of his book to a detailed explanation of Blum's solution, and Fletcher (1975) appears to have recently obtained the same solution independently. Since the problem describes an interesting physiological process, it is important to provide the correct analysis, and this is done in the present section. A brief description of Blum's analysis is given in appendix A, where it is shown why his solution is wrong. Numerical examples are presented for a particular choice of physiological data. No examples were given by Blum, presumably because of the contradictory nature of his results.

4.1. Analysis

The equations can be put into dimensionless form by normalizing the concentrations with respect to C_A, the arteriole concentration, and normalizing the radial and axial distances $\bar{r}$ and $\bar{z}$ with respect to R_t and L, respectively. Therefore, the non-dimensional variables are $C = \frac{C_b}{C_A}$, $c = \frac{c_t}{C_A}$, $r = \frac{\bar{r}}{R_t}$ and $z = \frac{\bar{z}}{L}$. The governing equations (4.2)-(4.5), (4.11), (4.12) and (4.8) are then

$$\frac{1}{r}\frac{\partial}{\partial r} r \frac{\partial c}{\partial r} + \theta \frac{\partial^2 c}{\partial z^2} = M , \quad 0 \le z \le 1 , \quad R \le r \le 1 , \tag{4.13}$$

$$\left.\frac{\partial c}{\partial r}\right|_{r=1} = 0 , \quad 0 \le z \le 1 , \tag{4.14}$$

$$\left.\frac{\partial c}{\partial z}\right|_{z=0} = 0 , \quad R \le r \le 1 , \tag{4.15}$$

$$\left.\frac{\partial c}{\partial z}\right|_{z=1} = 0 , \quad R \le r \le 1 , \tag{4.16}$$

$$\left.\frac{\partial c}{\partial r}\right|_{r=R} = -h[C(z)-c(R,z)] , \quad 0 \le z \le 1 , \tag{4.17}$$

$$\beta \frac{dC}{dz} = \left.\frac{\partial c}{\partial r}\right|_{r=R} , \quad 0 \le z \le 1 , \tag{4.18}$$

$$C(0) = 1 , \tag{4.19}$$

where

$$R = \frac{R_c}{R_t} , \quad \theta = \frac{R_t^2 D_z}{L^2 D_r} , \quad M = \frac{R_t^2 M_o}{D_r C_A} , \quad h = \frac{H R_t}{D_r}$$

$$\text{and} \quad \beta = \frac{q}{2\pi R D_r L} .$$

Eqn. (4.13) is the two dimensional diffusion equation with constant sink. Methods of solution may be found in Carslaw and Jaeger (1959), and Crank (1975). The solution to eqns. (4.13)-(4.17) will be obtained in terms of $C(z)$, and this solution will be substituted into eqn. (4.18) to obtain a single equation for $C(z)$.

A solution to eqn. (4.13) satisfying the boundary conditions, eqns. (4.15) and (4.16), is given by the eigenfunction expansion

$$c(r,z) = \frac{Mr^2}{4} + y_1 + y_2 \ell n\, r + \sum_{n=1}^{\infty} [\bar{A}_n I_o(\rho_n r) + \bar{B}_n K_o(\rho_n r)] \cos(n\pi z), \quad (4.20)$$

where K_o and I_o are the modified Bessel functions of order zero. y_1, y_2, $\bar{A}_n$ and $\bar{B}_n$ are constants, and $\rho_n = \sqrt{\theta}\, n\pi$. Using the boundary condition eqn. (4.14) gives

$$c(r,z) = \frac{M}{2}\left(\frac{r^2}{2} - \ell n\, r - \frac{R^2}{2} + \ell n\, R\right) + B_o + \sum_{n=1}^{\infty} B_n [K_1(\rho_n) I_o(\rho_n r) + I_1(\rho_n) K_o(\rho_n r)] \cos(n\pi z), \quad (4.21)$$

where constant y_1 has been written as $B_o - \frac{M}{2}\left(\frac{R^2}{2} - \ell n\, R\right)$ for convenience, and $B_n = \frac{\bar{B}_n}{I_1(\rho_n)}$. These constants are determined by substituting the solution into the remaining boundary condition, eqn. (4.17). Writing

$$u_n = \rho_n [K_1(\rho_n) I_1(\rho_n R) - I_1(\rho_n) K_1(\rho_n R)] \ , \qquad (4.22)$$

and

$$v_n = K_1(\rho_n) I_o(\rho_n R) + I_1(\rho_n) K_o(\rho_n R) \ , \qquad (4.23)$$

this substitution yields

$$B_o + \sum_{n=1}^{\infty} B_n \left(v_n - \frac{1}{h} u_n\right) \cos(n\pi z) = C(z) + \frac{M}{2h} \left(R - \frac{1}{R}\right) \ . \qquad (4.24)$$

From this equation and the orthogonality properties of $\cos(n\pi z)$, it follows that

$$B_o = \frac{M}{2h} \left(R - \frac{1}{R}\right) + \int_o^1 C(z) dz \ , \qquad (4.25)$$

and

$$B_n = \frac{2}{v_n - \frac{1}{h} u_n} \int_o^1 C(z) \cos(n\pi z) dz \ . \qquad (4.26)$$

Substituting eqns. (4.25) and (4.26) into eqn. (4.21), we have

$$c(r,z) = \frac{M}{2h} \left(R - \frac{1}{R}\right) + \int_o^1 C(\zeta) d\zeta + \frac{M}{2} \left(\frac{r^2}{2} - \ell n \ r - \frac{R^2}{2} + \ell n \ R\right)$$

$$+ \sum_{n=1}^{\infty} \frac{2}{v_n - \frac{1}{h} u_n} [K_1(\rho_n) I_o(\rho_n r) + I_1(\rho_n) K_o(\rho_n r)]$$

$$\cos(n\pi z) \int_o^1 C(\zeta) \cos(n\pi\zeta) d\zeta \ . \qquad (4.27)$$

This gives $c(r,z)$ explicitly in terms of the capillary concentration $C(z)$.

Substituting eqn. (4.27) into eqn. (4.18) yields

an integro-differential equation for $C(z)$:

$$\frac{dC}{dz} = \frac{M}{2\beta}\left(R - \frac{1}{R}\right) + \sum_{n=1}^{\infty} \frac{2u_n}{\beta\left(v_n - \frac{1}{h}u_n\right)} \cos(n\pi z) \int_o^1 C(\zeta)\cos(n\pi\zeta)d\zeta. \quad (4.28)$$

Integrating with respect to z and applying the boundary condition, eqn. (4.19), yields a Fredholm integral equation of the second kind with separable kernel, for the function $C(z)$:

$$C(z) = 1 + \frac{M}{2\beta}\left(R - \frac{1}{R}\right)z + \sum_{n=1}^{\infty} \frac{2u_n}{\beta n\pi\left(v_n - \frac{1}{h}u_n\right)} \sin(n\pi z) \int_o^1 C(\zeta)\cos(n\pi\zeta)d\zeta . \quad (4.29)$$

Multiplying eqn. (4.29) by $\cos(m\pi z)$ and integrating from $z=0$ to $z=1$, gives

$$a_m = b_m + \sum_{n=1}^{\infty} e_{mn}a_n , \quad m=1,2,3,... \quad (4.30)$$

where

$$a_m = \int_o^1 C(z)\cos(m\pi z)dz , \quad (4.31)$$

$$b_m = \int_o^1 \left[1 + \frac{M}{2\beta}\left(R - \frac{1}{R}\right)z\right]\cos(m\pi z)dz$$

$$= \begin{cases} 0 & , \quad m=2i \quad , \quad i=1,2,3,... \\ -\dfrac{M}{\beta m^2\pi^2}\left(R - \dfrac{1}{R}\right) & , \quad m=2i-1 \quad , \quad i=1,2,3,... \end{cases} , \quad (4.32)$$

and

$$e_{mn} = \frac{2u_n}{\beta n\pi\left(v_n - \frac{1}{h}\,u_n\right)} \int_o^1 \sin(n\pi z)\cos(m\pi z)\,dz$$

$$= \begin{cases} 0 & , \quad m=n \quad \text{or} \quad m+n \quad \text{even} \\ \dfrac{4u_n}{\beta\left(v_n - \frac{1}{h}\,u_n\right)(n^2-m^2)\pi^2} & , \quad m+n \quad \text{odd} \,. \end{cases} \qquad (4.33)$$

Eqn. (4.30) represents an infinite set of linear algebraic equation for the infinite set of unknown constants a_m . The corresponding truncated or "reduced" system of equations,

$$\hat{a}_m = b_m + \sum_{n=1}^{N} e_{mn}\hat{a}_n \,, \quad m=1,2,3,\ldots,N \,, \qquad (4.34)$$

can readily be solved for the N unknowns $\hat{a}_m$, and it can be shown that the $\hat{a}_m$ converge to the desired constants a_m as $N\to\infty$ (Kantorovich and Krylov 1958, Mikhlin 1964). Therefore, a solution of any desired accuracy can be obtained by choosing N sufficiently large. Once the a_m have been determined, C(z) and c(r,z) are found from

$$C(z) = 1 + \frac{M}{2\beta}\left(R - \frac{1}{R}\right)z + \sum_{n=1}^{\infty} \frac{2a_n u_n}{\beta n\pi\left(v_n - \frac{1}{h}\,u_n\right)} \sin(n\pi z) \,, \qquad (4.35)$$

and

$$c(r,z) = \frac{M}{2h}\left(R - \frac{1}{R}\right) + \int_o^1 C(\zeta)\,d\zeta + \frac{M}{2}\left(\frac{r^2}{2} - \ell n\ r - \frac{R^2}{2} + \ell n\ R\right)$$

$$+ \sum_{n=1}^{\infty} \frac{2a_n}{v_n - \frac{1}{h}\,u_n} \left[K_1(\rho_n)I_o(\rho_n r) + I_1(\rho_n)K_o(\rho_n r)\right] \cos(n\pi z) \,, \qquad (4.36)$$

where

$$\int_0^1 C(\zeta)d\zeta = 1 + \frac{M}{4\beta}\left(R - \frac{1}{R}\right) + \sum_{n=1}^{\infty} \frac{2a_n u_n}{\beta(n\pi)^2\left(v_n - \frac{1}{h}u_n\right)}\left[1-\cos(n\pi)\right] , \quad (4.37)$$

is used in eqn. (4.36).

For the linear problem of oxygen transport to tissue, an infinitely permeable capillary wall is considered and eqn. (4.17) must be replaced by

$$c(R,z) = C(z) , \quad 0 \leq z \leq 1 . \quad (4.38)$$

It can be shown that the corresponding solutions $C(z)$ and $c(r,z)$ for the linear problem of oxygen transport to tissue are obtained directly from eqns. (4.36) and (4.37) by setting $1/h = 0$ and using q^* instead of q in the definition of non-dimensional parameter β. We have

$$C(z) = 1 + \frac{M}{2\beta^*}\left(R - \frac{1}{R}\right)z + \sum_{n=1}^{\infty} \frac{2a_n u_n}{\beta^* n\pi v_n} \sin(n\pi z) , \quad (4.39)$$

and

$$c(r,z) = \int_0^1 C(\zeta)d\zeta + \frac{M}{2}\left(\frac{r^2}{2} - \ell n\ r - \frac{R^2}{2} + \ell n\ R\right) + \sum_{n=1}^{\infty} \frac{2a_n}{v_n}\left[K_1(\rho_n)I_o(\rho_n r)+I_1(\rho_n)K_o(\rho_n r)\right]\cos(n\pi z) , \quad (4.40)$$

where a_n are the solutions of an infinite set of

linear algebraic equations

$$a_n = b_n + \sum_{k=1}^{\infty} e_{nk} a_k \ , \quad n=1,2,3,\ldots \ , \tag{4.41}$$

with

$$a_n = \int_o^1 C(z)\cos(n\pi z)dz \ , \tag{4.42}$$

$$b_n = \begin{cases} 0 \ , & n=2i \ , \quad i=1,2,\ldots \ , \\ -\dfrac{M}{\beta^* n^2 \pi^2}\left(R - \dfrac{1}{R}\right), & n=2i-1 \ , \quad i=1,2,\ldots \ , \end{cases} \tag{4.43}$$

$$e_{nk} = \begin{cases} 0 \ , & n=k \ \text{ or } \ n+k \ \text{ even} \\ \dfrac{4u_n}{\beta^* v_n (k^2-n^2)\pi^2} \ , & n+k \ \text{ odd} \ , \end{cases} \tag{4.4}$$

$$\beta^* = \frac{q^*}{2\pi R D_r L} \ , \tag{4.45}$$

and

$$\int_o^1 C(\zeta)d\zeta = 1 + \frac{M}{4\beta^*}\left(R - \frac{1}{R}\right) + \sum_{n=1}^{\infty} \frac{2a_n u_n}{\beta^* (n\pi)^2 v_n}\left[1-\cos(n\pi)\right] \ , \tag{4.46}$$

is used in eqn. (4.40).

4.2. Numerical Results and Discussion

Numerical examples will be presented for a 110 μm diameter Krogh cylinder surrounding a 10 μm diameter capillary 1000 μm long. The axial and radial diffusivities are both 900 $\mu m^2/sec$, and the capillary blood flow rate is 3.1416×10^4 $\mu m^3/sec$. To determine the normalized concentrations $C(z)$ and $c(r,z)$, it is necessary only to specify the ratio M_o/C_A , and not both quantities separately. The examples correspond to $M_o/C_A = 0.002$ sec^{-1} .

The results are illustrated for a range of capillary permeabilities, including an infinitely permeable capillary wall. It can be shown that the solution for infinite h is obtained directly from the above solution for finite h simply by setting $1/h = 0$. Some available data on capillary permeability for certain substrates can be found in Landis and Pappenheimer (1963) and Crone and Lassen (1970).

Figure 4 shows the substrate concentration in the capillary for various values of H . In all cases, $C = 0.4$ at $z=1$, since the amount of substrate consumed is independent of the capillary permeability. For the large values of H , the concentration decreases more rapidly at the arterial end. The more permeable

capillary permits a rapid entry of substrate into the capillary at the arterial end, and this substrate reaches other regions of the tissue by axial diffusion. The limiting case $H=\infty$ is approximated fairly closely by the solution for finite H when $H > 50$ μm/sec .

Figures 5-7 show the tissue concentration, as a function of axial position, at the capillary wall, midway between the capillary wall and the outer edge of the Krogh cylinder, and at the outer edge of the Krogh cylinder, respectively. The concentration decreases with decreasing H , since less substrate enters the tissue when the endothelium of the capillary wall is less permeable. At a value slightly less than $H=2$, the substrate concentration becomes negative over some portion of the tissue. Since this is physically impossible, the solutions obtained are not valid for such values of H . Below some critical value of capillary permeability, it is impossible for sufficient substrate to enter the capillary to be consumed at the uniform rate M_o . A new solution must be obtained in which regions with zero substrate concentration appear in the tissue. An approximate analysis of this type has been given recently for oxygen transport to tissue (Salathé and Beaudet 1978).

The concentration profiles show zero slope at $z=0$

and $z=1$, in accordance with the boundary conditions, eqns. (4.15) and (4.16). An exception occurs at $r=R$ for $H=\infty$, since $c(R,z) = C(z)$, and $z=0,1$, $r=R$ are singular points for this solution.

Figures 8-10 show the concentration profiles as a function of radial position, at $z=0$, $z=0.3$ and $z=1.0$. These profiles are rather flat, as a result of the relatively large tissue diffusivity. Not only does large diffusivity permit radial diffusion into the tissue from the capillary to occur at low concentration gradients, but also permits substrate delivery by axial diffusion from the arterial end. When the diffusivity is low, the radial gradients are steeper. However, each section of the capillary then supplies substrate mainly to the tissue surrounding it at that location, since axial diffusion is of less significance. The result is an approximately linear profile in the capillary. This can be seen in figure 11, for fixed permeability $H=50$ μm/sec and varying tissue diffusivity. The capillary substrate concentration for $D_r=D_z=900$ $\mu m^2/sec$ has been shown in figure 4. Decreasing the diffusivity to 300 $\mu m^2/sec$ results in a concentration profile in the capillary that is approximately linear. Increasing the diffusivity to 2700 $\mu m^3/sec$ results in a rapid decrease in concentration at the arterial end.

Much of the substrate leaves the capillary at the arterial end and is delivered to the tissue through axial diffusion. In all three cases, $C=0.4$ at $z=1$, since the amount of substrate consummed is independent of tissue diffusivity.

Since the solution is obtained as an infinite series, it must be truncated after a finite number of terms for numerical computations. In addition, the truncation of the infinite set of algebraic equations at N terms, leading to eqn. (4.34), means that the N numbers $\hat{a}_n$ only approximate the correct values a_n. Therefore, the accuracy of the solution should be examined. Since all of the governing equations except eqn. (4.17) are satisfied exactly, the error can be determined by calculating

$$\left| \frac{\frac{\partial c}{\partial r}\Big|_{r=R} + h[C(z)-c(R,z)]}{h[C(z)-c(R,z)]} \right| .$$

In the example shown, 100 terms were used in the expansion. and the error was exceedingly small. Only at $z=0$, for $H=\infty$, did the error rise to a few percent. By choosing $N=120$, the above ratio was 4.7×10^{-2} at this singular point, but at $z=0.01$, it had already decreased to 6.2×10^{-4}.

The solutions $C(z)$ and $c(r,z)$, from eqns. (4.39) and (4.40), respectively, for the linear problem of

oxygen transport to tissue will be presented in section 6.1, figures 20-25, and compared with the method of solution which is used in solving oxygen transport with nonlinear oxyhemoglobin dissociation relationship. The analysis of nonlinear problem of oxygen transport will be presented in the next section.

5. NONLINEAR PROBLEM

Although linearizing the oxyhemoglobin dissociation relationship for the oxygen transport problem makes the mathematics tractable, the results do not describe important characteristics of oxygen transport. According to the oxyhemoglobin dissociation relationship, fig. 2, a significant drop in blood oxygen concentration occurs at the beginning of the capillary for a high incoming arterial oxygen concentration. As blood oxygen concentration decreases, more oxygen is released from hemoglobin, slowing the drop of blood oxygen concentration. Using the linear oxyhemoglobin relationship, this phenomena can not be described properly (see the results of Davis et al. 1974). Therefore, a nonlinear oxyhemoglobin dissociation relationship (see Roughton 1964, Lambertsen 1974) must be used, and the mathematical model for the steady state oxygen transport to tissue discussed in section 4 becomes a nonlinear problem. The analysis is much more difficult than the linear problem, and the method used in section 4 results in a complicated nonlinear Fredholm integral equation, where the reduction to an infinite set of linear algebraic equations cannot be applied. The analysis will be more complicated when we consider axial diffusion in the capillary. No analytical solutions have been

obtained for such a model including axial diffusion and nonlinear oxyhemoglobin dissociation relationship, even for the steady state problem. Based on the geometrical property of the Krogh cylinder and the diffusional nature in the tissue, the analytical solutions for this nonlinear problem can be obtained by using perturbation methods. This method will be presented in the present section.

Axial diffusion in the capillary is generally less important than axial diffusion in the tissue, but it can be included in the present analysis without any difficulty. Therefore, the governing equations for this nonlinear problem of steady state oxygen transport to tissue are

$$D_r \frac{1}{\bar{r}} \frac{\partial}{\partial \bar{r}} \bar{r} \frac{\partial c_t}{\partial \bar{r}} + D_z \frac{\partial^2 c_t}{\partial \bar{z}^2} = M_o \ , \quad R_c \le \bar{r} \le R_t \ , \quad 0 \le \bar{z} \le L \ , \tag{5.1}$$

$$\left. \frac{\partial c_t}{\partial \bar{r}} \right|_{\bar{r}=R_t} = 0 \ , \quad 0 \le \bar{z} \le L \ , \tag{5.2}$$

$$\left. \frac{\partial c_t}{\partial \bar{z}} \right|_{\bar{z}=0} = 0 \ , \quad R_c \le \bar{r} \le R_t \ , \tag{5.3}$$

$$\left. \frac{\partial c_t}{\partial \bar{z}} \right|_{\bar{z}=L} = 0 \ , \quad R_c \le \bar{r} \le R_t \ , \tag{5.4}$$

$$c_t(R_c, \bar{z}) = C_b(\bar{z}) \ , \quad 0 \le \bar{z} \le L \ , \tag{5.5}$$

$$q \frac{d}{d\bar{z}} [C_b + \bar{Q} S^*(C_b)] = 2\pi R_c D_r \left. \frac{\partial c_t}{\partial \bar{r}} \right|_{\bar{r}=R_c} + \pi R_c^2 D_b \frac{d^2 C_b}{d\bar{z}^2} \ , \quad 0 \le \bar{z} \le L \tag{5.6}$$

$$C_b(0) = C_A \ , \qquad (5.7)$$

where the oxyhemoglobin dissociation relationship, $S^*(C_b)$, is considered to be a nonlinear function of blood oxygen concentration, C_b . Reneau et al. (1967, 1969, 1970), Hyman (1973), Hyman et al. (1975) used the empirical formula for $S^*(C_b)$ which is given by eqn. (2.1), while Middleman (1972), Fletcher (1975, 1976) used a graphical representation. Lambertsen (1974) suggested a more complicated formula for $S^*(C_b)$,

$$S^*(C_b) = \frac{\left(\frac{1+W_1 C_b}{W_1 C_b}\right)^3 + W_2 - 1}{\left(\frac{1+W_1 C_b}{W_1 C_b}\right)^4 + W_2 - 1} \ , \qquad (5.8)$$

where W_1 and W_2 are constants and depend on the pH, carbon dioxide concentration, and temperature of the blood. The particular form of this nonlinear relationship makes no difference in the present analysis.

5.1. Method of Solution

In terms of the non-dimensional variables $C = \frac{C_b}{C_A}$, $c = \frac{c_t}{C_A}$, $r = \frac{\bar{r}}{R_t}$ and $z = \frac{\bar{z}}{L}$, the governing equations (5.1)-(5.7) become

$$\frac{1}{r}\frac{\partial}{\partial r} r \frac{\partial c}{\partial r} + \varepsilon^2 \frac{\partial^2 c}{\partial z^2} = M , \quad R \le r \le 1 , \quad 0 \le z \le 1 , \tag{5.9}$$

$$\left.\frac{\partial c}{\partial r}\right|_{r=1} = 0 , \quad 0 \le z \le 1 , \tag{5.10}$$

$$\left.\frac{\partial c}{\partial z}\right|_{z=0} = 0 , \quad R \le r \le 1 , \tag{5.11}$$

$$\left.\frac{\partial c}{\partial z}\right|_{z=1} = 0 , \quad R \le r \le 1 , \tag{5.12}$$

$$c(R,z) = C(z) , \quad 0 \le z \le 1 , \tag{5.13}$$

$$\beta \frac{d}{dz}[C+QS(C)] = \left.\frac{\partial c}{\partial r}\right|_{r=R} + \varepsilon^2 \delta \frac{d^2 C}{dz^2} , \quad 0 \le z \le 1 , \tag{5.14}$$

$$C(0) = 1 , \tag{5.15}$$

where

$$\varepsilon = \frac{R_t}{L}\sqrt{\frac{D_z}{D_r}} , \quad R = \frac{R_c}{R_t} , \quad M = \frac{R_t^2 M_o}{D_r C_A} ,$$

$$\beta = \frac{q}{2\pi D_r L R} , \quad Q = \frac{\bar{Q}}{C_A} , \quad \delta = \frac{R D_b}{2 D_z} ,$$

and

$$S(C) = S^*(C_A C) .$$

The Krogh cylinder is an appropriate model for

capillary beds consisting of regular parallel arrays of vessels, in which the distance separating the capillaries is small compared to their length. The Krogh cylinder is therefore long and slender and ε is a small parameter. Alternatively, when the tissue axial oxygen diffusivity is small compared to the tissue radial oxygen diffusivity, ε is small. The parameter ε therefore indicates geometric and diffusional properties of the Krogh cylinder. The above eqns. (5.9)-(5.15) may be solved for small ε by using perturbation methods (Cole 1968, Van Dyke 1975). The dominant behavior is found by setting $\varepsilon=0$, and corresponds to neglecting axial diffusion in the tissue and the capillary; the higher order terms in the expansion give the effect of axial diffusion. Previously, analytical solutions have been obtained only by neglecting the axial diffusion terms (Hyman 1973). Although Blum (1960) and Davis et al. (1974) attempted to obtain the analytical solution including axial diffusion in the tissue, they failed to include the nonlinear oxyhemoglobin dissociation relationship in their model. As pointed out in section 4, Blum's method of solution was incorrect.

For extremely small capillary spacing, neglecting axial diffusion provides a sufficiently good approximation, but significant errors will be introduced for

less dense capillary networks. In this section, the effect of axial diffusion will be examined analytically, and it will be possible to ascertain when these effects can be neglected and when they must be taken into account.

The solutions for $C(z)$ and $c(r,z)$ will be obtained in the form of an asymptotic series, applicable for small ε :

$$C(z;\varepsilon) \sim C_o(z) + \varepsilon^2 C_1(z) + \ldots , \qquad (5.16)$$

$$c(r,z;\varepsilon) \sim c_o(r,z) + \varepsilon^2 c_1(r,z) + \ldots . \qquad (5.17)$$

The oxyhemoglobin dissociation relationship $S(C)$ can also be expanded in the form of asymptotic series by using the Taylor series expansion,

$$S(C;\varepsilon) \sim S(C_o) + \varepsilon^2 C_1 S'(C_o) + \ldots . \qquad (5.18)$$

The leading terms, C_o and c_o , satisfy eqns. (5.9) and (5.14) with $\varepsilon=0$. Therefore the equations for $C_o(z)$ and $c_o(r,z)$ are

$$\frac{1}{r}\frac{\partial}{\partial r} r \frac{\partial c_o}{\partial r} = M , \quad R \le r \le 1 , \quad 0 \le z \le 1 , \qquad (5.19)$$

$$\left.\frac{\partial c_o}{\partial r}\right|_{r=1} = 0 , \quad 0 \le z \le 1 , \qquad (5.20)$$

$$c_o(R,z) = C_o(z) , \quad 0 \le z \le 1 , \qquad (5.21)$$

$$\beta \frac{d}{dz}\left[C_o+QS(C_o)\right] = \left.\frac{\partial c_o}{\partial r}\right|_{r=R} , \quad 0\leq z\leq 1 , \qquad (5.22)$$

$$C_o(0) = 1 . \qquad (5.23)$$

The solution to eqns. (5.19)-(5.21) is

$$c_o(r,z) = C_o(z) + \frac{M}{2}\left(\frac{r^2}{2} - \ell n\ r - \frac{R^2}{2} + \ell n\ R\right) . \qquad (5.24)$$

Substituting this into eqn. (5.22) and using the boundary condition, eqn. (5.23), it follows that

$$C_o + QS(C_o) = \frac{M}{2\beta}\left(R - \frac{1}{R}\right)z + 1 + QS(1) . \qquad (5.25)$$

Eqn. (5.25) gives z explicitly in terms of C_o. For any choice of $S(C_o)$, $z(C_o)$ can be computed, starting at $C_o=1$, where $z=0$, and continuing until $z=1$ is obtained. It can be shown that this function is monotonic, and so gives, by inversion, the function $C_o(z)$. In the absence of a region of anoxia (and therefore failure of metabolism) in the Krogh cylinder, eqn. (5.25) may be used as a simple mass balance equation to determine the venous end oxygen concentration (Lightfoot 1973).

Equations for $C_1(z)$ and $c_1(r,z)$ are obtained by substituting the expansions, eqns. (5.16)-(5.18), into eqns. (5.9), (5.10), (5.13)-(5.15) and retaining terms of order ε^2. This gives

$$\frac{1}{r}\frac{\partial}{\partial r}\, r\, \frac{\partial c_1}{\partial r} = -\frac{\partial^2 c_o}{\partial z^2} \quad , \quad R \le r \le 1 \quad , \quad 0 \le z \le 1 \quad , \tag{5.26}$$

$$\left.\frac{\partial c_1}{\partial r}\right|_{r=1} = 0 \quad , \quad 0 \le z \le 1 \quad , \tag{5.27}$$

$$c_1(R,z) = C_1(z) \quad , \quad 0 \le z \le 1 \quad , \tag{5.28}$$

$$\beta \frac{d}{dz}\left[C_1 + QC_1 S'(C_o)\right] = \left.\frac{\partial c_1}{\partial r}\right|_{r=R} + \delta \frac{d^2 C_o}{dz^2} \quad , \quad 0 \le z \le 1 \quad , \tag{5.29}$$

$$C_1(0) = 0 \quad , \tag{5.30}$$

respectively, and includes the axial diffusion terms. The solution to eqn. (5.26) is easily found, using the boundary conditions, eqns. (5.27) and (5.28), to be

$$c_1(r,z) = C_1(z) - \frac{C_o''(z)}{2}\left(\frac{r^2}{2} - \ell n\ r - \frac{R^2}{2} + \ell n\ R\right), \tag{5.31}$$

where $C_o(z)$ is already known from eqn. (5.25). Substituting this into eqn. (5.29) and integrating with respect to z gives

$$C_1(z)\left[1+QS'(C_o(z))\right] - C_1(0)\left[1+QS'(1)\right] = \frac{1}{\beta}\left[\delta - \frac{1}{2}\left(R - \frac{1}{R}\right)\right]\left[C_o'(z) - C_o'(0)\right] \quad . \tag{5.32}$$

Using the boundary condition, eqn. (5.30), in eqn. (5.32) completes the solution for $C_1(z)$. It is not correct to use this boundary condition, however, because the solutions obtained in the form of the expansion given by eqns. (5.16) and (5.17) are not

valid at the end $z=0$. The assumption that axial diffusion is a small effect which can be included as a perturbation method is not correct at the ends of Krogh cylinder $z=0$ and $z=1$.

It has not been possible in the present analysis to satisfy the boundary condition expressed by eqns. (5.11) and (5.12), and the solution $c_o(r,z)+\varepsilon^2 c_1(r,z)$ gives non-zero oxygen flux through the ends of the cylinder. In the end regions the character of the solution changes radically from that obtained above, and radial and axial diffusion are of equal importance.

In order to determine the unknown constant $C_1(0)$ and complete the solution for $C_1(z)$, eqn. (5.32), it is necessary to examine the solution in the region near $z=0$. The procedure for doing this involves the technique of matched asymptotic expansions (Cole 1968, Van Dyke 1975). The expansion must be joined in an appropriate sense to the solution already obtained for the region bounded away from the ends. The matching of the two expansions will yield the required constant $C_1(0)$.

5.2. The Boundary Layer Solution Near $z=0$

The solutions obtained in section 5.1 are based on the assumption that as $\varepsilon \to 0$ axial diffusion becomes negligible compared to radial diffusion. This assumption is valid everywhere except near the ends, where no matter how small ε is, there always exists a narrow region, or boundary layer, in which radial and axial diffusion are of equal importance. In these regions, the character of the solution is entirely different from that already obtained and satisfied the boundary condition of no flux through the ends of the Krogh cylinder. The solutions in these regions must joint smoothly at the outer edge of the boundary layers to the solutions obtained previously.

The boundary layer at the arterial end occupies a vanishing small region about $z=0$ in the limit $\varepsilon \to 0$. Therefore, it cannot be described in terms of physical variable z, since no matter how small z is, it is possible to choose ε sufficiently small that z is not in the boundary layer. The appropriate boundary layer variable is $Z = \frac{z}{\varepsilon}$, which has the property $z \to 0$ as $\varepsilon \to 0$ for fixed Z. In terms of this variable the governing equations (5.9) and (5.14) are

$$\frac{1}{r}\frac{\partial}{\partial r} r \frac{\partial \bar{c}}{\partial r} + \frac{\partial^2 \bar{c}}{\partial Z^2} = M , \quad R \leq r \leq 1 , \quad Z \geq 0 , \qquad (5.33)$$

$$\beta \frac{d}{dZ} [\bar{C}+QS(\bar{C})] = \varepsilon \left.\frac{\partial \bar{c}}{\partial r}\right|_{r=R} + \varepsilon\delta \frac{d^2\bar{C}}{dZ^2} , \quad Z\geq 0 , \quad (5.34)$$

where $\bar{C}(Z) = C(\varepsilon Z)$ and $\bar{c}(r,Z) = c(r,\varepsilon Z)$. In these variables, the radial and axial diffusion terms in eqn. (5.33) are of equal importance. The boundary conditions are

$$\left.\frac{\partial \bar{c}}{\partial r}\right|_{r=1} = 0 , \quad Z\geq 0 , \quad (5.35)$$

$$\left.\frac{\partial \bar{c}}{\partial Z}\right|_{Z=0} = 0 , \quad R\leq r\leq 1 , \quad (5.36)$$

$$\bar{c}(R,Z) = \bar{C}(Z) , \quad Z\geq 0 , \quad (5.37)$$

$$\bar{C}(0) = 1 . \quad (5.38)$$

These must be supplemented by the requirements imposed by matching these solutions with the solutions obtained earlier. The matching conditions are

$$\bar{C}\to C , \quad \bar{c}\to c , \quad \text{as} \quad Z\to\infty . \quad (5.39)$$

In order to construct solutions to these equations in the form of an asymptotic series in ε which join properly to the previous solutions, it is necessary to examine the behavior of those solutions as $z\to 0$. Since $z\to 0$ is equivalent to the limit $\varepsilon\to 0$, Z fixed (c.f. $z=\varepsilon Z$), this can be done by rewriting the solutions $C_o+\varepsilon^2 C_1$, $c_o+\varepsilon^2 c_1$ in terms of r and Z , and

expanding the results in a series in ε (Taylor series expansion at $z=0$). This gives

$$C \sim 1 + \varepsilon\alpha Z + \varepsilon^2[\phi Z^2 + C_1(0)] + O(\varepsilon^3) , \quad (5.40)$$

$$c \sim 1 + \frac{M}{2}\left(\frac{r^2}{2} - \ell n\ r - \frac{R^2}{2} + \ell n\ R\right) + \varepsilon\alpha Z + \varepsilon^2\left[\phi Z^2 + C_1(0) - \frac{C_o''(0)}{2}\left(\frac{r^2}{2} - \ell n\ r - \frac{R^2}{2} + \ell n\ R\right)\right] + O(\varepsilon^3) , \quad (5.41)$$

where

$$\alpha = \frac{M\left(R - \frac{1}{R}\right)}{2\beta[1+QS'(1)]} = C_o'(0) , \quad (5.42)$$

$$\phi = -\frac{\alpha^2 QS''(1)}{2[1+QS'(1)]} = \frac{C_o''(0)}{2} . \quad (5.43)$$

It follows from these expressions that the boundary layer expansions for $\bar{C}(Z)$ and $\bar{c}(r,Z)$ are of the form

$$\bar{C} \sim 1 + \varepsilon\alpha Z + \varepsilon^2 P(Z) , \quad (5.44)$$

$$\bar{c} \sim 1 + \frac{M}{2}\left(\frac{r^2}{2} - \ell n\ r - \frac{R^2}{2} + \ell n\ R\right) + \varepsilon U(r,Z) + \varepsilon^2 V(r,Z) , \quad (5.45)$$

where equations and boundary conditions for P, U and V are found by substituting eqns. (5.44) and (5.45) into eqns. (5.33)-(5.38), comparing eqns. (5.40)-(5.41) and eqns. (5.44)-(5.45) and using eqn. (5.39) yields the matching conditions for P, U and V. We then have the following problem:

(I) $$\beta \frac{d}{dZ}\left[P(Z)(1+QS'(1))+\frac{1}{2}\alpha^2 Z^2 QS''(1)\right] = \left.\frac{\partial U}{\partial r}\right|_{r=R}, \quad Z\geq 0 , \tag{5.46}$$

$$P(0) = 0 , \tag{5.47}$$

with the matching condition

$$P(Z) \to \phi Z^2 + C_1(0) , \quad \text{as} \quad Z\to\infty . \tag{5.48}$$

(II) $$\frac{1}{r}\frac{\partial}{\partial r} r \frac{\partial U}{\partial r} + \frac{\partial^2 U}{\partial Z^2} = 0 , \quad R\leq r\leq 1 , \quad Z\geq 0 , \tag{5.49}$$

$$\left.\frac{\partial U}{\partial r}\right|_{r=1} = 0 , \quad Z\geq 0 , \tag{5.50}$$

$$\left.\frac{\partial U}{\partial Z}\right|_{Z=0} = 0 , \quad R\leq r\leq 1 , \tag{5.51}$$

$$U(R,Z) = \alpha Z , \quad Z\geq 0 , \tag{5.52}$$

matching condition:

$$U(r,Z) \to \alpha Z , \quad \text{as} \quad Z\to\infty , \quad R\leq r\leq 1 . \tag{5.53}$$

(III) $$\frac{1}{r}\frac{\partial}{\partial r} r \frac{\partial V}{\partial r} + \frac{\partial^2 V}{\partial Z^2} = 0 , \quad R\leq r\leq 1 , \quad Z\geq 0 , \tag{5.54}$$

$$\left.\frac{\partial V}{\partial r}\right|_{r=1} = 0 , \quad Z\geq 0 , \tag{5.55}$$

$$\left.\frac{\partial V}{\partial Z}\right|_{Z=0} = 0 , \quad R\leq r\leq 1 , \tag{5.56}$$

$$V(R,Z) = P(Z) , \quad Z\geq 0 , \tag{5.57}$$

matching condition:

$$V(r,Z) \to \phi Z^2 + C_1(0) - \frac{C_o''(0)}{2}\left(\frac{r^2}{2} - \ell n\ r - \frac{R^2}{2} + \ell n\ R\right) ,$$

$$\text{as } Z\to\infty , \quad R\le r\le 1 . \qquad (5.58)$$

Eqns. (5.46) and (5.47) of Problem (I) can be solved for $P(Z)$, and the solution is

$$P(Z) = \phi Z^2 + \frac{1}{\beta[1+QS'(1)]} \int_o^Z \left.\frac{\partial U(r,\zeta)}{\partial r}\right|_{r=R} d\zeta . \qquad (5.59)$$

Substituting eqn. (5.59) into eqn. (5.48), we have

$$C_1(0) = \frac{1}{\beta[1+QS'(1)]} \int_o^\infty \left.\frac{\partial U}{\partial r}\right|_{r=R} dZ , \qquad (5.60)$$

where $U(r,Z)$ is the solution of problem (II). It is therefore necessary to solve problem (II) for U, which is defined on the semi-infinite strip $Z\ge 0$, $R\le r\le 1$. By introducing

$$U(r,Z) = \alpha Z + \alpha u(r,Z) \qquad (5.61)$$

into problem (II), we have

$$\frac{1}{r}\frac{\partial}{\partial r}\, r\, \frac{\partial u}{\partial r} + \frac{\partial^2 u}{\partial Z^2} = 0 , \quad R\le r\le 1 , \quad Z\ge 0 , \qquad (5.62)$$

$$\left.\frac{\partial u}{\partial r}\right|_{r=1} = 0 , \quad Z\ge 0 , \qquad (5.63)$$

$$\left.\frac{\partial u}{\partial Z}\right|_{Z=0} = -1 , \quad R\le r\le 1 , \qquad (5.64)$$

$$u(R,Z) = 0 , \quad Z\ge 0 , \qquad (5.65)$$

$$u(r,Z) \to 0 , \quad \text{as } Z\to\infty , \quad R\le r\le 1 . \qquad (5.66)$$

A solution to this problem can be obtained by an eigenfunction expansion of the composite Bessel functions. The solution for $U(r,Z)$ is

$$u(r,Z) = -4\pi \sum_{n=1}^{\infty} \frac{\Psi_n(r)e^{-\lambda_n Z}}{\lambda_n^3\pi^2\Psi_n^2(1)-4\lambda_n} , \qquad (5.67)$$

where eigenfunctions $\Psi_n(r)$ are defined in terms of the Bessel functions J_o and Y_o by

$$\Psi_n(r) = Y_o(\lambda_n R)J_o(\lambda_n r) - J_o(\lambda_n R)Y_o(\lambda_n r) , \quad n=1,2,3,... \qquad (5.68)$$

and the eigenvalues λ_n , $n=1,2,3,...$, are the roots of

$$J_o(\lambda R)Y_1(\lambda) - Y_o(\lambda R)J_1(\lambda) = 0 . \qquad (5.69)$$

Here, J_o, Y_o and J_1, Y_1 are zero and first order of the first and second kind of Bessel functions, respectively. It has been shown (Watson 1952) that eqn. (5.69) has no imaginary or repeated roots, and it has an infinite number of positive roots, λ_n , $n=1,2,3,...$. These roots do not exist in the literature for the values of R which are of physiological interest, except for a few that were calculated and presented by Apelblat et al. (1974). In our numerical examples, additional eigenvalues will be calculated and used for different values of R .

Substituting eqn. (5.67) into eqn. (5.61) gives

$$U(r,Z) = \alpha Z - 4\pi\alpha \sum_{n=1}^{\infty} \frac{\Psi_n(r)e^{-\lambda_n Z}}{\lambda_n^3\pi^2\Psi_n^2(1)-4\lambda_n} . \quad (5.70)$$

The integrations in eqns. (5.59) and (5.60) can be calculated by using eqn. (5.70) and the property

$$\left.\frac{d\Psi_n(r)}{dr}\right|_{r=R} = -\frac{2}{\pi R} , \quad \text{for all eigenvalues } \lambda_n . \quad (5.71)$$

This property can be found in Watson (1952). We have

$$\int_o^Z \left.\frac{\partial U(r,\zeta)}{\partial r}\right|_{r=R} d\zeta = 8\alpha \sum_{n=1}^{\infty} A_n\left(1-e^{-\lambda_n Z}\right) , \quad (5.72)$$

and

$$\int_o^{\infty} \left.\frac{\partial U}{\partial r}\right|_{r=R} dZ = 8\alpha \sum_{n=1}^{\infty} A_n , \quad (5.73)$$

where

$$A_n = (R\pi^2\lambda_n^4\Psi_n^2(1)-4R\lambda_n^2)^{-1} . \quad (5.74)$$

Substituting these into eqn. (5.59) and (5.60), yields

$$P(Z) = \phi Z^2 + C_1(0) - \frac{4M\left(R-\frac{1}{R}\right)}{\beta^2[1+QS'(1)]^2} \sum_{n=1}^{\infty} A_n e^{-\lambda_n Z} \quad (5.75)$$

and

$$C_1(0) = \frac{4M\left(R-\frac{1}{R}\right)}{\beta^2[1+QS'(1)]^2} \sum_{n=1}^{\infty} A_n . \quad (5.76)$$

Eqn. (5.76) provides the required constant $C_1(0)$.

To solve problem (III) for the higher order tissue

boundary layer solution $V(r,Z)$, which is defined on the semi-infinite strip $Z \geq 0$, $R \leq r \leq 1$, it is necessary to introduce a proper transformation which is of the form

$$V(r,Z) = v(r,Z) + \phi Z^2 + C_1(0) - \xi \sum_{n=1}^{\infty} A_n e^{-\lambda_n Z} - \phi\left(\frac{r^2}{2} - \ell n\ r - \frac{R^2}{2} + \ell n\ R\right) , \qquad (5.77)$$

where

$$\xi = \frac{4M\left(R - \frac{1}{R}\right)}{\beta^2[1+QS'(1)]^2} . \qquad (5.78)$$

Applying eqns. (5.43), (5.75), (5.77) and (5.78) to problem (III) yields Poisson's equation for $v(r,Z)$:

$$\frac{1}{r}\frac{\partial}{\partial r} r \frac{\partial v}{\partial r} + \frac{\partial^2 v}{\partial Z^2} = \xi \sum_{n=1}^{\infty} \lambda_n^2 A_n e^{-\lambda_n Z} , \quad R \leq r \leq 1 , \quad Z \geq 0 , \qquad (5.79)$$

with homogeneous boundary conditions with respect to radial direction

$$\left.\frac{\partial v}{\partial r}\right|_{r=1} = 0 , \quad Z \geq 0 , \qquad (5.80)$$

$$v(R,Z) = 0 , \quad Z \geq 0 , \qquad (5.81)$$

and inhomogeneous boundary condition at $Z=0$

$$\left.\frac{\partial v}{\partial Z}\right|_{Z=0} = -\xi \sum_{n=1}^{\infty} \lambda_n A_n , \quad R \leq r \leq 1 , \qquad (5.82)$$

$$\text{as} \quad Z \to \infty , \quad R \leq r \leq 1 , \quad v(r,Z) \to 0 . \qquad (5.83)$$

Since the boundary condition are homogeneous in

the r direction, a solution in the form of an eigenfunction expansion with respect to r for the related homogeneous problem can be found similarly to the solution $u(r,Z)$. It is proposed to find a solution of Poisson's equation (5.79) with eqns. (5.80)-(5.83) in the form of a series of the form eqn. (5.67), but in which the function $e^{-\lambda_n Z}$ are replaced by a more general function $E_n(Z)$. The solution will be a series

$$v(r,Z) = \sum_{k=1}^{\infty} E_k(Z)\Psi_k(r) \ . \qquad (5.84)$$

The orthogonality property of the eigenfunctions $\Psi_k(r)$ are (see appendix B)

$$\int_R^1 r\Psi_m(r)\Psi_n(r)dr = 0 \ , \quad \text{for} \quad m\neq n \ , \qquad (5.85)$$

and

$$\int_R^1 r\Psi_k^2(r)dr = \frac{1}{2}\left[\Psi_k^2(1) - \frac{4}{\lambda_k^2\pi^2}\right] , \quad k=1,2,3,\ldots$$

$$= (\Phi_k)^{-1} \ . \qquad (5.86)$$

Applying this orthogonality property to eqn. (5.84), the coefficient functions $E_k(Z)$ are related to the (still unknown) solution $v(r,Z)$ by the formula

$$E_k(Z) = \Phi_k \int_R^1 rv(r,Z)\Psi_k(r)dr \ . \qquad (5.87)$$

Assuming that $\frac{\partial^2 v}{\partial Z^2}$ is a continuous function in the region $R\leq r\leq 1$, $Z\geq 0$, we obtain, referring to eqn. (5.79),

$$E_k''(Z) = -\Phi_k \int_R^1 \frac{\partial}{\partial r} r \frac{\partial v}{\partial r} \Psi_k(r)dr + \Phi_k\left(\xi \sum_{n=1}^{\infty} \lambda_n^2 A_n e^{-\lambda_n Z}\right)\int_R^1 r\Psi_k(r)dr \ . \qquad (5.88)$$

It can be shown that (see appendix B)

$$\int_R^1 r\Psi_k(r)dr = -\frac{2}{\lambda_k^2 \pi} \ . \qquad (5.89)$$

The first term on the right hand side of eqn. (5.88) will be transformed by using Green's formula and applying the homogeneous boundary conditions and the properties of eigenfunctions $\Psi_k(r)$. We have

$$-\Phi_k \int_R^1 \frac{\partial}{\partial r} r \frac{\partial v}{\partial r} \Psi_k(r)dr = \lambda_k^2 \Phi_k \int_r^1 rv(r,Z)\Psi_k(r)dr = \lambda_k^2 E_k(Z) \ , \qquad (5.90)$$

where eqn. (5.87) for $E_k(Z)$ is used.

Substituting eqns. (5.89) and (5.90) into eqn. (5.88) gives a second order nonhomogeneous ordinary differential equation for $E_k(Z)$

$$E_k''(Z) - \lambda_k^2 E_k(Z) = -\frac{2\xi\Phi_k}{\lambda_k^2 \pi} \sum_{n=1}^{\infty} \lambda_n^2 A_n e^{-\lambda_n Z} \ . \qquad (5.91)$$

The general solution for eqn. (5.91) is

$$E_k(Z) = C_k^{(1)} e^{\lambda_k Z} + C_k^{(2)} e^{-\lambda_k Z} - \frac{2\xi\Phi_k}{\lambda_k^2 \pi} \sum_{\substack{n=1 \\ n\neq k}}^{\infty} \frac{\lambda_n^2 A_n}{\lambda_n^2 - \lambda_k^2} e^{-\lambda_n Z} + \frac{\xi\Phi_k A_k}{\lambda_k \pi} Ze^{-\lambda_k Z} \ , \qquad (5.92)$$

where $C_k^{(1)}$ and $C_k^{(2)}$ are arbitrary constants and will be determined by boundary conditions. Taking the limit of eqn. (5.87) as $Z\to\infty$, we see that

$$\lim_{Z\to\infty} E_k(Z) = \lim_{Z\to\infty} \Phi_k \int_R^1 rv(r,Z)\Psi_k(r)dr$$

$$= \Phi_k \int_R^1 r\left(\lim_{Z\to\infty} v(r,Z)\right)\Psi_k(r)dr \ . \qquad (5.93)$$

Applying the boundary condition, eqn. (5.83), to eqn. (5.93) gives

$$\lim_{Z\to\infty} E_k(Z) = 0 \ . \qquad (5.94)$$

Applying this property to eqn. (5.92) gives

$$C_k^{(1)} \equiv 0 \ . \qquad (5.95)$$

Differentiating eqn. (5.87) at $Z=0$ yields

$$E_k'(0) = \Phi_k \int_R^1 r\left(\frac{\partial v}{\partial Z}\Big|_{Z=0}\right)\Psi_k(r)dr \ . \qquad (5.96)$$

Applying the boundary condition, eqn. (5.82), to eqn. (5.96) and using eqn. (5.89), gives

$$E_k'(0) = \frac{2\xi\Phi_k}{\lambda_k^2\pi} \sum_{n=1}^{\infty} \lambda_n A_n$$

or

$$E_k'(0) = \frac{2\xi\Phi_k}{\lambda_k^2\pi} \sum_{\substack{n=1 \\ n\neq k}}^{\infty} \lambda_n A_n + \frac{2\xi\Phi_k A_k}{\lambda_k \pi} \ . \qquad (5.97)$$

From eqns. (5.92) with eqn. (5.95), we can obtain

$$E_k'(0) = -\lambda_k C_k^{(2)} + \frac{2\xi\Phi_k}{\lambda_k^2\pi} \sum_{\substack{n=1 \\ n\neq k}}^{\infty} \frac{\lambda_n^3 A_n}{\lambda_n^2-\lambda_k^2} + \frac{\xi\Phi_k A_k}{\lambda_k\pi} . \quad (5.98)$$

Combining eqn. (5.97) and (5.98) yields

$$C_k^{(2)} = \frac{2\xi\Phi_k}{\lambda_k\pi}\left(\sum_{\substack{n=1 \\ n\neq k}}^{\infty} \frac{\lambda_n A_n}{\lambda_n^2-\lambda_k^2}\right) - \frac{\xi\Phi_k A_k}{\lambda_k^2\pi} .$$

Therefore we have

$$E_k(Z) = \frac{2\xi\Phi_k}{\lambda_k^2\pi}\left[\left(\sum_{\substack{n=1 \\ n\neq k}}^{\infty} \frac{\lambda_n A_n}{\lambda_n^2-\lambda_k^2}\right)\lambda_k e^{-\lambda_k Z} - \sum_{\substack{n=1 \\ n\neq k}}^{\infty} \frac{\lambda_n^2 A_n}{\lambda_n^2-\lambda_k^2} e^{-\lambda_n Z}\right]$$

$$+ \frac{\xi\Phi_k A_k}{\lambda_k^2\pi} (\lambda_k Z-1)e^{-\lambda_k Z} . \quad (5.99)$$

Substituting eqns. (5.99) and (5.84) into eqn. (5.77), yields

$$V(r,Z) = \sum_{k=1}^{\infty} E_k(Z)\Psi_k(r) + \phi Z^2 + C_1(0) - \xi \sum_{k=1}^{\infty} A_k e^{-\lambda_k Z}$$

$$- \phi\left[\frac{r^2}{2} - \ell n\ r - \frac{R^2}{2} + \ell n\ R\right] . \quad (5.100)$$

This completes the boundary layer solutions at the arterial ends.

5.3. The Boundary Layer Solution Near $z=1$

The solutions which are valid away from both ends, and the solutions of the boundary layer at the arterial end have been solved by using the technique of matched asymptotic expansions. Since the boundary condition for $c(r,z)$ at $z=1$ has not been satisfied, the solution in the neighborhood of $z=1$ must be obtained. Following the same reasoning used in obtaining the boundary layer expansions at the arterial end, a boundary layer variable at the venous end must be selected. The appropriate boundary layer variable at the venous end is $X = \frac{1-z}{\varepsilon}$, which has the property $z \to 1$ as $\varepsilon \to 0$ for fixed X. In terms of this variable the governing equations (5.9) and (5.14) are

$$\frac{1}{r}\frac{\partial}{\partial r} r \frac{\partial \hat{c}}{\partial r} + \frac{\partial^2 \hat{c}}{\partial X^2} = M , \quad R \leq r \leq 1 , \quad X \geq 0 , \tag{5.101}$$

$$-\beta \frac{d}{dX}[\hat{C}+QS(\hat{C})] = \varepsilon \left.\frac{\partial \hat{c}}{\partial r}\right|_{r=R} + \varepsilon\delta \frac{d^2\hat{C}}{dX^2} , \quad X \geq 0 , \tag{5.102}$$

where $\hat{C}(X) = C(1-\varepsilon X)$ and $\hat{c}(r,X) = c(r,1-\varepsilon X)$. In these variables, the radial and axial diffusion terms in eqn. (5.101) are of equal importance. The boundary conditions are

$$\left.\frac{\partial \hat{c}}{\partial r}\right|_{r=1} = 0 , \quad X \geq 0 , \tag{5.103}$$

$$\left.\frac{\partial \hat{c}}{\partial X}\right|_{X=0} = 0 , \quad R \leq r \leq 1 , \tag{5.104}$$

$$\hat{c}(R,X) = \hat{C}(X) \ , \quad X \geq 0 \ . \tag{5.105}$$

For simplicity, the oxygen concentration at the venous end, $\hat{C}(0)$, may be assumed to be $C_o(1)$, which can be determined from the mass balance equation (5.25) if axial diffusion in the capillary is not considered. Therefore, $C_o(1)$ is given implicitly by

$$C_o(1) + QS(C_o(1)) = \frac{M}{2\beta}\left(R - \frac{1}{R}\right) + 1 + QS(1) \ . \tag{5.106}$$

An additional boundary condition is therefore

$$\hat{C}(0) = C_o(1) \ . \tag{5.107}$$

The matching conditions are

$$\hat{C} \to C \ , \quad \hat{c} \to c \ , \quad \text{as} \quad X \to \infty \ . \tag{5.108}$$

Rewriting the solutions $C_o+\varepsilon^2 C_1$, $c_o+\varepsilon^2 c_1$ in terms of r and X and using Taylor expansions at $z=1$ gives C and c as a series in ε :

$$C \sim C_o(1) + \varepsilon\hat{\alpha}X + \varepsilon^2[\hat{\phi}X^2 + C_1(1)] + O(\varepsilon^3) \ , \tag{5.109}$$

$$c \sim C_o(1) + \frac{M}{2}\left(\frac{r^2}{2} - \ell n\ r - \frac{R^2}{2} + \ell n\ R\right) + \varepsilon\hat{\alpha}X + \varepsilon^2\left[\hat{\phi}X^2 + C_1(1) - \frac{C_o''(1)}{2}\left(\frac{r^2}{2} - \ell n\ r - \frac{R^2}{2} + \ell n\ R\right)\right] + O(\varepsilon^3) \ , \tag{5.110}$$

where

$$\hat{\alpha} = -\frac{M\left(R - \frac{1}{R}\right)}{2\beta[1+QS'(C_o(1))]} = -C_o'(1) \ , \tag{5.111}$$

$$\hat{\phi} = -\frac{\hat{\alpha}^2 QS''(C_o(1))}{2[1+QS'(C_o(1))]} = \frac{C_o''(1)}{2} . \qquad (5.112)$$

It follows that the boundary layer expansions for $\hat{C}(X)$ and $\hat{c}(r,X)$ are of the forms

$$\hat{C} \sim C_o(1) + \varepsilon\hat{\alpha}X + \varepsilon^2\hat{P}(X) , \qquad (5.113)$$

$$\hat{c} \sim C_o(1) + \frac{M}{2}\left(\frac{r^2}{2} - \ell n\ r - \frac{R^2}{2} + \ell n\ R\right) + \varepsilon\hat{U}(r,X) + \varepsilon^2\hat{V}(r,X) , \qquad (5.114)$$

where equations and boundary conditions for $\hat{P}$, $\hat{U}$ and $\hat{V}$ are found by substituting eqns. (5.113) and (5.114) into eqns. (5.101)-(5.105), and (5.107). Applying eqns. (5.109) and (5.110), (5.113) and (5.114) into eqn. (5.108) yields the matching conditions for $\hat{P}$, $\hat{U}$ and $\hat{V}$. We then have the following problems:

(I') $$-\beta \frac{d}{dX}\left[\hat{P}(X)\left(1+QS'(C_o(1))\right) + \frac{1}{2}\hat{\alpha}^2X^2S''(C_o(1))\right] = \left.\frac{\partial\hat{U}}{\partial r}\right|_{r=R} , \quad X\geq 0$$

$$\hat{P}(0) = 0$$

with matching condition:

$$\hat{P}(X) \to \hat{\phi}X^2 + C_1(1) , \quad \text{as} \quad X\to\infty .$$

(II') $$\frac{1}{r}\frac{\partial}{\partial r} r \frac{\partial\hat{U}}{\partial r} + \frac{\partial^2\hat{U}}{\partial X^2} = 0 , \quad R\leq r\leq 1 , \quad X\geq 0 ,$$

$$\left.\frac{\partial\hat{U}}{\partial r}\right|_{r=1} = 0 , \quad X\geq 0 ,$$

$$\left.\frac{\partial \hat{U}}{\partial X}\right|_{X=0} = 0 \ , \quad R \leq r \leq 1 \ ,$$

$$\hat{U}(R,X) = \hat{\alpha} X \ , \quad X \geq 0 \ ,$$

matching condition:

$$\hat{U}(r,X) \to \hat{\alpha} X \ , \quad \text{as} \quad X \to \infty \ , \quad R \leq r \leq 1 \ .$$

(III') $$\frac{1}{r} \frac{\partial}{\partial r} r \frac{\partial \hat{V}}{\partial r} + \frac{\partial^2 \hat{V}}{\partial X^2} = 0 \ , \quad R \leq r \leq 1 \ , \quad X \geq 0 \ ,$$

$$\left.\frac{\partial \hat{V}}{\partial r}\right|_{r=1} = 0 \ , \quad X \geq 0 \ ,$$

$$\left.\frac{\partial \hat{V}}{\partial X}\right|_{X=0} = 0 \ , \quad R \leq r \leq 1 \ ,$$

$$\hat{V}(R,X) = \hat{P}(X) \ , \quad X \geq 0 \ ,$$

matching condition:

$$\hat{V}(r,X) \to \hat{\phi} X^2 + C_1(1) - \frac{C_o''(1)}{2}\left(\frac{r^2}{2} - \ell n \ r - \frac{R^2}{2} + \ell n \ R\right) \ ,$$

$$\text{as} \quad X \to \infty \ , \quad R \leq r \leq 1 \ .$$

The problems (I'), (II') and (III') for $\hat{P}$, $\hat{U}$ and $\hat{V}$ are similar to problems (I), (II) and (III) for P, U and V, respectively. The methods of solution for P, U and V are used here for $\hat{P}$, $\hat{U}$ and $\hat{V}$, respectively, without any further discussion.

The solution for $\hat{U}(r,X)$ can be found as a series of eigenfunction expansions, this is

$$\hat{U}(r,X) = \hat{\alpha}X - 4\pi\hat{\alpha} \sum_{n=1}^{\infty} \frac{\Psi_n(r)e^{-\lambda_n X}}{\lambda_n^3\pi^2\Psi_n^2(1)-4\lambda_n}, \qquad (5.115)$$

where eigenfunctions $\Psi_n(r)$ and eigenvalues λ_n are defined in eqns. (5.68) and (5.69), respectively.

In terms of $\hat{U}(r,X)$, the solution for $\hat{P}(X)$ is

$$\hat{P}(X) = \hat{\phi}X^2 - \frac{1}{\beta[1+QS'(C_o(1))]} \int_o^X \left.\frac{\partial\hat{U}(r,\zeta)}{\partial r}\right|_{r=R} d\zeta . \qquad (5.116)$$

Substituting eqn. (5.115) into eqn. (5.116), yields

$$\hat{P}(X) = \hat{\phi}X^2 + C_1(1) - \frac{4M\left(R-\frac{1}{R}\right)}{\beta[1+QS'(C_o(1))]^2} \sum_{n=1}^{\infty} A_n e^{-\lambda_n X}, \qquad (5.117)$$

where $C_1(1)$ is determined from matching process in problem (I'),

$$C_1(1) = -\frac{1}{\beta[1+QS'(C_o(1))]} \int_o^{\infty} \left.\frac{\partial\hat{U}}{\partial r}\right|_{r=R} dX$$

$$= \frac{4M\left(R-\frac{1}{R}\right)}{\beta^2[1+QS'(C_o(1))]^2} \sum_{n=1}^{\infty} A_n , \qquad (5.118)$$

and A_n is defined in eqn. (5.74).

The higher order tissue venous boundary layer solution $\hat{V}(r,X)$, which is presented in problem (III'), can be obtained by using the similar format of the solution $V(r,Z)$, eqn. (5.100). We have

$$\hat{V}(r,X) = \sum_{k=1}^{\infty} \hat{E}_k(X)\Psi_k(r) + \hat{\phi}X^2 + C_1(1)$$

$$- \hat{\xi} \sum_{k=1}^{\infty} A_k e^{-\lambda_k X} - \hat{\phi}\left[\frac{r^2}{2} - \ell n\, r - \frac{R^2}{2} + \ell n\, R\right], \qquad (5.119)$$

where

$$\hat{E}_k(X) = \frac{2\hat{\xi}\Phi_k}{\lambda_k^2\pi}\left[\left(\sum_{\substack{n=1\\ n\neq k}}^{\infty}\frac{\lambda_n A_n}{\lambda_n^2-\lambda_k^2}\right)\lambda_k e^{-\lambda_k X} - \sum_{\substack{n=1\\ n\neq k}}^{\infty}\frac{\lambda_n^2 A_n}{\lambda_n^2-\lambda_k^2}\, e^{-\lambda_n X}\right]$$

$$+ \frac{\hat{\xi}\Phi_k A_k}{\lambda_k^2\pi}(\lambda_k X-1)e^{-\lambda_k X}, \qquad (5.120)$$

$$\hat{\xi} = \frac{4M\left(R-\frac{1}{R}\right)}{\beta^2[1+QS'(C_o(1))]^2}, \qquad (5.121)$$

and Φ_k is defined in eqn. (5.86). The boundary layer solutions at venous end are now completed.

The boundary layer solution at the venous end differs from that at the arterial end in an essential manner. The venous boundary layer starts at $z=1$, where the capillary oxygen concentration is known and is given by $C_o(1)$, determined from eqn. (5.106). As part of the boundary layer solution and the matching, $C_1(1)$ is determined (eqn. 5.118) in a manner analogous to $C_1(0)$ (eqn. 5.76). However, $C_1(0)$ was an unknown to be determined from the arterial boundary layer analysis, but $C_1(1)$ is known. It is the value of $C_1(z)$ at $z=1$ and is found from eqn. (5.32). It is therefore necessary to establish that $C_1(1)$ determined from eqn. (5.118) is the same as $C_1(1)$ determined from (5.32). This will be done in the next section.

5.4. Consistency of the Solutions

We have already solved boundary layer solutions at both ends independently by using the technique of matched asymptotic expansions. The solutions $C_o+\varepsilon^2 C_1$, $c_o+\varepsilon^2 c_1$ are uniquely determined when the unknown constant $C_1(0)$ is determined by the arterial boundary layer analysis. Then $C_1(1)$ can be calculated from eqn. (5.32) with $z=1$. This can also be calculated independently from solving the boundary layer solutions at the venous end, and is given in eqn. (5.118). In this analysis, for simplicity, the axial diffusion in the capillary is neglected.

As noted at the end of the previous section, no matter how $C_1(1)$ is determined, the two methods must be consistent. Combining eqn. (5.32), with $z=1$, and eqn. (5.118), yields a consistency equation

$$\frac{C_1(0)[1+QS'(1)]-\frac{1}{2\beta}\left(R-\frac{1}{R}\right)[C_o'(1)-C_o'(0)]}{1+QS'(C_o(1))}$$

$$= -\frac{1}{\beta[1+QS'(C_o(1))]}\int_o^\infty \left.\frac{\partial \hat{U}}{\partial r}\right|_{r=R} dX \ . \qquad (5.122)$$

Since $C_1(0)$ is given in eqn. (5.60), substituting this into eqn. (5.122), we have the following consistency relationship

$$\int_o^\infty \left.\frac{\partial U}{\partial r}\right|_{r=R} dZ + \int_o^\infty \left.\frac{\partial \hat{U}}{\partial r}\right|_{r=R} dX = \frac{1}{2}\left(\frac{1}{R}-R\right)[C_o'(0)-C_o'(1)] \ . \qquad (5.123)$$

This relationship will now be proven.

The function $U(r,Z)$ is a solution of the pure diffusional problem for oxygen in the tissue without consumption. The problem for $U(r,Z)$ is defined on the semi-infinite strip $Z \geq 0$, $R \leq r \leq 1$, and is given in section 5.2, problem (II). The total oxygen flux across the capillary wall at $r=R$ into the tissue from $Z=0$ to $Z \to \infty$ is

$$2\pi R \int_0^\infty \left. \frac{\partial U(r,Z)}{\partial r} \right|_{r=R} dZ \ .$$

The total oxygen flux through the edge of the boundary layer ($Z \to \infty$) from $r=R$ to $r=1$ is

$$2\pi \int_R^1 r \left. \frac{\partial U(r,Z)}{\partial Z} \right|_{Z \to \infty} dr \ .$$

According to Laplace's equation for $U(r,Z)$ with zero-flux boundary at $Z=0$ and $r=1$, no oxygen is consumed in the tissue, and the total flux coming in across the capillary wall must be equal to the total flux going out through the edge of the boundary layer. Therefore, we must have

$$2\pi R \int_0^\infty \left. \frac{\partial U(r,Z)}{\partial r} \right|_{r=R} dZ = 2\pi \int_R^1 r \left. \frac{\partial U(r,Z)}{\partial Z} \right|_{Z \to \infty} dr \ . \quad (5.124)$$

Differentiating eqn. (5.70) with respect to Z at $Z \to \infty$, we get

$$\left.\frac{\partial U(r,Z)}{\partial Z}\right|_{Z\to\infty} = \alpha \ .$$

Substituting this into the right hand side of eqn. (5.124), yields

$$\int_o^\infty \left.\frac{\partial U}{\partial r}\right|_{r=R} dZ = \frac{\alpha}{2}\left(\frac{1}{R} - R\right) \ . \qquad (5.125)$$

Using eqn. (5.42), eqn. (5.125) becomes

$$\int_o^\infty \left.\frac{\partial U}{\partial r}\right|_{r=R} dZ = \frac{C_o'(0)}{2}\left(\frac{1}{R} - R\right) \ . \qquad (5.126)$$

The problem for $\hat{U}(r,X)$, which is given in section 5.3, problem (II'), is equivalent to that of $U(r,Z)$. Similarly, we should have

$$\int_o^\infty \left.\frac{\partial \hat{U}}{\partial r}\right|_{r=R} dX = \frac{\hat{\alpha}}{2}\left(\frac{1}{R} - R\right) \ . \qquad (5.127)$$

Using eqn. (5.111), eqn. (5.127) becomes

$$\int_o^\infty \left.\frac{\partial \hat{U}}{\partial r}\right|_{r=R} dX = -\frac{C_o'(1)}{2}\left(\frac{1}{R} - R\right) \ . \qquad (5.128)$$

Adding eqns. (5.126) and (5.128), the relationship in eqn. (5.123) is proven.

Physically, this consistency relationship states that the difference between the oxygen flux across the capillary wall in the arterial boundary layer and the venous boundary layer is equal to the difference between the oxygen flux through the edges of the arterial boundary layer and the venous boundary layer.

Substituting eqns. (5.126) and (5.128) into eqns. (5.60) and (5.118), respectively, yields

$$C_1(0) = \frac{\left(\frac{1}{R} - R\right)C_o'(0)}{2\beta[1+QS'(1)]} , \qquad (5.129)$$

and

$$C_1(1) = \frac{\left(\frac{1}{R} - R\right)C_o'(1)}{2\beta[1+QS'(C_o(1))]} . \qquad (5.130)$$

Comparing eqns. (5.129) and (5.130) with eqns. (5.76) and (5.118), respectively, and using eqns. (5.42) and (5.111) for $C_o'(0)$ and $C_o'(1)$, respectively, we always have

$$\sum_{n=1}^{\infty} A_n = \frac{1}{16}\left(\frac{1}{R} - R\right) . \qquad (5.131)$$

From this equation we find that the summation of the infinite series A_n, which involve R dependent eigenvalues λ_n, can be replaced by a known function of $R = \frac{R_c}{R_t}$, $F(R)$. Here $F(R)$ is defined as

$$F(R) = \frac{1}{16}\left(\frac{1}{R} - R\right) . \qquad (5.132)$$

We now define

$$F_N(R) = \sum_{n=1}^{N} A_n , \qquad (5.133)$$

where N eigenvalues λ_n, $n=1,\ldots,N$, are used in summing the series. The error in the calculation of $F_N(R)$ is dependent on N, and is defined as

$$\text{Error}(N) = \frac{|F(R)-F_N(R)|}{F(R)} \,. \qquad (5.134)$$

For example, at $R = 0.1$, the error is negligible (0.092%) using 40 eigenvalues, and the error is still small (0.46%) even using 8 eigenvalues. The physiological interesting region of R is selected as $0.05 \leq R \leq 0.20$. In this region, $F(R)$, $F_N(R)$ and $\text{Error}(N)$ are calculated for $N=8$, and the graphs of $F(R)$ and $F_N(R)$, and $\text{Error}(N)$, as a function of R are plotted in figures 12 and 13, respectively. Figure 13 shows that the error increases linearly as R increases, but the maximum error is still less than 1%.

From now on, the calculations made by $C_1(0)$ and $C_1(1)$ will be found using the exact form, $F(R)$, instead of summing the series. Thus, $C_1(0)$ and $C_1(1)$ are of the form

$$C_1(0) = -\frac{M\left(R-\frac{1}{R}\right)^2}{4\beta^2[1+QS'(1)]^2} \,, \qquad (5.135)$$

$$C_1(1) = -\frac{M\left(R-\frac{1}{R}\right)^2}{4\beta^2[1+QS'(C_o(1))]^2} \,. \qquad (5.136)$$

These not only simplify the computation but also make the results more accurate.

5.5. Composite Solution

The perturbation solution presented in section 5.1 is valid in the region bounded away from both ends, but it fails in the end regions, where the boundary layer effect occurs. In these regions, the boundary layer solutions can be obtained by introducing appropriate boundary layer variables, $Z = \frac{z}{\varepsilon}$ and $X = \frac{1-z}{\varepsilon}$, as shown in sections 5.2 and 5.3, respectively. This oxygen transport problem, which is represented by these different solutions, may raise practical questions of where the solution shifts from one to the other. Fortunately, the perturbation solution has common regions of validity with both boundary layer solutions. In these common regions, they have some terms in common, namely those terms that are matched. We can construct a single uniformly valid solution from them by adding them together and subtracting the common terms. This uniformly valid solution throughout the whole region is called a composite solution. The purpose of this section is to obtain a uniformly valid composite solution for normalized blood and tissue oxygen concentration.

It can be found by inspecting eqns. (5.40), (5.44) and (5.75) that the common part of both C and $\bar{C}$, say $\bar{C}_{cp}$, in terms of arterial boundary layer variable Z, is

$$\bar{C}_{cp} = 1 + \varepsilon\alpha Z + \varepsilon^2[\phi Z^2 + C_1(0)] \ . \qquad (5.137)$$

Similarly, inspecting eqns. (5.109), (5.113) and (5.117), the common part of both C and $\hat{C}$, say $\hat{C}_{cp}$, in terms of venous boundary layer variable X, is

$$\hat{C}_{cp} = C_o(1) + \varepsilon\hat{\alpha}X + \varepsilon^2[\hat{\phi}X^2 + C_1(1)] \ . \qquad (5.138)$$

The composite solution for normalized blood oxygen concentration is given by

$$C(z) \sim C_o(z) + \varepsilon^2 C_1(z) + \ldots + [\bar{C}(Z) - \bar{C}_{cp}] + [\hat{C}(X) - \hat{C}_{cp}] \ . \qquad (5.139)$$

Substituting eqns. (5.44), (5.75), (5.113), (5.117), (5.137) and (5.138) into eqn. (5.139), yields

$$C(z) \sim C_o(z) + \varepsilon^2 \left[C_1(z) - \frac{4M\left(R - \frac{1}{R}\right)}{\beta^2[1+QS'(1)]^2} \sum_{n=1}^{\infty} A_n e^{-\lambda_n Z} - \frac{4M\left(R - \frac{1}{R}\right)}{\beta^2[1+QS'(C_o(1))]^2} \sum_{n=1}^{\infty} A_n e^{-\lambda_n X} \right] + \ldots \ . \qquad (5.140)$$

This composite solution $C(z)$ is uniformly valid everywhere. In the region away from both ends $e^{-\lambda_n Z}$ and $e^{-\lambda_n X}$ become exponentially small, the dominant behavior is $C_o(z)+\varepsilon^2 C_1(z)$. In the arterial boundary layer $e^{-\lambda_n X}$ becomes exponentially small, and in terms of arterial boundary layer variable Z

$$C_o(\varepsilon Z) + \varepsilon^2\left[C_1(\varepsilon Z) - \frac{4M\left(R - \frac{1}{R}\right)}{\beta^2[1+QS'(1)]^2} \sum_{n=1}^{\infty} A_n e^{-\lambda_n Z}\right]$$

becomes the boundary layer solution at the arterial end. Similarly, in the venous boundary layer $e^{-\lambda_n Z}$ becomes exponentially small, and

$$C_o(1-\varepsilon X) + \varepsilon^2\left[C_1(1-\varepsilon X) - \frac{4M\left(R - \frac{1}{R}\right)}{\beta^2[1+QS'(C_o(1))]^2} \sum_{n=1}^{\infty} A_n e^{-\lambda_n X}\right]$$

becomes the boundary layer solution at the venous end.

The composite solution for normalized tissue oxygen concentration can be obtained by using the same method as used for the normalized blood oxygen concentration. The common parts $\bar{c}_{cp}$ and $\hat{c}_{cp}$ for c and $\bar{c}$, and c and $\hat{c}$, respectively, are

$$\begin{aligned}\bar{c}_{cp} &= 1 + \frac{M}{2}\left(\frac{r^2}{2} - \ell n\ r - \frac{R^2}{2} + \ell n\ R\right) + \varepsilon\alpha Z \\ &\quad + \varepsilon^2\left[\phi Z^2 + C_1(0) - \phi\left(\frac{r^2}{2} - \ell n\ r - \frac{R^2}{2} + \ell n\ R\right)\right], \\ \hat{c}_{cp} &= C_o(1) + \frac{M}{2}\left(\frac{r^2}{2} - \ell n\ r - \frac{R^2}{2} + \ell n\ R\right) + \varepsilon\hat{\alpha}X \\ &\quad + \varepsilon^2\left[\hat{\phi}X^2 + C_1(1) - \hat{\phi}\left(\frac{r^2}{2} - \ell n\ r - \frac{R^2}{2} + \ell n\ R\right)\right].\end{aligned} \tag{5.141}$$

The composite solution for normalized tissue oxygen concentration is given by

$$c(r,z) \sim c_o(r,z) + g_o(r,Z,X) + \varepsilon^2[c_1(r,z)+g_1(r,Z,X)] \ ,$$

where

$$g_o(r,Z,X) = \varepsilon\left[-4\pi\alpha \sum_{n=1}^{\infty} \frac{\Psi_n(r)e^{-\lambda_n Z}}{\lambda_n^3\pi^2\Psi_n^2(1)-4\lambda_n}\right.$$

$$\left. - 4\pi\hat{\alpha} \sum_{n=1}^{\infty} \frac{\Psi_n(r)e^{-\lambda_n X}}{\lambda_n^3\pi^2\Psi_n^2(1)-4\lambda_n}\right], \tag{5.142}$$

$$g_1(r,Z,X) = -\frac{4M\left(R-\frac{1}{R}\right)}{\beta^2[1+QS'(1)]^2} \sum_{n=1}^{\infty} A_n e^{-\lambda_n Z}$$

$$- \frac{4M\left(R-\frac{1}{R}\right)}{\beta^2[1+QS'(C_o(1))]^2} \sum_{n=1}^{\infty} A_n e^{-\lambda_n X} + \sum_{n=1}^{\infty} [E_n(Z)+\hat{E}_n(X)]\Psi_n(r).$$

Here, $E_n(Z)$ and $\hat{E}_n(X)$ are defined in sections 5.2 and 5.3, respectively, and are given by eqns. (5.99) and (5.120), respectively.

The analysis for the nonlinear steady state problem of oxygen transport to tissue is now completed.

5.6. An Exact Solution

In the beginning of section 5, we noted that the analysis of the nonlinear oxygen transport problem is much more difficult than the linear problem. Inside the tissue, the governing equation and boundary conditions are the same for both linear and nonlinear problems, so that the solution for normalized tissue oxygen concentration, $c(r,z)$ can be taken from eqns. (4.40) and (4.42). We have

$$c(r,z) = \int_0^1 C(\zeta)d\zeta + \frac{M}{2}\left(\frac{r^2}{2} - \ell n\ r - \frac{R^2}{2} + \ell n\ R\right) + \sum_{n=1}^{\infty} \frac{2}{v_n} [K_1(\rho_n)I_o(\rho_n r)+I_1(\rho_n)K_o(\rho_n r)] \cos(n\pi z) \int_0^1 C(\zeta)\cos(n\pi\zeta)d\zeta \ , \qquad (5.143)$$

where K_o , K_1 and I_o , I_1 are the modified Bessel functions of order zero and one, respectively. C is the normalized blood oxygen concentration, which must satisfy the following non-dimensional equations:

$$\beta \frac{d}{dz} [C+QS(C)] = \left.\frac{\partial c}{\partial r}\right|_{r=R} , \quad 0\leq z\leq 1$$
$$C(0) = 1 . \qquad (5.144)$$

Applying eqn. (5.143) to eqn. (5.144) yields

$$C(z) + QS(C(z)) = 1 + QS(1) + \frac{M}{2\beta}\left(R - \frac{1}{R}\right)z + \sum_{n=1}^{\infty} \frac{2u_n}{\beta n\pi v_n} \sin(n\pi z) \int_0^1 C(\zeta)\cos(n\pi\zeta)d\zeta, \qquad (5.145)$$

where u_n and v_n are defined by eqns. (4.22) and (4.23), respectively. This is a nonlinear Fredholm integral equation for $C(z)$. The method, used in section 4, of reducing the integral equation to an infinite set of linear algebraic equations cannot be applied here. The method of solution for this nonlinear Fredholm integral equation is suggested by using successive approximations. Let $C^{(o)}(z)$ be the starting solution, which is given implicitly by

$$C^{(o)} + QS(C^{(o)}) = 1 + QS(1) + \frac{M}{2\beta}\left(R - \frac{1}{R}\right)z \ . \qquad (5.146)$$

Once $C^{(o)}(z)$ is known for $0 \le z \le 1$, the first iteration solution $C^{(1)}$ can be solved from

$$C^{(1)} + QS(C^{(1)}) = 1 + QS(1) + \frac{M}{2\beta}\left(R - \frac{1}{R}\right)z + \int_o^1 K(z,\zeta)C^{(o)}(\zeta)d\zeta \ ,$$

where $K(z,\zeta) = \sum_{n=1}^{\infty} \frac{2u_n}{\beta n\pi v_n} \sin(n\pi z)\cos(n\pi\zeta)$, is a degenerate kernel.

In general, we have

$$C^{(i+1)} + QS(C^{(i+1)}) = 1 + QS(1) + \frac{M}{2\beta}\left(R - \frac{1}{R}\right)z + \int_o^1 K(z,\zeta)C^{(i)}(\zeta)d\zeta \ . \qquad (5.147)$$

It can be shown that the integrand $K(z,\zeta)C^{(i)}(\zeta)$ satisfies a Lipschitz condition

$$|K(z,\zeta)C^{(i+1)}(\zeta)-K(z,\zeta)C^{(i)}(\zeta)| \leq L|C^{(i+1)}(\zeta)-C^{(i)}(\zeta)| ,$$

where L is a upper bound of $K(z,\zeta)$. It can be proven that the solution $C(z)$ of eqn. (5.145) is the uniform limit of the successive approximations $C^{(i)}(z)$ defined by eqns. (5.146) and (5.147) (Ref. Saaty and Bram 1964, Saaty 1967).

Once $C(z)$ is determined for $0 \leq z \leq 1$, the normalized tissue oxygen concentration can be determined from eqn. (5.143) for $0 \leq z \leq 1$ and $R \leq r \leq 1$. An exact solution for this nonlinear problem of oxygen transport to tissue can therefore be obtained.

5.7. A Modification of the Krogh Model

The isolated Krogh cylinder is treated as a functional unit of entire capillary beds which begin from arterioles and end at the venules. The regularity of the capillary beds provides this conceptual physical geometry. However, near the arterioles and venules there are tissue regions which are not included in the Krogh cylinder but still require oxygen for metabolism. The oxygen supply to these tissue regions may be from the nearest Krogh cylinder where oxygen diffuses through the tissue boundary. Therefore, the isolated Krogh tissue cylinder can be modified by assuming non-zero flux through the tissue boundary at $\bar{z}=0$ and $\bar{z}=L$. Then the boundary conditions eqns. (5.3) and (5.4) become

$$D_z \left.\frac{\partial c_t}{\partial \bar{z}}\right|_{\bar{z}=0} = f_1 , \quad R_c \leq \bar{r} \leq R_t , \tag{5.148}$$

$$D_z \left.\frac{\partial c_t}{\partial \bar{z}}\right|_{\bar{z}=L} = - f_2 , \quad R_c \leq \bar{r} \leq R_t , \tag{5.149}$$

where f_1 and f_2 (cm^3O_2/cm^2tissue boundary-sec) are constant oxygen fluxes through both the arterial and venous ends of the tissue boundary, respectively. The sign indicates the direction of oxygen flux according to Fick's first law.

In terms of nondimensional variables $z = \frac{\bar{z}}{L}$, $r = \frac{\bar{r}}{R_t}$,

and $c = \frac{c_t}{C_A}$, eqns. (5.148) and (5.149) become

$$\left.\frac{\partial c}{\partial z}\right|_{z=0} = f_A \ , \quad R \leq r \leq 1 \ , \tag{5.150}$$

$$\left.\frac{\partial c}{\partial z}\right|_{z=1} = - f_V \ , \quad R \leq r \leq 1 \ , \tag{5.151}$$

where $f_A = \frac{f_1 L}{D_z C_A}$ and $f_V = \frac{f_2 L}{D_z C_A}$. These two boundary conditions replace eqn. (5.11) and (5.12). The perturbation analysis in the region bounded away from the ends does not change, because the method of solution did not employ these two boundary conditions. But the perturbation solution involved the constant $C_1(0)$, which will be changed when we solve the boundary layer solution and apply non-zero flux at the arterial end of tissue boundary, eqn. (5.150). In terms of the arterial boundary layer variables $Z = \frac{z}{\varepsilon}$ and $\bar{c}(r,Z) = c(r,\varepsilon Z)$, eqn. (5.150) becomes

$$\left.\frac{\partial \bar{c}}{\partial Z}\right|_{Z=0} = \varepsilon f_A \ , \quad R \leq r \leq 1 \ . \tag{5.152}$$

We use this instead of eqn. (5.36) in the boundary layer problem at the arterial end. We then obtain

$$P(Z) = \phi Z^2 + C_1(0) - \frac{8(\alpha - f_A)}{\beta[1+QS'(1)]} \sum_{n=1}^{\infty} A_n e^{-\lambda_n Z}, \tag{5.153}$$

$$C_1(0) = \frac{8(\alpha - f_A)}{\beta[1+QS'(1)]} F(R) \ , \tag{5.154}$$

$$U(r,Z) = \alpha Z - 4\pi(\alpha-f_A)\sum_{n=1}^{\infty} \frac{\Psi_n(r)e^{-\lambda_n Z}}{\lambda_n^3\pi^2\Psi_n^2(1)-4\lambda_n} . \quad (5.155)$$

The higher order tissue boundary layer solution, $V(r,Z)$, has the same form as eqn. (5.100), obtained in section 5.2, except ξ in eqn. (5.28) is changed to $8(\alpha-f_A)/\beta[1+QS'(1)]$.

For simplicity, we do not consider axial diffusion in the capillary. The amount of oxygen lost from the capillary is equal to the oxygen consumed in the tissue and the oxygen diffused out through the tissue boundary, $\bar{z}=0$ and $\bar{z}=L$. We have the mass balance equation for oxygen transport

$$\pi R_c^2 q[C_A+\bar{Q}S^*(C_A)-C_V-\bar{Q}S^*(C_V)] = M_o\pi(R_t^2-R_c^2)L + (f_1+f_2)\pi(R_t^2-R_c^2) . \quad (5.156)$$

We define a nondimensional constant $C_o(1)$,

$$C_o(1) = \frac{C_V}{C_A} .$$

Substituting this into eqn. (5.156), gives $C_o(1)$ implicitly by

$$C_o(1) + QS(C_o(1)) = \frac{M_oL+f_1+f_2}{q\,C_A\,R}(R-\frac{1}{R}) + 1 + QS(1). \quad (5.157)$$

This normalized venous oxygen concentration, $C_o(1)$, can be used in solving the boundary layer problem at venous end with a non-zero flux boundary.

Similarly, in terms of venous boundary layer variables $X = \frac{1-z}{\varepsilon}$ and $\hat{c}(r,X) = c(r,1-\varepsilon X)$, eqn. (5.151) becomes

$$\left.\frac{\partial \hat{c}}{\partial X}\right|_{X=0} = \varepsilon f_V \ , \quad R \leq r \leq 1 \ . \tag{5.158}$$

This can be used instead of eqn. (5.104) in the boundary layer problem at the venous end. Then the solutions for $\hat{P}(X)$, $\hat{U}(r,X)$ and $\hat{V}(r,X)$, and the constant $C_1(1)$ can be obtained as follows:

$$\hat{P}(X) = \hat{\phi}X^2 + C_1(1) + \frac{8(\hat{\alpha}-f_V)}{\beta[1+QS'(C_o(1))]} \sum_{n=1}^{\infty} A_n e^{-\lambda_n X} , \tag{5.159}$$

$$C_1(1) = -\frac{8(\hat{\alpha}-f_V)}{\beta[1+QS'(C_o(1))]} F(R) \ , \tag{5.160}$$

$$\hat{U}(r,X) = \hat{\alpha}X - 4\pi(\hat{\alpha}-f_V) \sum_{n=1}^{\infty} \frac{\Psi_n(r)e^{-\lambda_n X}}{\lambda_n^3 \pi^2 \Psi_n^2(1) - 4\lambda_n} \ , \tag{5.161}$$

The higher order tissue boundary layer solution, $\hat{V}(r,X)$, has the same form as we have already obtained in section 5.3, eqn. (5.119), except $\hat{\xi}$ in eqn. (5.121) is changed to $-8(\hat{\alpha}-f_V)/\beta[1+QS'(C_o(1))]$.

The consistency relationship for this modified model can be obtained by directly applying the results for $C_1(0)$ and $C_1(1)$, eqns. (5.154) and (5.160), respectively. It is given by

$$\int_o^{\infty} \left.\frac{\partial U}{\partial r}\right|_{r=R} dZ + \int_o^{\infty} \left.\frac{\partial \hat{U}}{\partial r}\right|_{r=R} dX = \frac{1}{2}\left(\frac{1}{R}-R\right)[C_o(0)-C_o(1)-(f_A+f_V)] \ . \tag{5.162}$$

The composite solution for $C(z)$ and $c(r,Z)$ are of the form

$$C(z) = C_o(z) + \varepsilon^2\left[C_1(z) - \frac{8(\alpha-f_A)}{\beta[1+QS'(1)]}\sum_{n=1}^{\infty}A_n e^{-\lambda_n Z} + \frac{8(\hat{\alpha}-f_V)}{\beta[1+QS'(C_o(1))]}\sum_{n=1}^{\infty}A_n e^{-\lambda_n X}\right] + \ldots ,$$

(5.163)

$$c(r,z) = c_o(r,z) + g_o(r,Z,X) + \varepsilon^2[c_1(r,z)+g_1(r,Z,X)] + \ldots ,$$

where

$$g_o(r,Z,X) = \varepsilon\left[-4\pi(\alpha-f_A)\sum_{n=1}^{\infty}\frac{\Psi_n(r)e^{-\lambda_n Z}}{\lambda_n^3\pi^2\Psi_n^2(1)-4\lambda_n} - 4\pi(\hat{\alpha}-f_V)\sum_{n=1}^{\infty}\frac{\Psi_n(r)e^{-\lambda_n X}}{\lambda_n^3\pi^2\Psi_n^2(1)-4\lambda_n}\right],$$

(5.164)

$$g_1(r,Z,X) = -\frac{8(\alpha-f_A)}{\beta[1+QS'(1)]}\sum_{n=1}^{\infty}A_n e^{-\lambda_n Z} + \frac{8(\hat{\alpha}-f_V)}{\beta[1+QS'(C_o(1))]}\sum_{n=1}^{\infty}A_n e^{-\lambda_n X} + \sum_{n=1}^{\infty}[E_n(Z)+\hat{E}_n(X)]\Psi_n(r) .$$

The previous analysis in sections 5.1-5.5 can be considered as a special case of the present model by taking $f_1=f_2=0$. As noted in section 3, Reneau et al. (1967,1969) assumed zero flux at the arterial tissue boundary and non-zero flux at venous tissue boundary. However, they chose the wrong direction for oxygen flux,

taking it to be influx. This made axial diffusion less important, as shown in their results. The numerical examples of the effect of the outflux from tissue cylinder will be given in the next section.

6. NUMERICAL RESULTS AND DISCUSSION

Numerical examples are presented in this section. Using the linear theory, in section 6.1 it is shown that the perturbation method is a good approximation to the exact solution. Several numerical examples for the non-linear problem are presented. In section 6.2, the effect of axial diffusion is studied, and it is ascertained when this effect can be neglected and when it must be taken into account. In section 6.3, numerical examples of a modified Krogh model with outflux of oxygen through the ends of the Krogh cylinder are presented. The results are compared with the corresponding results of the isolated Krogh model shown in section 6.2.

6.1. Comparison of the Perturbation Solution with the Exact Solution Obtained by Using Linear Oxyhemoglobin Dissociation Relationship

From the normal oxyhemoglobin dissociation curve shown in fig. 2(II), we pick up two points (0.00323 cm^3O_2/cm^3blood, 0.958) and (0.00162 cm^3O_2/cm^3blood, 0.829) and use the straight line which passes through these two points, instead of the nonlinear relationship. The equation is

$$S^*(C_b) = S_1^* C_b + S_o^* , \qquad (6.1)$$

where $S_1^*=80$ and $S_o^*=0.7$. In terms of normalized blood oxygen concentration C , we have

$$S(C) = S_1^* C_A C + S_o^* \qquad (6.2)$$

and

$$S'(C) = S_1^* C_A . \qquad (6.3)$$

We can see that $S'(C)$ is a constant and is independent of C . Then,

$$S''(C) = 0 . \qquad (6.4)$$

Substituting eqn. (6.2) into eqn. (5.25), gives C_o as a linear function of z . For given $0 \le z \le 1$, the corresponding value of C_o can be calculated from

$$C_o(z) = \frac{M(R-\frac{1}{R})}{2\beta(1+QS_1^* C_A)} z + 1 . \qquad (6.5)$$

Once C_o is known, the oxygen distribution in the tissue, c_o, can be determined from eqn. (5.24) as a linear function of z for a given radial location r.

From eqn. (6.5), we can see that

$$C_o'(z) = \frac{M(R-\frac{1}{R})}{2\beta(1+QS_1^*C_A)} \text{ , independent of } z \text{ , } \quad (6.6)$$

and

$$C_o''(z) = 0 \text{ .} \quad (6.7)$$

By applying eqns. (6.3) and (6.6) to eqn. (5.32), C_1 can be found to be a constant, given by

$$C_1(z) = C_1(0) = -\frac{M(R-\frac{1}{R})^2}{4\beta^2(1+QS_1^*C_A)^2} \text{ .} \quad (6.8)$$

Substituting eqn. (6.7) into eqn. (5.31) yields

$$c_1(r,z) = C_1(z) \text{ , independent of } r \text{ .}$$

The boundary layer solutions at the arterial and venous ends, $\bar{C}$, $\bar{c}$, and $\hat{C}$, $\hat{c}$, from sections 5.2 and 5.3, respectively, can be simplified by using the following results

$$\alpha = -\hat{\alpha} = C_o'(z) \text{ ,}$$

$$\xi = \hat{\xi} = \frac{4M(R-\frac{1}{R})}{\beta^2(1+QS_1^*C_A)^2} \text{ ,}$$

and

$$\phi = \hat{\phi} = 0 \text{ .}$$

For this linear problem, the matched constant $C_1(1)$ is

equal to $C_1(0)$.

Numerical examples are given for two sets of data, shown in table I. To determine the solutions, 40 eigenvalues, λ_n , n=1,2,...,40 , are calculated and used. In these particular examples the ratio $R = \frac{R_c}{R_t}$ is equal to 0.1 . A list of 40 eigenvalues for $R = 0.1$ is shown in table II.

Example (1) corresponds to a short capillary, high diffusivity, and high metabolic rate. The results of the perturbation solution using the linear oxyhemoglobin dissociation relationship are illustrated in figures 14-16. Figure 14 shows the normalized oxygen concentration in the capillary. The perturbation solutions without and with axial diffusion, for the region bounded away from the ends, $C_o(z)$ and $C_o(z) + \varepsilon^2 C_1(z)$, respectively, are linear functions of axial position z because of the use of a linear oxyhemoglobin dissociation relationship. The boundary layer solutions, $\bar{C}$ and $\hat{C}$, provide the description in the regions near $z=0$ and $z=1$, respectively. These boundary layer solutions can be seen to be very close to the composite solution, which is uniformly valid over the whole region. Figures 15 and 16 show the normalized oxygen concentration in the tissue without and with axial diffusion, for the region bounded away from the ends, $c_o(r,z)$ and $c_o(r,z) + \varepsilon^2 c_1(r,z)$.

They are seen to be linear functions of z . The figures are shown for a location midway between the capillary wall and the outer edge of the Krogh cylinder, and at the outer edge of the Krogh cylinder, respectively. These solutions are not valid near $z=0,1$, and it can be seen that they do not have zero slope there. The boundary layer solutions at arterial and venous end are shown in the figures. These solutions have zero slope at $z=0,1$, so that no oxygen diffuses out through the ends of the tissue cylinder. Again, these boundary layer solutions can be seen to be very close to the uniformly valid composite solution.

Figures 17-19 show similar results for the second set of data, example (2), in table I, which corresponds to a long capillary, low diffusivity, and low metabolic rate compared with example (1).

The exact solution of the oxygen transport problem with a linear oxyhemoglobin dissociation relationship, which has been obtained in section 4.1, eqns. (4.39) and (4.40), can be compared with the composite solution to check the accuracy of the perturbation method. The results are shown in figures 20-25. Figures 20-22 show good agreement between the composite solution and the exact solution even when the diameter of the Krogh cylinder is one third of its length $(\varepsilon = \frac{1}{6})$. Figures 23-25

show better agreement between the two solutions for smaller ε , $\varepsilon = \frac{1}{10}$. These indicate that the perturbation methods are a good approximate solution to the problem with small parameter ε .

6.2. Numerical Examples of Nonlinear Problem

Numerical results for the nonlinear problem can easily be obtained from the perturbation solutions which are presented in section 5. For given $C_o \leq 1$, the corresponding value of $z \geq 0$ can be computed directly from eqn. (5.25) for any choice of $S(C_o)$, even if this function is given graphically or in tabular form. Once C_o is known, the normalized oxygen concentration in the tissue, c_o, can be determined from eqn. (5.24) as a function of r at the corresponding location z. To determine $C_1(z)$ from eqn. (5.32), the constant $C_1(0)$ must first be calculated from eqn. (5.135). Then C_1 can be found at the location z corresponding to C_o by substituting C_o into eqn. (5.32). To facilitate the computation, C_o' has been derived as a function of C_o, and is given by

$$C_o'(z) = \frac{M(R-\frac{1}{R})}{2\beta[1+QS'(C_o(z))]}, \qquad (6.9)$$

where the empirical formula, eqn. (2.1), is used for the oxyhemoglobin dissociation relationship, and $S'(C_o(z))$ is

$$S'(C_o(z)) = \frac{KxC_A^x C_o^{x-1}(z)}{[1+KC_A^x C_o^x(z)]^2} \qquad (6.10)$$

The slope of the oxyhemoglobin dissociation curves in fig. 2 are shown in fig. 26 as a function of blood oxygen concentration. It can be seen that the slope of

the oxyhemoglobin dissociation curve increases as blood oxygen concentration decreases in the higher concentration region. When the slope reaches its maximum value at a certain low blood oxygen concentration, it then decreases rapidly to zero as blood oxygen concentration decreases to zero. The maximum value of the slope differs considerably for the different curves, and depends on the physiological constant K and x.

Eqn. (5.31) gives c_1 as a function of r at the given axial location z. The function $C_o''(z)$ appearing in this equation can also be determined as a function of C_o, and is given by

$$C_o''(z) = -\frac{M(R-\frac{1}{R})QS''(C_o(z))C_o'(z)}{2\beta[1+QS'(C_o(z))]^2}, \qquad (6.11)$$

where

$$S''(C_o(z)) = \frac{Kx(x-1)C_A^x C_o^{x-2}(z) - K^2x(x+1)C_A^{2x}C_o^{2x-2}(z)}{[1+KC_A^xC_o^x(z)]^3}. \qquad (6.12)$$

The oxygen distribution in the capillary and the tissue have been calculated for the three sets of data shown in table III. The first set of data shown in table III corresponds to a long capillary under a hyperbaric oxygen condition and large volume blood flow rate, and the corresponding results are illustrated in figs. 27-29. The high arterial oxygen concentration, 400 mm Hg, used in this example is typical of O_2 levels used for therapeutic

purposes, as, for example, in oxygen tents and masks. The eigenvalues shown in table II have been used in this example since the ratio $R = \frac{R_c}{R_t}$ is equal to 0.1 . Fig. 27 shows the normalized blood oxygen concentration, with and without axial diffusion, corresponding to $C_o(z)$ and $C_o(z) + \varepsilon^2 C_1(z)$, respectively. The solution with axial diffusion provides an accurate description except in the boundary layers. Keeping higher order terms does not improve the accuracy of the solution inside the boundary layer, since the expansion is not valid there. The oxygen concentration near both ends are determined by the expansions given in sections 5.2 and 5.3, and these solutions are indicated in the figure by a dotted line. It can be seen that the venous boundary layer is negligible compared with the arterial boundary layer, because $S'(C_o(1))$ is much larger than $S'(1)$, so that $\varepsilon^2 C_1(1)$ is much smaller than $\varepsilon^2 C_1(0)$. A detailed discussion of this will be given later. A uniformly valid composite solution given in section 5.5 is shown in the figure by the dashed line.

Figs. 28 and 29 show the oxygen distribution in the tissue, with and without axial diffusion, as a function of axial position z at a radial location midway between the capillary wall and the outer edge of the Krogh cylinder, and at the outer edge of the Krogh cylinder,

respectively. Again, these solutions are not valid near $z=0$, and it can be seen that they do not have a zero slope there. The venous boundary layer is negligible, since the solutions show an approximately zero slope there. The proper solution in the arterial boundary layer is given by the expansion shown in section 5.2, and the solution is also indicated in the figure. The arterial boundary layer solution has a zero slope at $z=0$, so that no oxygen diffuses out through the end of the Krogh cylinder. A uniformly valid composite solution is also shown in the figure.

Corresponding results for the second set of data in table III are illustrated in figs. 30-32. This set of data corresponds to a low tissue metabolic rate and low volume blood flow rate. The ratio $R = \frac{R_c}{R_t}$ is 0.1 , so that the eigenvalues shown in table II are again used. Fig. 30 shows the nonlinear oxygen distribution over the length of the capillary. The arterial boundary layer is seen to be more important than the venous boundary layer. This indicates that axial diffusion has a more significant effect at the beginning of the capillary. The arterial boundary layer solution and composite solution are shown in the figure. Figs. 31 and 32 show that a small boundary layer exists at the venous end, since the solutions $c_o(r,z)$ and $c_o(r,z) + \varepsilon^2 c_1(r,z)$ do not have zero slope

at $z=1$. The boundary layer solution at the arterial end does not join smoothly with the solution with axial diffusion and only the value of $c(r,z)$ at $z=0$, determined by the boundary layer solution is shown in the figure. For fig. 31 this is indicated by the short dash at $c = 0.78$, and in fig. 32 by the short dash at $c = 0.76$. The inaccuracy of the boundary layer solution away from the immediate neighborhood of $z=0$ for this case will be discussed later.

The third set of data shown in table III is taken from Hyman et al. (1975), except $C_A=0.002$ cm^3O_2/cm^3blood. The ratio $R = \frac{R_c}{R_t}$ is equal to $\frac{3}{35}$. The eigenvalues corresponding to this R have been calculated and are shown in table IV. The results for this set are shown in figs. 33-35. Fig. 33 shows that the difference between the oxygen concentration in the capillary with and without axial diffusion is small and the composite solution is close to the solution without axial diffusion. Figs. 34 and 35, illustrating the oxygen distribution in the tissue, show two significant boundary layers. The boundary layer solution is indicated by the dashed lines in the figure. Both boundary layer solutions have a zero slope at the ends, so that no oxygen diffuses out through the ends of the Krogh cylinder. The tissue oxygen concentration at $z=0$ can be accurately determined by the arterial boundary layer solution.

The exact solution of the nonlinear oxygen transport problem, which has been obtained in section 5.6, can be calculated numerically and compared with the composite solution. The results, illustrated in figs. 36-38 for the three sets of data, show that the exact solution is close to the composite solution, verifying that the perturbation method is a good approximation. In fig. 38, the exact solution and the composite solution are so close together that their difference cannot be seen in the figure. Therefore these solutions are indicated by one solid line.

The oxygen distribution in the capillary and the tissue in the region bounded away from the arterial and venous ends can be calculated very simply even when axial diffusion is included, but the solution depends strongly on the conditions at the arterial end. Although the solution in that region is much more complex, it affects the oxygen concentration outside the arterial boundary layer only through the constant $\varepsilon^2 C_1(0)$. This constant is the difference between the oxygen concentration in the capillary without and with axial diffusion, $C_o(z)$ and $C_o(z) + \varepsilon^2 C_1(z)$, respectively, at $z=0$, and therefore plays an essential role in ascertaining the importance of axial diffusion. Since $C_1(0)$ is given by the simple expression in eqn. (5.135), it is very easy to determine

the influence of various physiological parameters on its magnitude, and therefore their influence on the importance of axial diffusion. Fig. 26 shows that the slope of the oxyhemoglobin dissociation curve, $S'(1)$, increases as arterial oxygen concentration, C_A, decreases. The larger $S'(1)$, the smaller $\varepsilon^2 C_1(0)$. The effect of axial diffusion is therefore less important as C_A decreases. This is shown in fig. 39 for four different arterial oxygen concentrations, $C_A = 0.0032$, 0.003, 0.0025 and 0.002 (cm^3O_2/cm^3blood). In all cases, the venous boundary layer is seen to be less important than the arterial boundary layer. This is because $S'(C_o(1))$ is much larger than $S'(1)$, so that $\varepsilon^2 C_1(1)$ is much smaller than $\varepsilon^2 C_1(0)$. Because of the nonlinear oxyhemoglobin dissociation relationship, the blood oxygen profile is nonlinear. It is interesting to see that each decrease of C_A makes the blood oxygen profile without axial diffusion flatter. This phenomenon is due to the characteristics of the oxyhemoglobin dissociation relationship, fig. 2, which has been described in section 2. The amount of oxygen being consumed in the tissue is locally constant. Starting from a high C_A, a large drop in blood oxygen concentration can be seen near the arterial end because only a small amount of oxygen is released from hemoglobin. This makes the profile steep. It can

be seen that during hyperbaric oxygen conditions ($C_A > 0.0032$ cm^3O_2/cm^3blood) , axial diffusion has a significant effect at the beginning of the capillary. The difference between the arterial and venous oxygen concentration is very large. Starting from low C_A , small changes in blood oxygen concentration cause large amounts of oxygen to dissociate from hemoglobin. This makes the blood oxygen profile rather flat. It also can be seen that during arterial hypoxia ($C_A < 0.001$ cm^3O_2/cm^3blood) , the effect of axial diffusion is negligible. The difference between arterial and venous oxygen concentrations is then relatively small.

The initial difference in the curves with and without axial diffusion, $\varepsilon^2 C_1(0)$, is also affected by the tissue oxygen consumption rate, the tissue oxygen diffusivity, the volume blood flow rate, the blood hemotocrit, and the shift of the oxyhemoglobin dissociation relationship. This can be seen from the formula for $C_1(0)$, eqn. (5.135). The value of $\varepsilon^2 C_1(0)$ is proportional to the tissue oxygen consumption rate and the tissue oxygen diffusivity. Their effects are shown in figs. 40 and 41, respectively. The data used for figs. 40 and 41 are taken from the third set of data in table III with $C_A = 0.003$ cm^3O_2/cm^3blood and varying M_o and D_r, D_z , respectively. Fig. 40 shows the effect of the tissue oxygen consumption rate

on the blood oxygen concentration with and without axial diffusion. Fig. 40(a) corresponds to normal tissue oxygen consumption rate, $M_o = 0.0005$ cm^3O_2/cm^3tissue-sec. Decreasing M_o by one half, fig. 40(b), makes the arterial boundary layer less important compared to fig. 40(a). Because less oxygen is consumed in the tissue, the blood oxygen concentration at the venous end is higher in comparison with fig. 40(a). Increasing M_o by 50%, fig. 40(c), results in a larger value of $\varepsilon^2 C_1(0)$ and a lower venous blood oxygen concentration. It also makes the solution without axial diffusion steeper. Fig. 41 shows the effect of the tissue oxygen diffusivity on the blood oxygen concentration with and without axial diffusion. Since the tissue oxygen consumption rate is constant in this example, varying tissue oxygen diffusivity does not change blood oxygen concentration without axial diffusion. Fig. 41(a) corresponds to tissue oxygen diffusivity, $D_r=D_z=1300$ $\mu m^2/sec$. Fig. 41(b) shows the effect of decreasing D_r, D_z, by one half. This makes the arterial boundary layer less important. The effect of increasing D_r, D_z by 50% is shown in fig. 41(c). More oxygen diffuses across the capillary wall into the tissue at the beginning of the capillary. It then diffuses rapidly in the axial direction in the tissue, making the arterial boundary layer more important.

The value of $\varepsilon^2 C_1(0)$ is inversely proportional to q^2 and approximately to $\bar{Q}^2$. The effect of these parameters are shown in figs. 42 and 43, respectively. The data used for figs. 42 and 43 are taken from the third set of data in table III with $C_A = 0.003$ cm^3O_2/cm^3blood and varying q and $\bar{Q}$, respectively. Fig. 42 shows the effect of the volume blood flow rate on the blood oxygen concentration with and without axial diffusion. Fig. 42(a) corresponds to normal blood flow rate, $q = 1.131\times10^4$ $\mu m^3/sec$. Decreasing q decreases the amount of oxygen delivered to the capillary. Since the same amount of oxygen has to diffuse into the tissue to supply the metabolic needs, a lower venous blood oxygen concentration results. A steeper blood oxygen concentration without axial diffusion is also expected. More oxygen remains in the capillary when q is increased, giving a higher venous blood oxygen concentration. The value of $\varepsilon^2 C_1(0)$ is sensitive to the variation of q. A decrease in q of 25%, shown in fig. 42(b), causes a large increase of $\varepsilon^2 C_1(0)$. Conversely, an increase of 25% in q, fig. 42(c), causes a large decrease of $\varepsilon^2 C_1(0)$. Similarly, the result of increasing or decreasing $\bar{Q}$ is almost the same as that of increasing or decreasing q, respectively, because the amount of oxygen delivery by the capillary almost equally depends upon the volume blood flow rate

and the blood hematocrit. As noted in section 2, the blood oxygen capacity is proportional to the blood hematocrit. The effect of the blood oxygen capacity on the blood oxygen concentration with and without axial diffusion is shown in fig. 43.

Venous hypoxia (venous oxygen concentration less than $0.001\ cm^3O_2/cm^3blood$) occurs with a large increase of tissue oxygen consumption rate, or a large decrease of volume blood flow rate (or blood oxygen capacity). During venous hypoxia, the effect of axial diffusion is very important at the beginning of the capillary.

The value of $\varepsilon^2 C_1(0)$ is also approximately inversely proportional to $[S'(1)]^2$. As can be seen from figs. 2 and 26, the comparison of the slope for oxyhemoglobin dissociation curves (I), (II) and (III) at $C_A = 0.003\ cm^3O_2/cm^3blood$ is (I)<(II)<(III). Using the third set of data shown in table III, where the constants K and x are referred to the normal physiological conditions of curve (II), the corresponding result is shown in fig. 44(a). Shifting the normal oxyhemoglobin dissociation curve (II) to the right, curve (III), increases the slope. This makes $\varepsilon^2 C_1(0)$ smaller, as shown in fig. 44(b). Conversely, shifting the normal curve (II) to the left, curve (I), decreases the slope. This makes $\varepsilon^2 C_1(0)$ larger, as shown in fig. 44(c).

It has been shown that increasing tissue oxygen consumption rate and tissue diffusivity, decreasing volume blood flow rate and blood oxygen capacity, or shifting the normal oxyhemoglobin dissociation curve to the left, a significant difference between blood oxygen profile with and without axial diffusion can be seen at the beginning of the capillary. In these conditions, therefore, the effect of the axial diffusion must be taken into account.

6.3. Numerical Examples for the Modified Krogh Model

The tissue regions near the arterioles and venules can be regarded as being oxygenated by the initial and final portions of the capillary, respectively, and an appreciable portion of oxygen could diffuse into these regions from the capillary. This can be accounted for by a modification of the Krogh model, in which a given amount of oxygen is assumed to diffuse out the ends of the Krogh cylinder. The analysis of this modified model was given in section 5.7, and numerical examples will be presented here. Two different examples are illustrated in figs. 45-50. The data used for figs. 45-47 are taken from the first set of data in table III and the corresponding eigenvalues in table II. In this example, the total outflux of oxygen at each end of the Krogh cylinder is taken to be 3% of the oxygen consumed in the Krogh cylinder. We have

$$\pi(R_t^2-R_c^2)f_1 = \pi(R_t^2-R_c^2)f_2 = 0.03\ M_o\pi(R_t^2-R_c^2)L \quad .(6.13)$$

The nondimensional parameters f_A and f_V, shown in eqns. (5.150) and (5.151), respectively, can be determined by

$$f_A = f_V = \frac{0.03\ M_o L^2}{D_z\ C_A} \quad . \qquad (6.14)$$

Fig. 45 shows that axial diffusion has a greater effect

on the blood oxygen concentration at the beginning of the capillary than the corresponding case for the isolated Krogh model shown in fig. 27. A small effect of axial diffusion can be seen at the venous end. The blood oxygen concentration at the venous end, $z = 1$, can be determined from eqn. (5.157), and it can be seen that this value is smaller than the solution without axial diffusion at $z = 1$, because of oxygen diffusion through the ends of Krogh tissue. The arterial boundary layer solution and composite solution are shown in the figure by the dotted and dashed lines, respectively.

Figs. 46 and 47 show the oxygen distribution in the tissue as a function of axial position at a radial location midway between the capillary wall and the outer edge of the Krogh cylinder, and at the outer edge of the Krogh cylinder, respectively. Again, it can be seen that axial diffusion has a more significant effect in comparison with the results of the isolated Krogh model shown in figs. 28 and 29. A small venous boundary layer can be seen in the figure. According to eqns. (5.150) and (5.151), the boundary layer solution at the arterial and venous ends have slope f_A and $-f_V$, respectively. From eqn. (6.14), we have $f_A = f_V = 0.926$, which indicates the quantity and direction of the oxygen flux at both ends. The transition to positive slope, required for oxygen loss

from the arterial end of the Krogh cylinder, occurs very close to $z = 0$, as seen in figures 46 and 47. The slope of the venous boundary layer solution is negative, since oxygen diffuses out through the venous end. Due to the outflux of oxygen through the ends of the Krogh cylinder, the oxygen level at both ends can be seen to be lower than for the corresponding isolated Krogh model shown in the figs. 28 and 29.

The data used for figs. 48-50 is taken from the third set of data in table III and the corresponding eigenvalues in table IV. In this example, the total outflux of oxygen at each end of the Krogh cylinder is taken to be 5% of the oxygen being consumed in the Krogh tissue. Using similar expressions shown in eqns. (6.13) and (6.14), the nondimensional parameters f_A and f_V, therefore, can be determined by

$$f_A = f_V = \frac{0.05\ M_o L^2}{D_z\ C_A} \quad . \qquad (6.15)$$

Fig. 48 shows that axial diffusion has a more significant effect on the blood oxygen concentration not only at the beginning of the capillary, but also at the venous end, in comparison with the result of the isolated Krogh model shown in fig. 33. Therefore, both arterial and venous boundary layers can be seen in the figure. The blood oxygen concentration at the venous end, $z = 1$, can be

determined from eqn. (5.157) and it can be seen that this value is smaller than the solution without axial diffusion at $z = 1$, because oxygen diffuses out through the ends of the Krogh cylinder.

Figs. 49 and 50 show the effect of axial diffusion on the tissue oxygen distribution, with outflux of oxygen through the ends of the Krogh cylinder. As shown in the figure, the slope of the composite solution is positive at the arterial end and negative at the venous end. The slope can be found from eqn. (6.15) to be $f_A = f_V = 1.178$. Both arterial and venous boundary layers can be seen to be equally important. In contrast to the results of the isolated Krogh model shown in figs. 34 and 35, the arterial boundary layer shows a non-zero (positive) slope at $z = 0$, while figs. 34 and 35 show a zero slope there. The venous boundary layer shows not only a non-zero (negative) slope at $z = 1$, but also a much lower oxygen concentration than the solution without axial diffusion, while figs. 34 and 35 show a zero slope and a higher oxygen concentration than the solution without axial diffusion.

6.4. Discussion

Since the perturbation analysis provides only approximate solutions, the results cannot be expected to be good for all possible situations. When the effect of axial diffusion is very large, the solutions will not be accurate. It can be seen, however, that the linear problem, figs. 14-16, and the non-linear problem with hyperbaric oxygen conditions, figs. 27-29, show a fairly significant effect of axial diffusion, but the perturbation method still provides accurate results.

Another factor limiting the accuracy of the solutions is the change in slope, in the boundary layer region, of the oxyhemoglobin dissociation relationship. The dissociation relationship, $S(C)$, was expanded in a Taylor series about $z = 0$ (c.f. eqn. (5.18)) to obtain the arterial boundary layer equations, and the initial slope, $S'(1)$, is used throughout the boundary layer. If oxygen enters the capillary at 95 mm Hg, for example, and the rate of consumption is very large, $S'(C_o(z))$ can change considerably from its initial value $S'(1)$, and the method of solution breaks down. This difficulty does not occur for the solution near the venous ends. In all cases it was found that either axial diffusion was insignificant or that it could be described very accurately by the boundary layer solution.

In general, the accuracy of the solution is indicated by the manner in which the boundary layer solution and the solution with axial diffusion join at their common boundary, and by the extent to which the composite solution agrees with them in their respective domains of applicability. A much quicker indication of whether the perturbation method will provide accurate results can be obtained by examining the capillary oxygen concentration solution with axial diffusion. This is easily obtained from eqns. (5.25) and (5.32). If the initial difference between the solution with and without axial diffusion, $\varepsilon^2 C_1(0)$, is extremely large, axial diffusion is probably too important to be regarded as a small perturbation. If the initial slope of the curve with axial diffusion is positive, as in figs. (39a) and (41c), for example, the slope of the oxyhemoglobin dissociation relationship is probably changing very fast, causing a very rapid convergence of the solution to the result without axial diffusion. Although the results still give a qualitative indication of the significance of axial diffusion, for accurate quantitative results the exact solution must be used in these cases.

7. SUMMARY

The isolated Krogh model for steady state oxygen transport to tissue with axial diffusion has been studied analytically for both linear and nonlinear problems. The perturbation method involving boundary layer theory and the technique of matched asymptotic expansions has been shown to be a good approximation for the linear theory. Although the linear theory does not consider the nonlinear oxyhemoglobin dissociation relationship, it is still applicable for determining the concentration of certain substrates not having chemical reaction with red blood cells. Physiologically, the nonlinearity of the oxyhemoglobin dissociation relationship plays an important role in oxygen transport to tissue. Several cases have been studied using the nonlinear theory. These solutions show the validity and smoothness of the boundary layer analysis and indicate the effect of axial diffusion. Axial diffusion has a greater effect on the oxygen distribution in the blood and tissue when any of the following conditions is satisfied: (1) high incoming arterial oxygen concentration, (2) high tissue oxygen consumption rate, (3) high tissue diffusivity, (4) low volume blood flow rate, (5) low blood oxygen capacity, (6) a shift in the normal oxyhemoglobin dissociation curve to the left (corresponding to low body temperature,

or high blood pH value, or low blood carbon dioxide concentration). When a modification of the Krogh model is considered, in which outflux of oxygen through the ends of the Krogh cylinder occurs, the results show that axial diffusion has a greater effect on oxygen distribution in the blood and tissue than the corresponding results of the isolated Krogh model.

TABLE I

Values of Parameters used in Section 6.1

Parameter	Example (1)	Example (2)
Arterial blood oxygen concentration C_A (cm^3O_2/cm^3blood)	0.003	0.003
Tissue diffusivity D_r, D_z (μm^2/sec)	2000	1500
Oxygen capacity of the blood at 100% saturation $\bar{Q}$ (cm^3O_2/cm^3blood)	0.204	0.204
Tissue oxygen consumption rate M_o (cm^3O_2/cm^3tissue-sec)	0.0008	0.0005
Capillary length L (μm)	150	250
Capillary radius R_c (μm)	2.5	2.5
Tissue radius R_t (μm)	25	25
Volume blood flow rate q (μm^3/sec)	7.854×10^3	7.854×10^3

TABLE II

Eigenvalues for R = 0.1

n	Eigenvalues λ_n
1	1.102694
2	4.978842
3	8.554285
4	12.086804
5	15.602901
6	19.110740
7	22.613796
8	26.113821
9	29.611803
10	33.108342
11	36.603824
12	40.098509
13	43.592578
14	47.086161
15	50.579356
16	54.072233
17	57.564849
18	61.057248
19	64.549463
20	68.041521
21	71.533445
22	75.025255
23	78.516963
24	82.008584
25	85.500127
26	88.991602
27	92.483016
28	95.974375
29	99.465686
30	102.956953
31	106.448181
32	109.939373
33	113.430532
34	116.921662
35	120.412764
36	123.903842
37	127.394897
38	130.885931
39	134.378945
40	137.867942

TABLE III

Values of Parameters used in Section 6.2

Parameter	1st set	2nd set	3rd set
Tissue oxygen diffusivity D_r, D_z (μm/sec)	1000	1700	1300
Oxygen capacity of the blood at 100% saturation $\bar{Q}$ (cm^3O_2/cm^3blood)	0.204	0.204	0.204
Tissue oxygen consumption rate M_o (cm^3O_2/cm^3tissue-sec)	0.0003	0.0002	0.0005
Capillary length L (μm)	1200	700	350
Capillary radius R_c (μm)	3	3	3
Tissue radius R_t (μm)	30	30	35
Constant K in oxyhemoglobin dissociation relationship	1.8695×10^7	6.6856×10^6	6.6856×10^6
Constant x in oxygemoglobin dissociation relationship	2.3	2.2	2.2
Volume blood flow rate q (μm^3/sec)	2.545×10^4	8.482×10^3	1.131×10^4
Arterial oxygen concentration C_A (cm^3O_2/cm^3blood)	0.014	0.00323	0.002

TABLE IV

Eigenvalues for R = 3/35

n	Eigenvalues λ_n
1	1.056554
2	4.882037
3	8.404731
4	11.884348
5	15.347278
6	18.801709
7	22.251159
8	25.697422
9	29.141517
10	32.584070
11	36.025486
12	39.466041
13	42.905928
14	46.345285
15	49.784216
16	53.222800
17	56.661097
18	60.099153
19	63.537007
20	66.974688
21	70.412220
22	73.849624
23	77.286917
24	80.724111
25	84.161220
26	87.598252
27	91.035216
28	94.472120
29	97.908969
30	101.345769
31	104.782525
32	108.219242
33	111.655921
34	115.092568
35	118.529184
36	121.965772
37	125.402335
38	128.838874
39	132.275392
40	135.711889

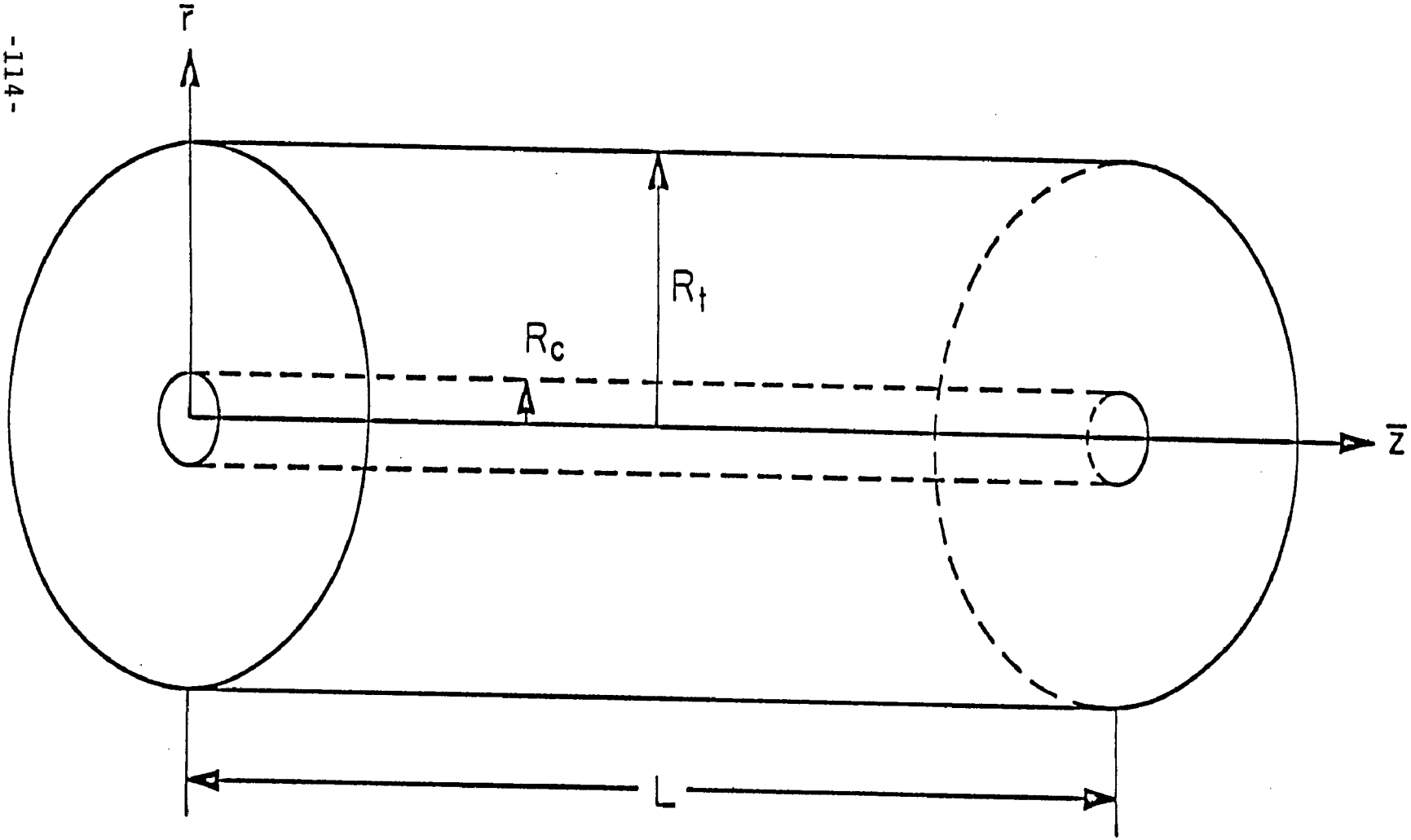

Figure 1. Geometry of the problem: a single capillary surrounded by a concentric cylinder of tissue.

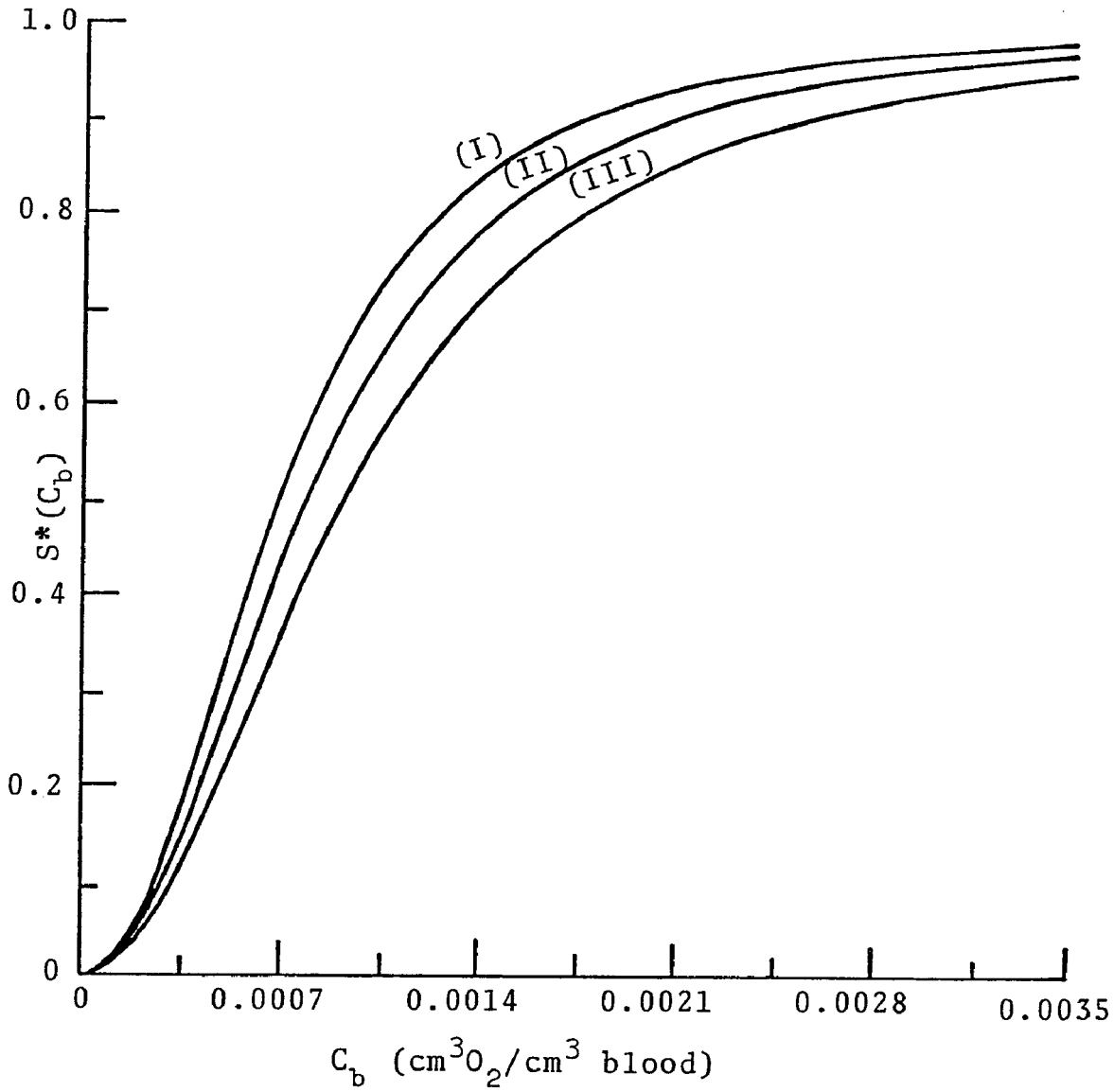

Figure 2. Oxyhemoglobin dissociation curves as a function of blood oxygen concentration for various values of physiological constants K and x . (K,x) is $(1.8695\times10^{7}, 2.3)$ for (I), $(6.6856\times10^{6}, 2.2)$ for (II), and $(2.3908\times10^{6}, 2.1)$ for (III). Curve (II) is for normal physiological conditions.

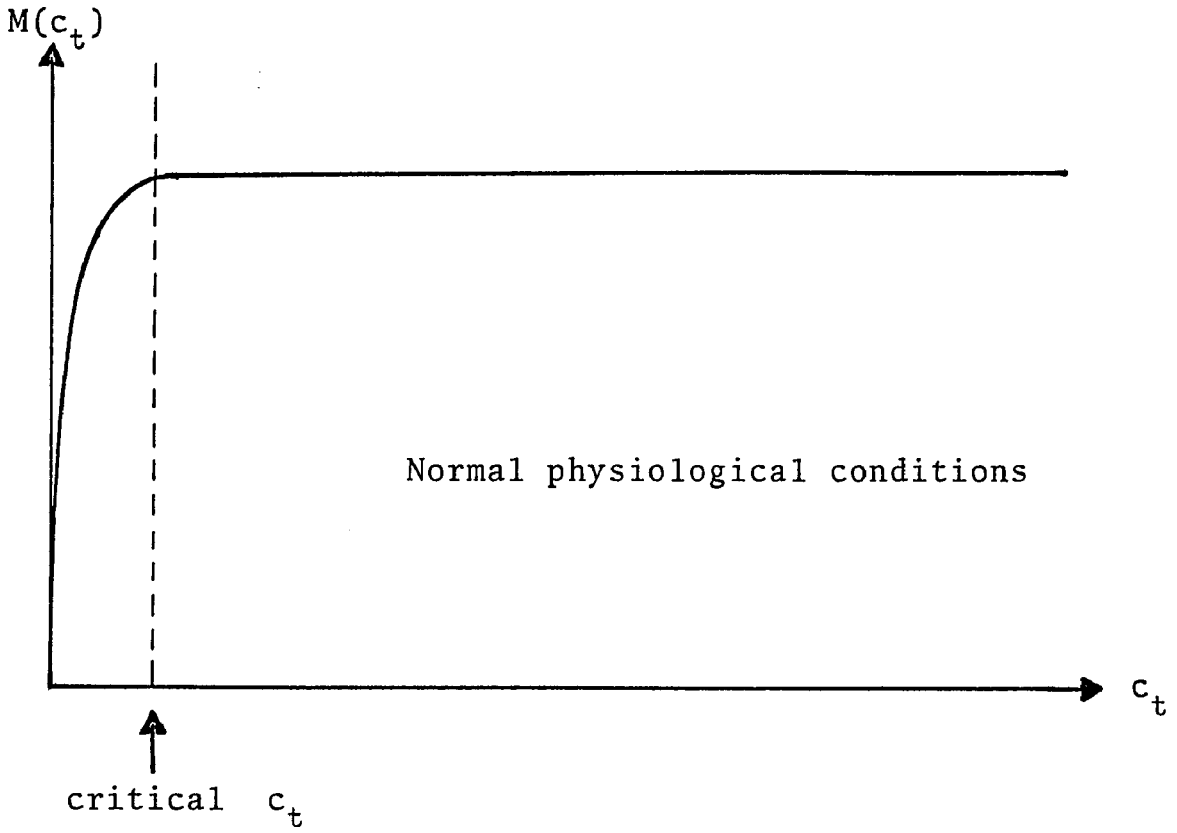

Figure 3. Tissue oxygen consumption rate, $M(c_t)$ (cm^3O_2/cm^3 tissue-sec), as a function of tissue oxygen concentration, c_t (cm^3O_2/cm^3 tissue).

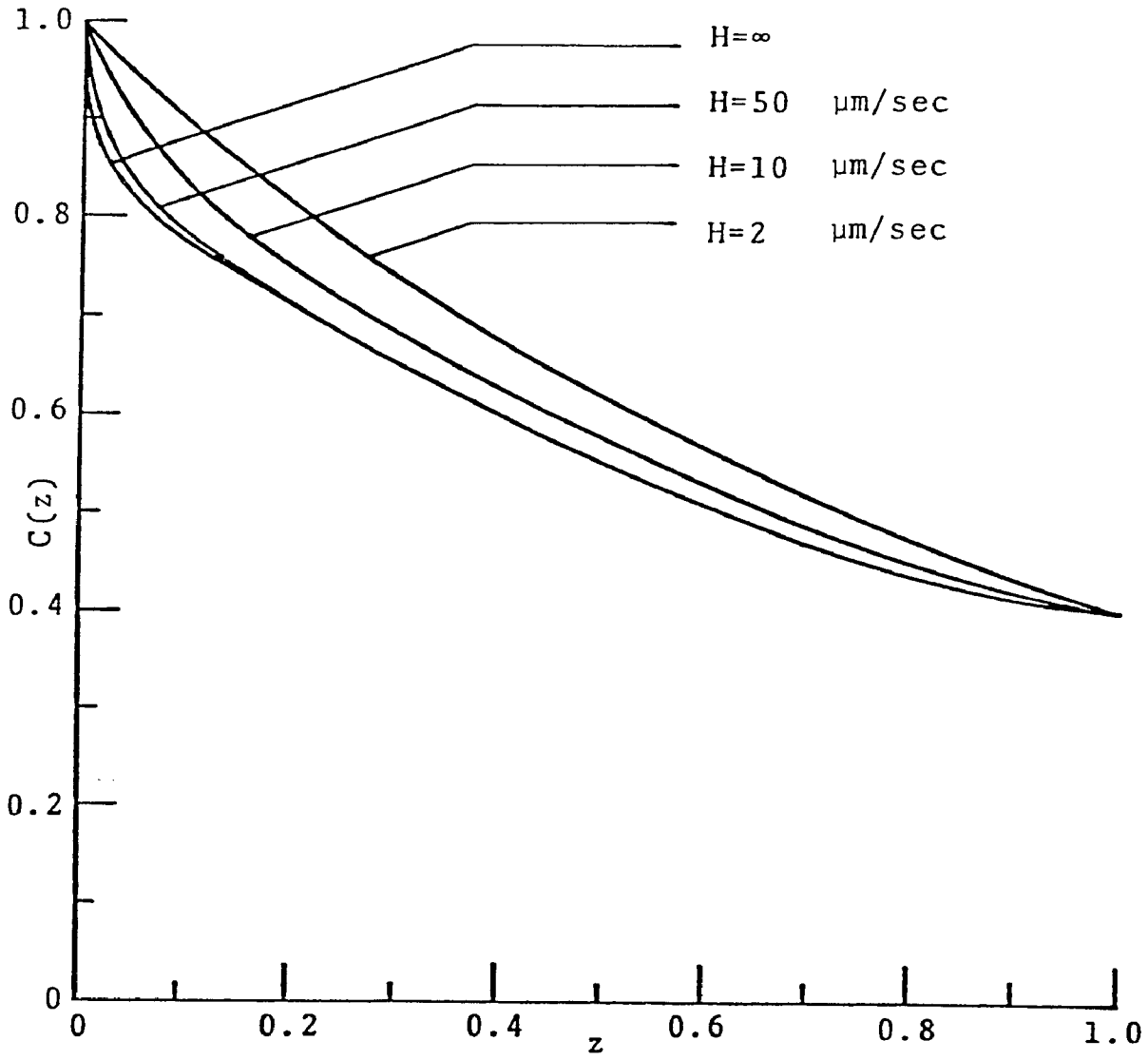

Figure 4. Normalized capillary concentration as a function of distance, for various values of the permeability H .

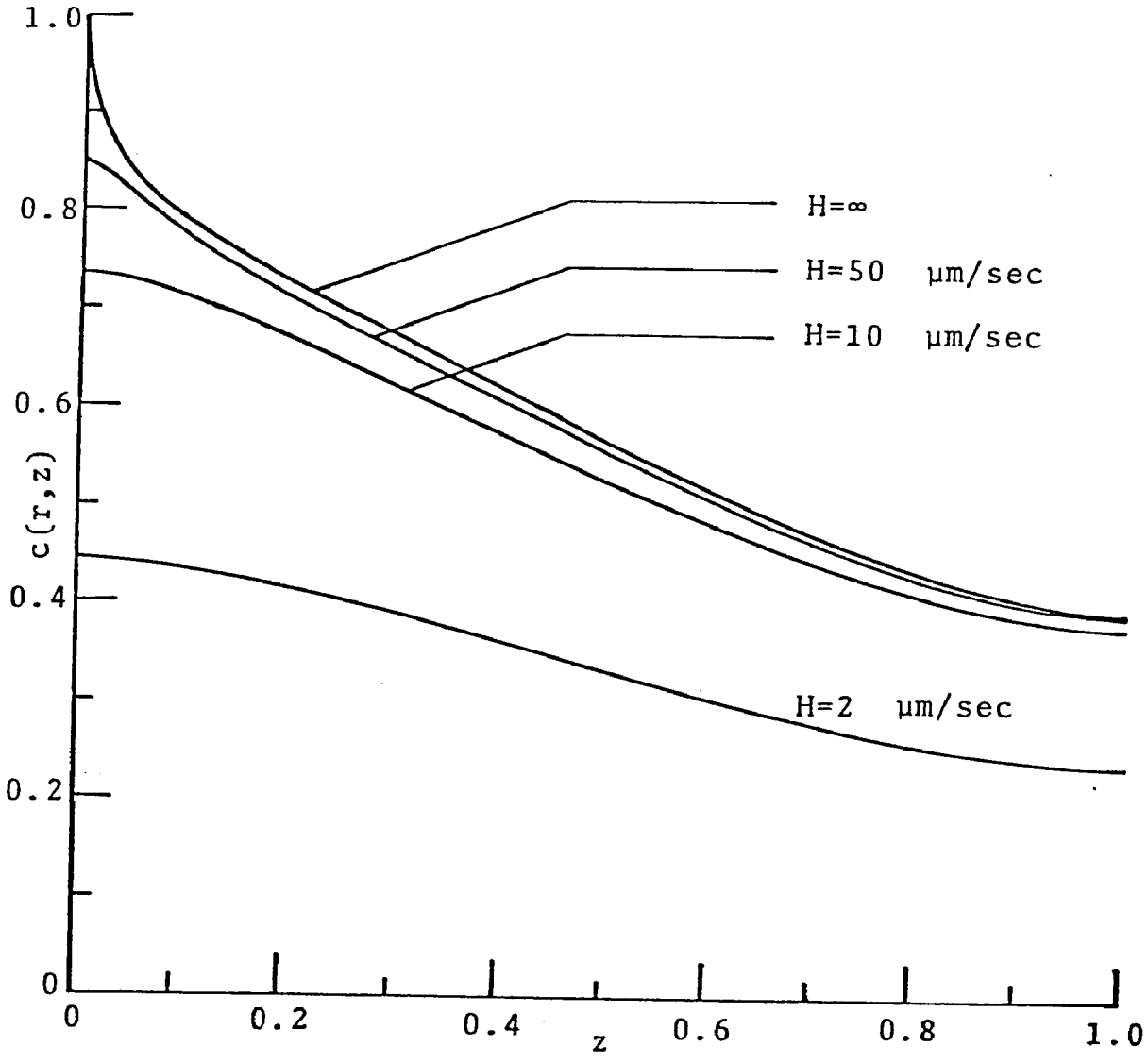

Figure 5. Normalized tissue concentration at the capillary wall as a function of axial position, for various values of the permeability H .

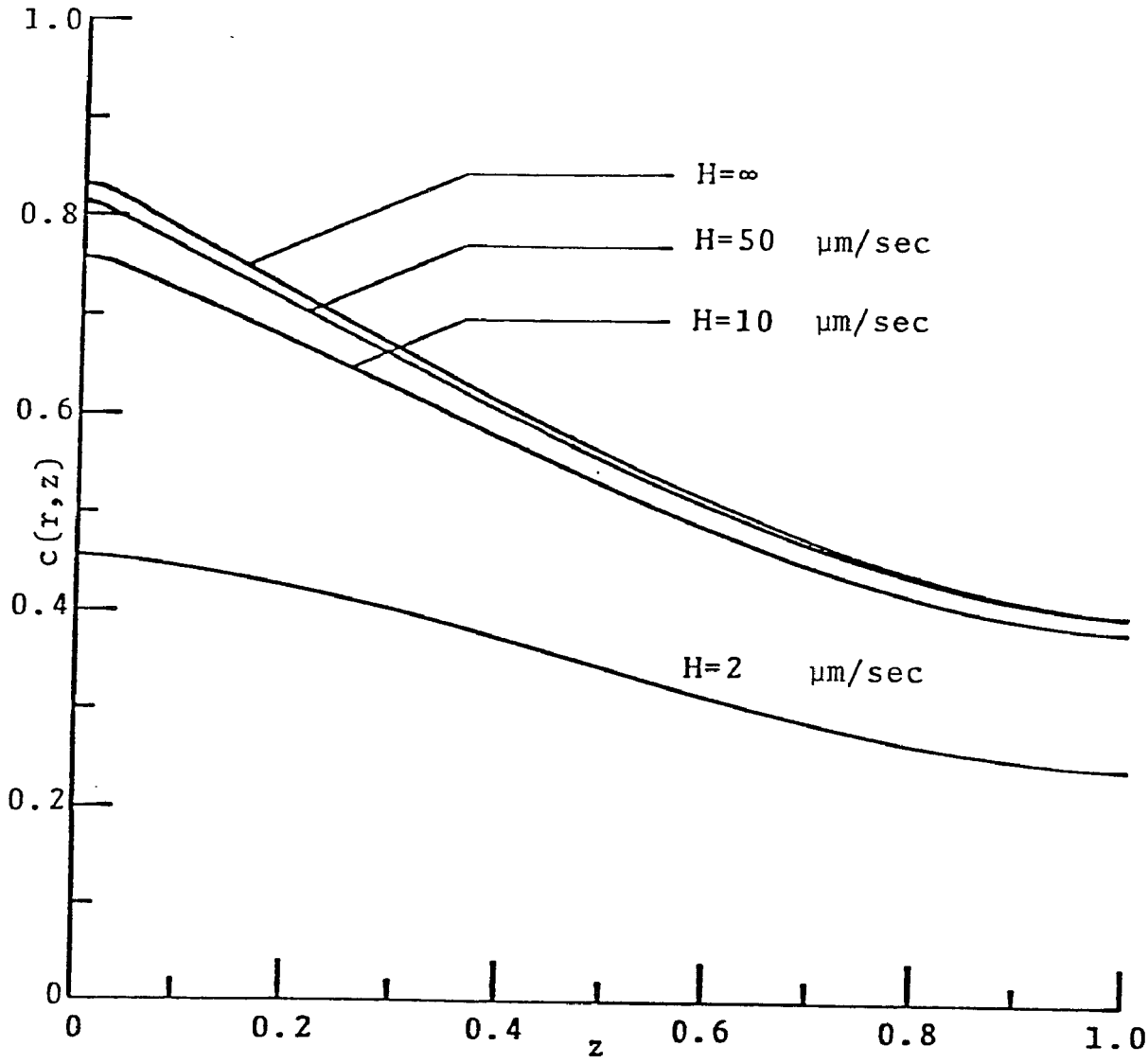

Figure 6. Normalized tissue concentration midway between the capillary wall and the outer edge of the tissue as a function of axial position, for various values of permeability H .

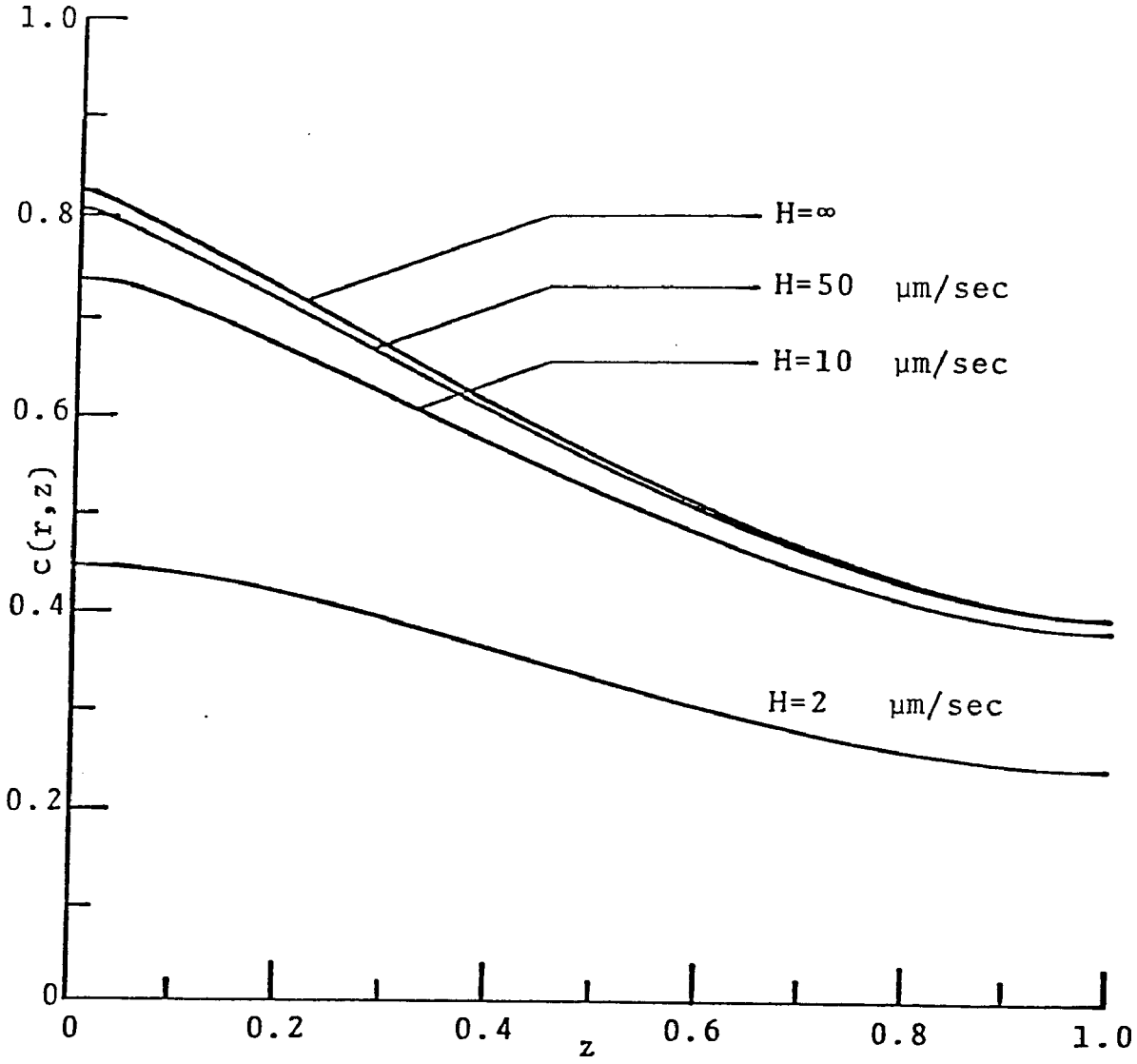

Figure 7. Normalized tissue concentration at the outer edge of the tissue as a function of axial position, for various values of permeability H .

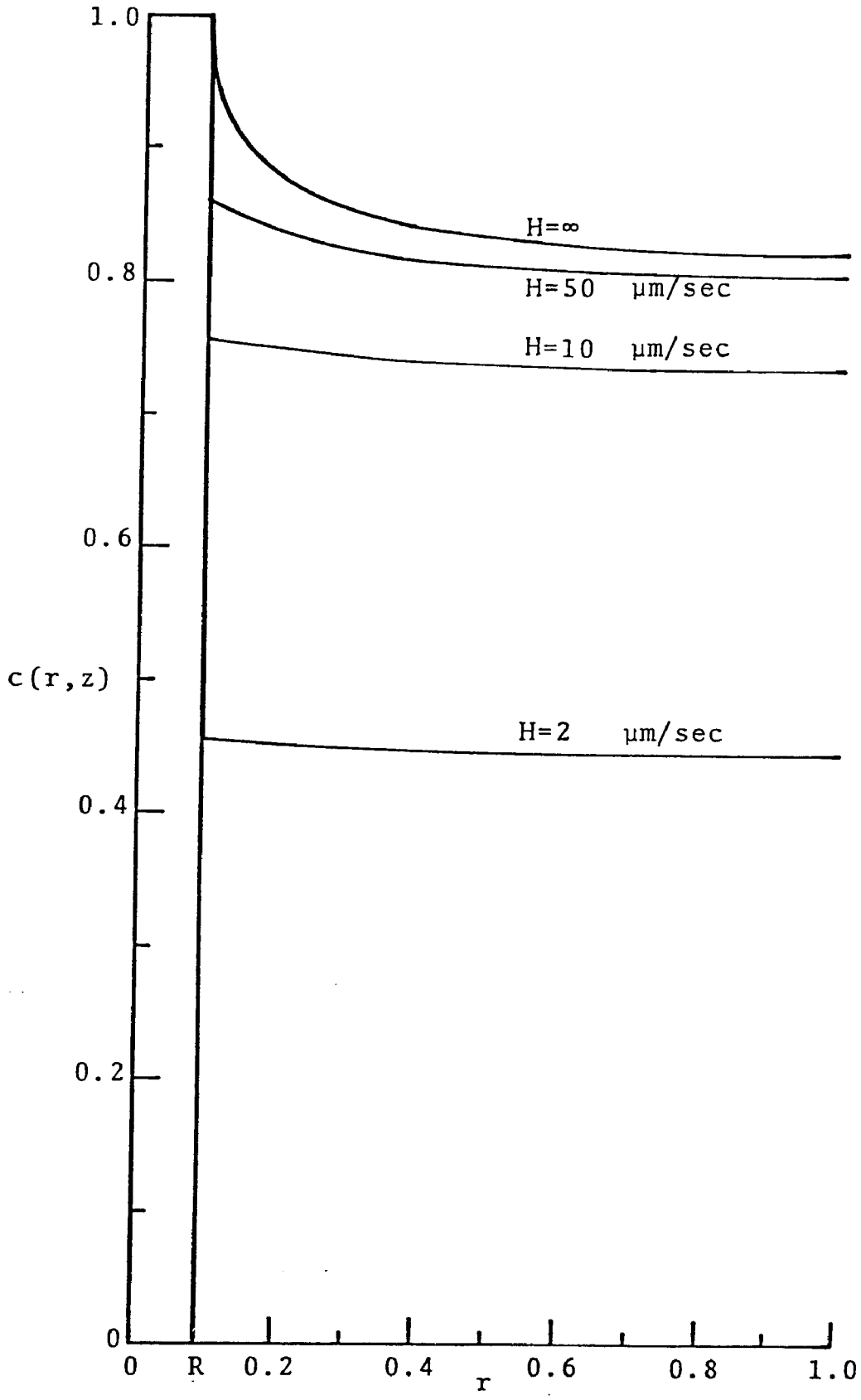

Figure 8. Normalized tissue concentration as a function of radial position at $z=0$, for various values of the permeability H.

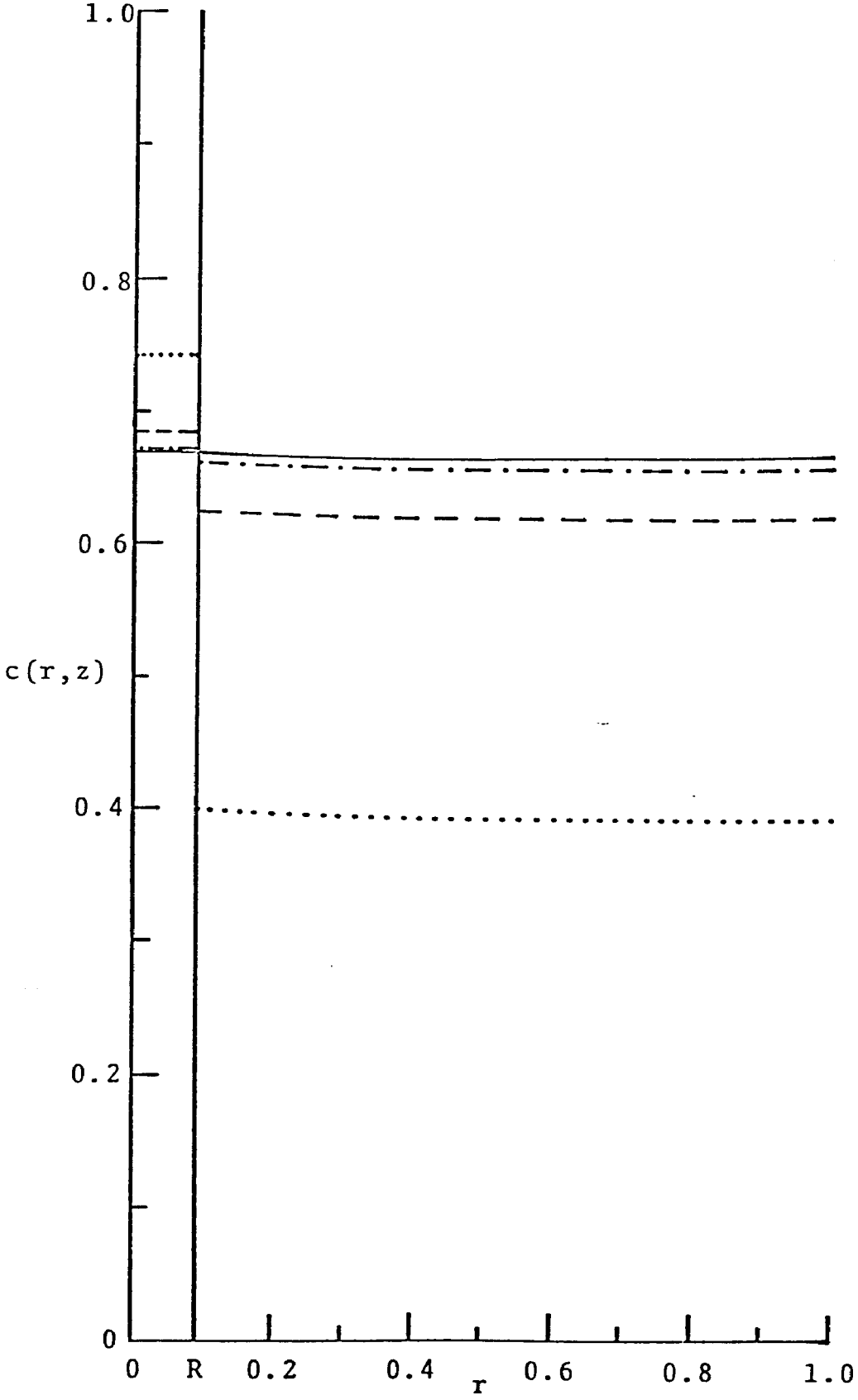

Figure 9. Normalized tissue concentration as a function of radial position at $z=0.3$. ——— $H=\infty$, — · — · — $H=50$, — — — $H=10$, ····· $H=2$.

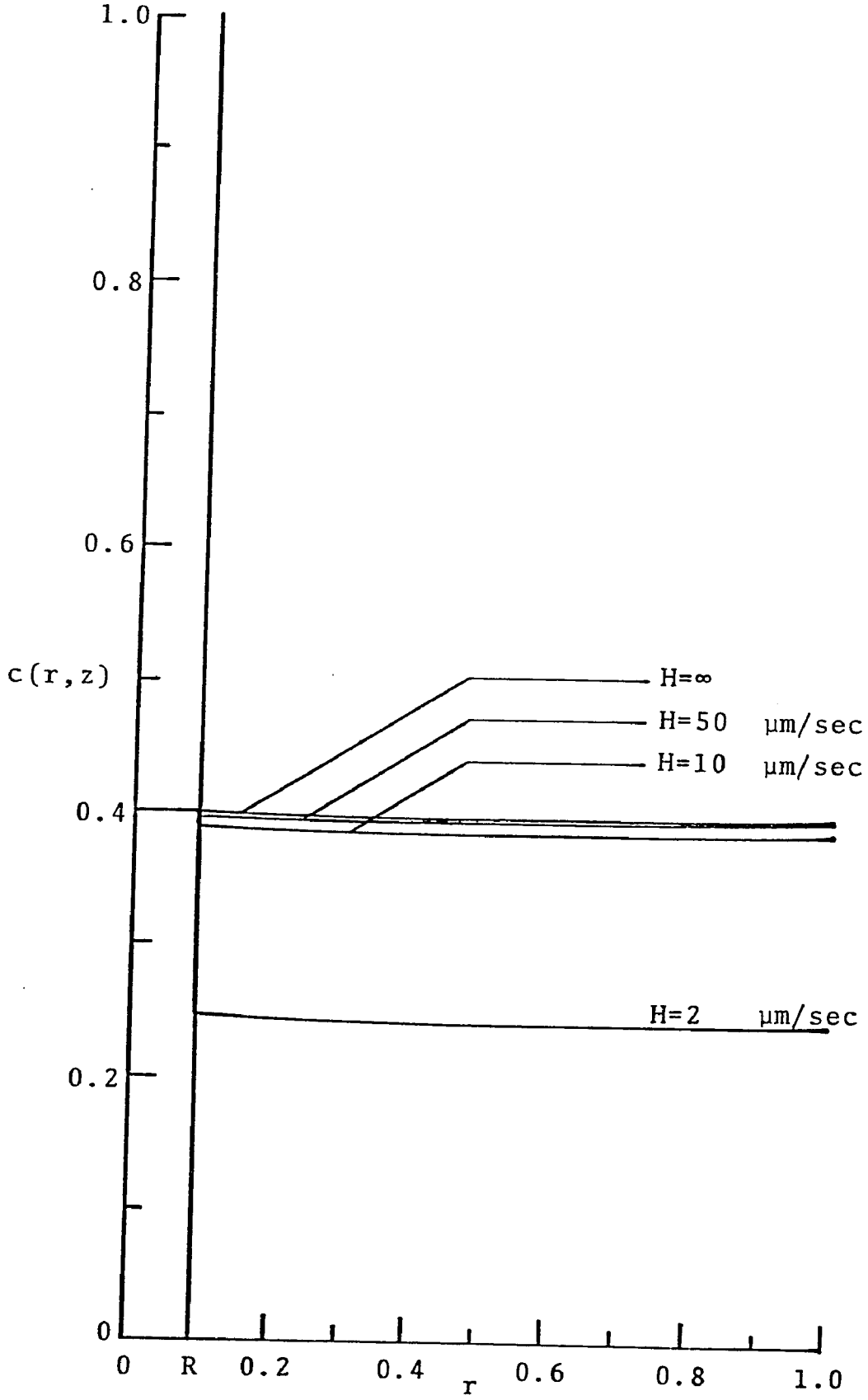

Figure 10. Normalized tissue concentration as a function of radial position at $z=1$, for various values of the permeability H.

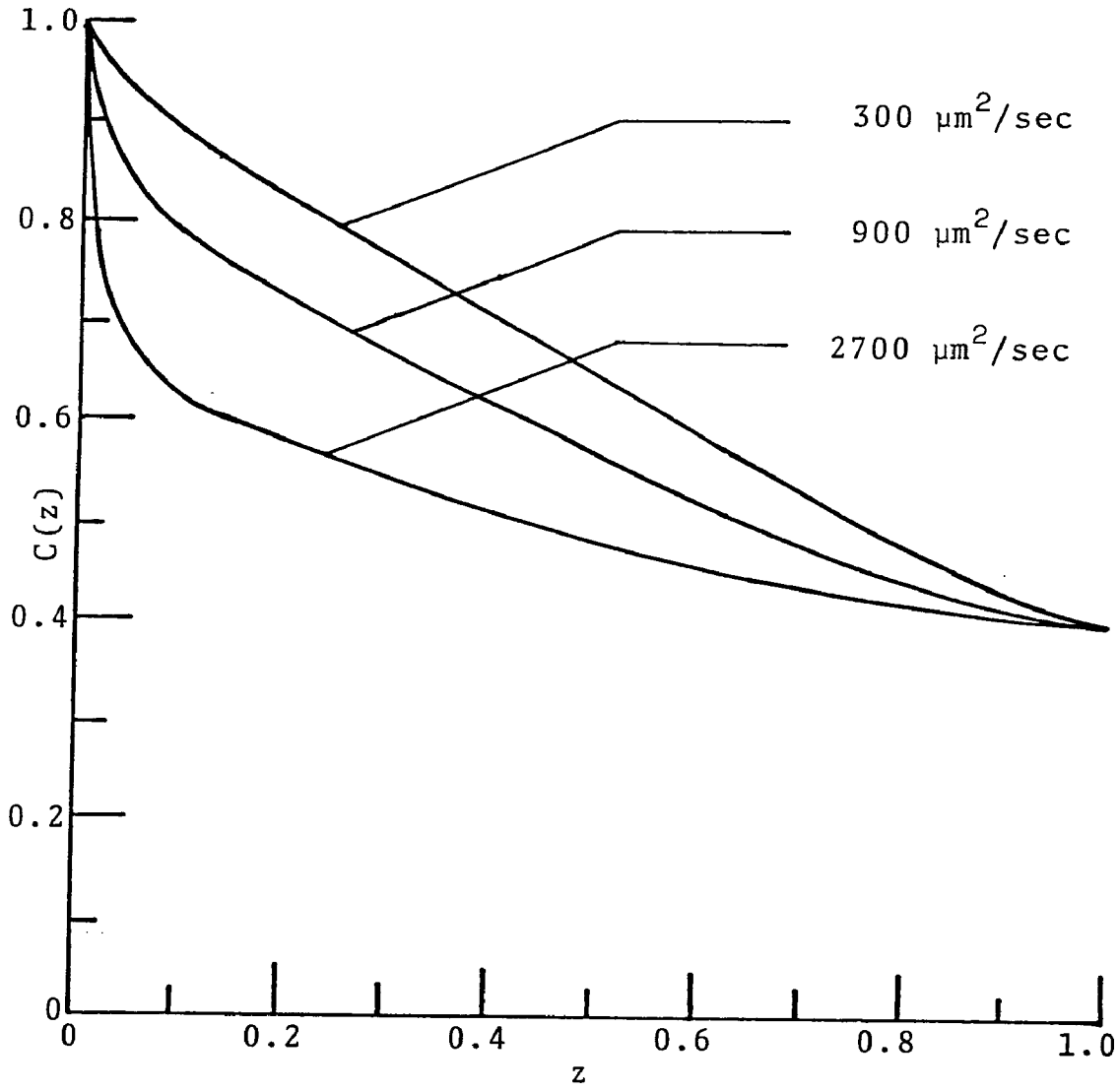

Figure 11. Normalized capillary concentration as a function of distance, for permeability H=50 μm/sec and various values of tissue diffusivity.

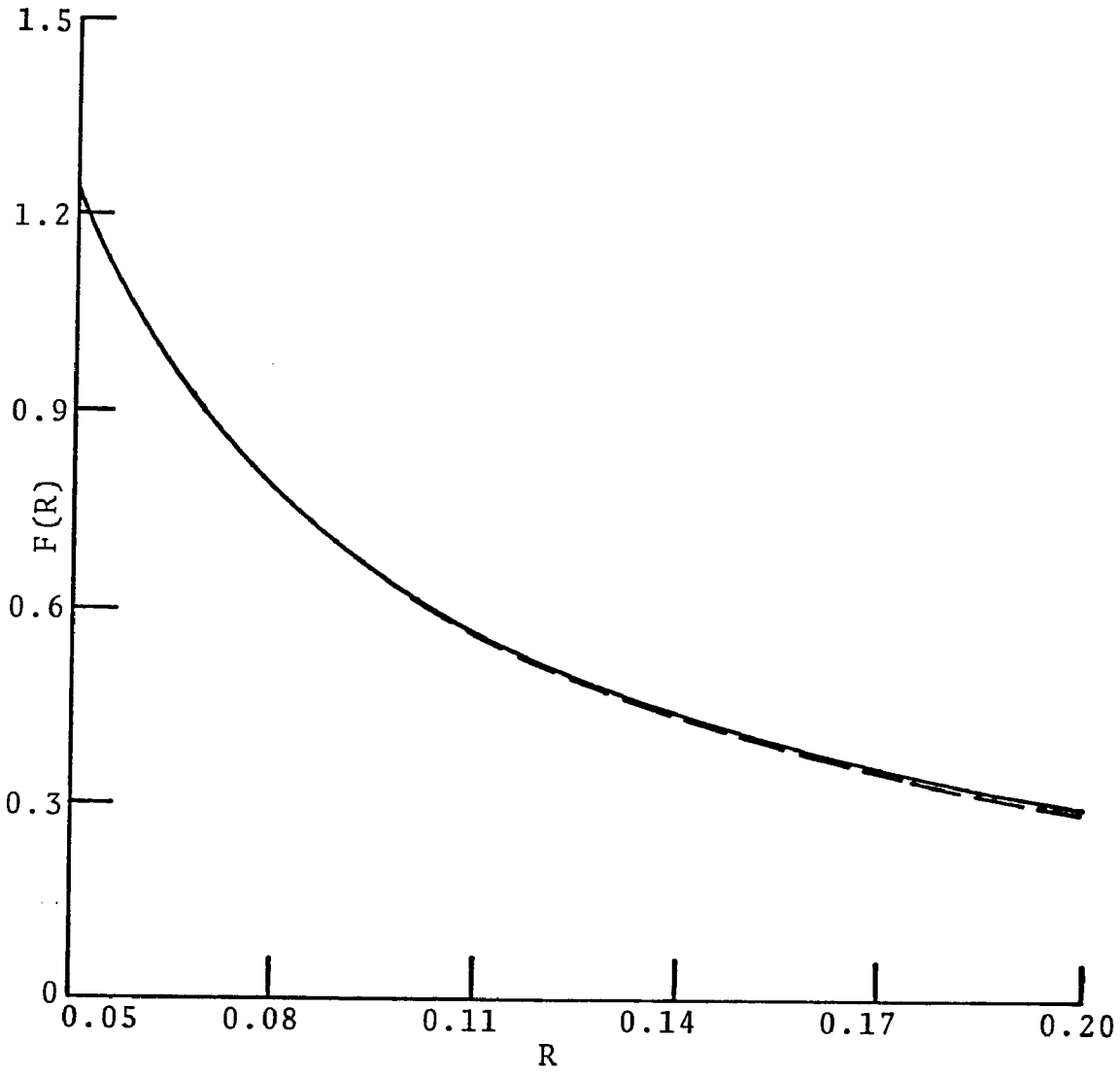

Figure 12. The function F(R) , defined by eqns. (5.132) and (5.133). ———————— exact form, — — — — — — approximate form, based on eight terms in the eigenfunction expansion.

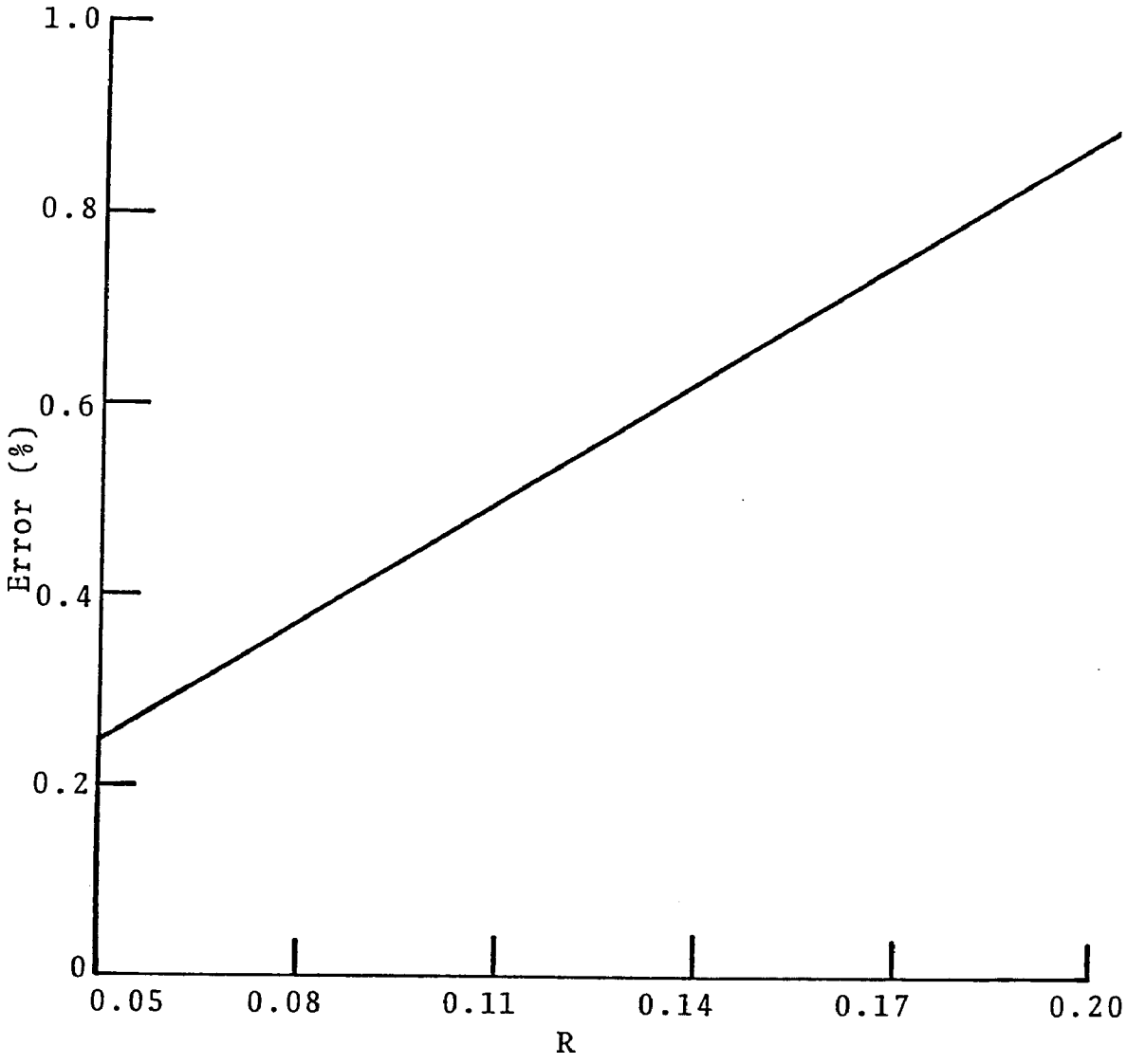

Figure 13. Error in F(R) as a function of R, resulting from using an eight term eigenfunction expansion.

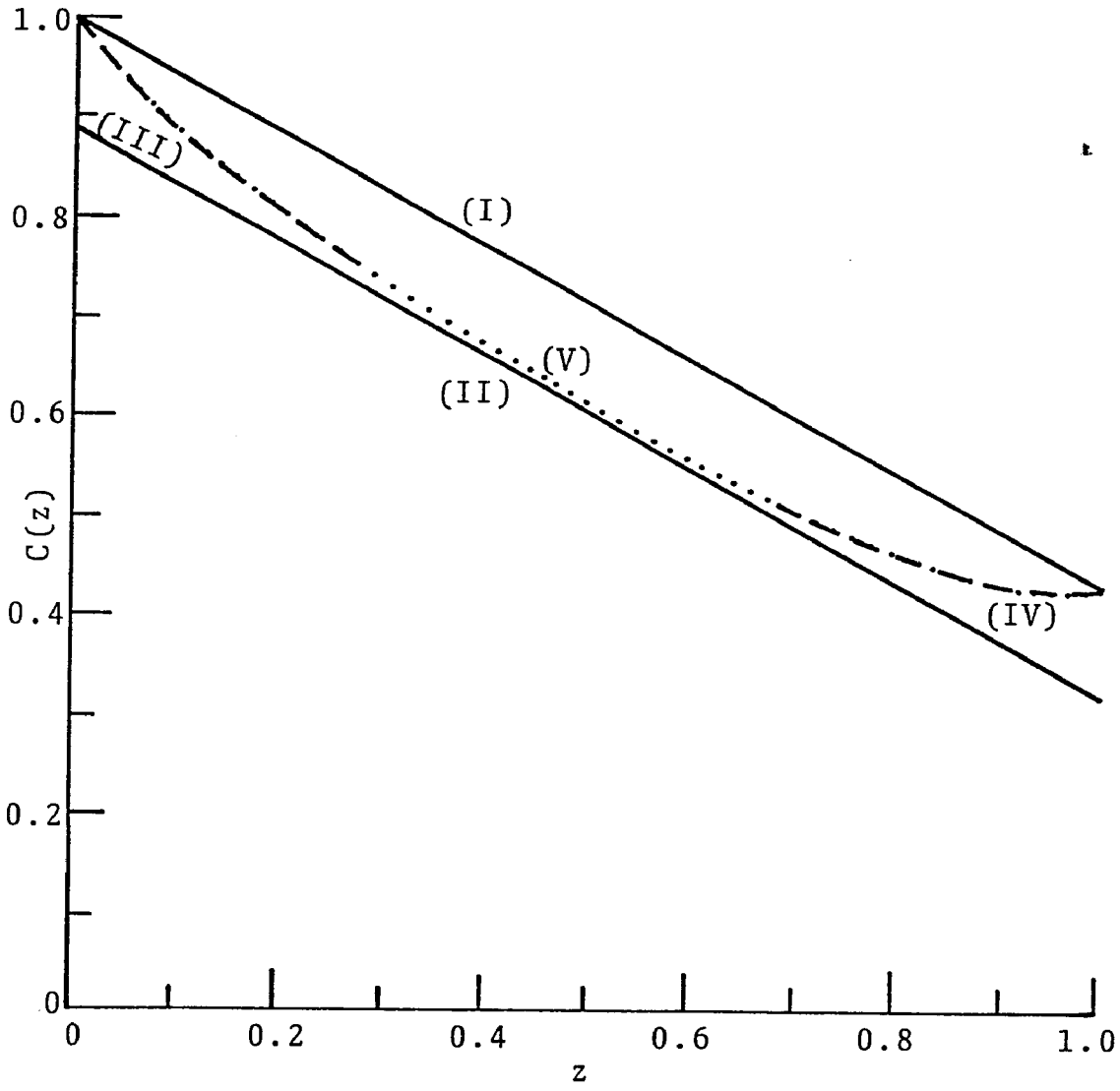

Figure 14. Normalized blood oxygen concentration as a function of distance, for example (1) in table I. (I) ———— without axial diffusion, (II) ———— with axial diffusion, (III) — — — — arterial boundary layer solution, (IV) — — — — venous boundary layer solution, (V) ····· composite solution.

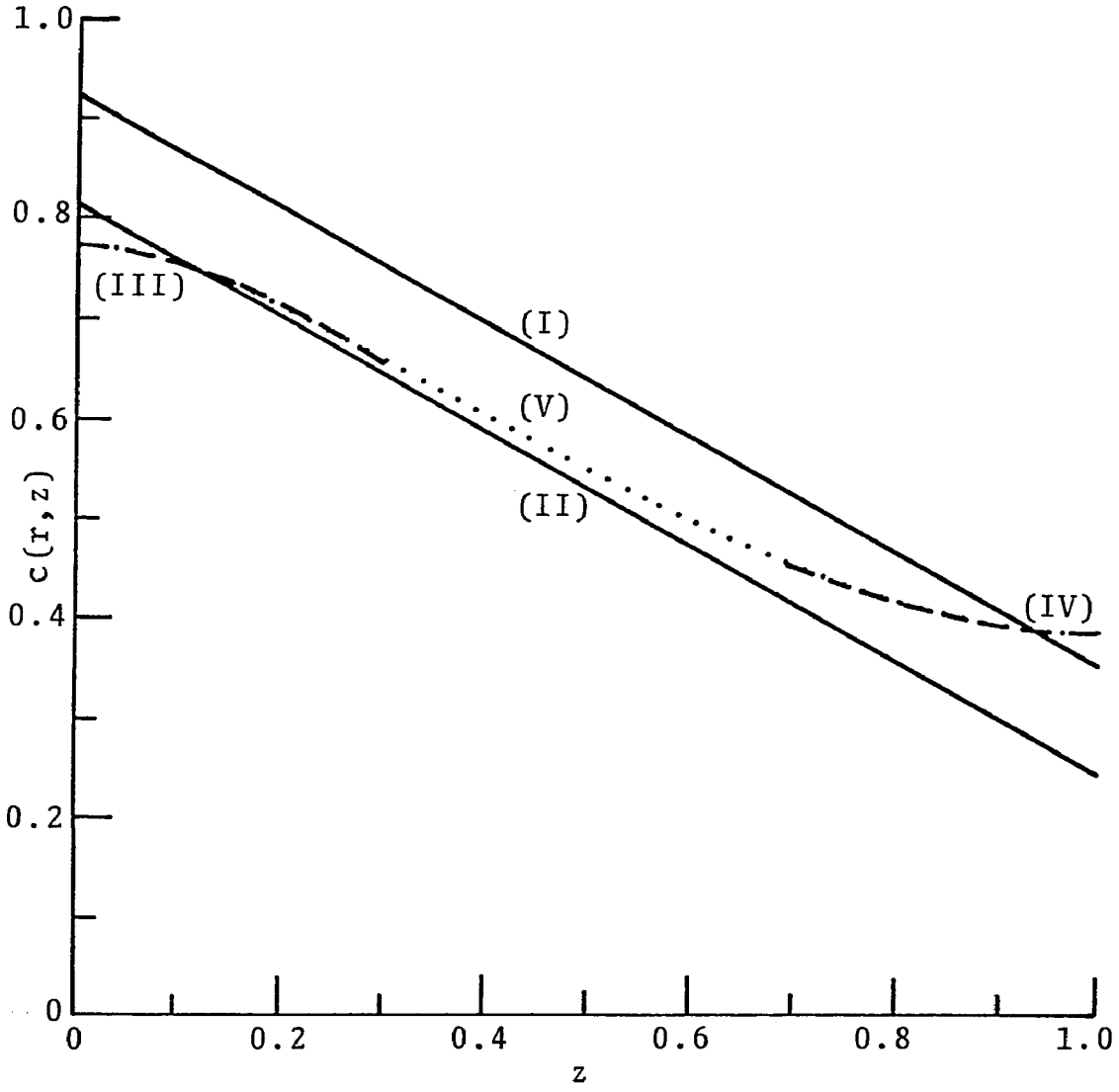

Figure 15. Normalized tissue oxygen concentration midway between the capillary wall and the outer edge of the tissue as a function of axial position, for example (1) in table I. (I) ———— without axial diffusion, (II) ———— with axial diffusion, (III) — — — — arterial boundary layer solution, (IV) — — — — venous boundary layer solution, (V) ····· composite solution.

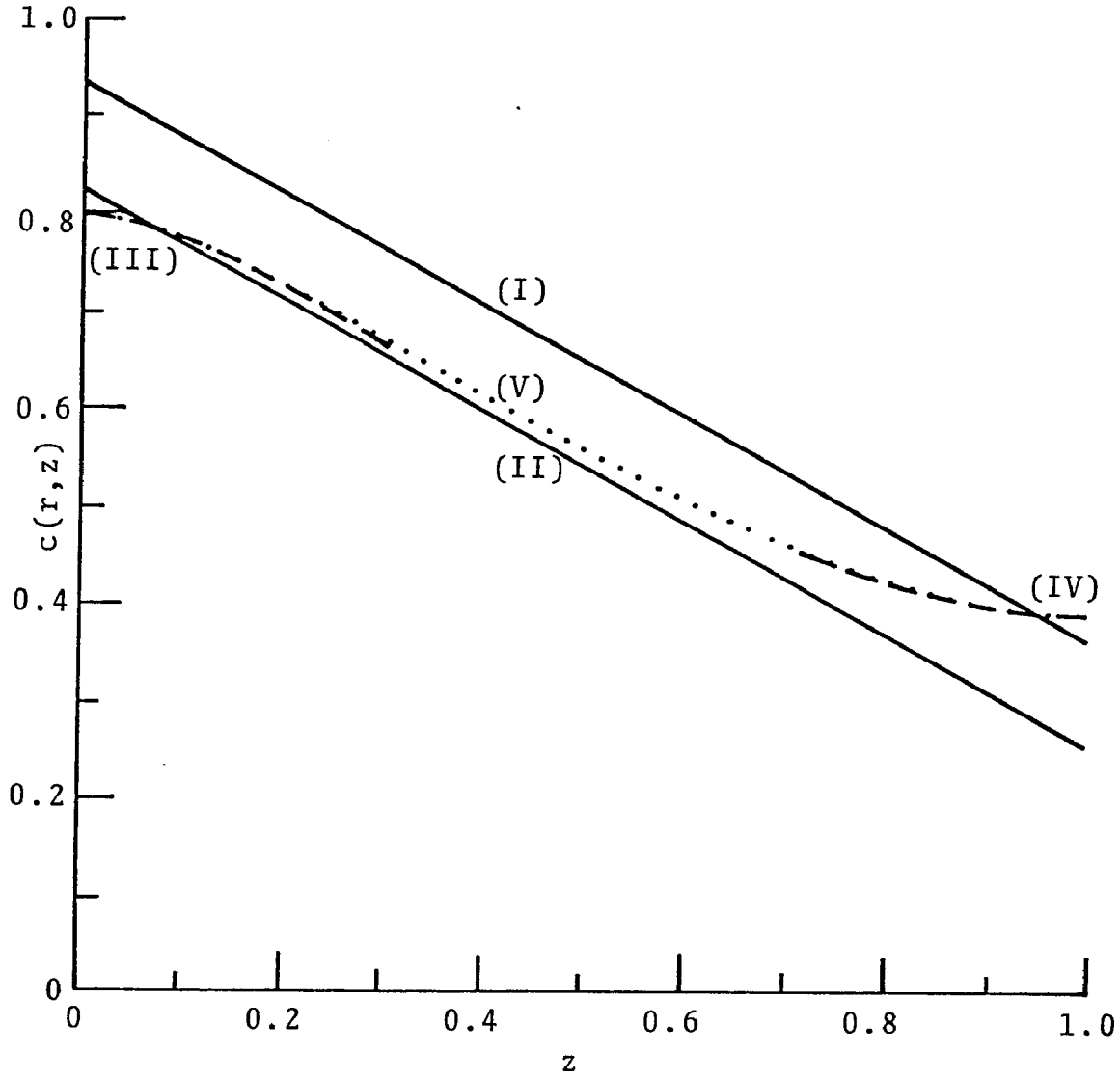

Figure 16. Normalized tissue oxygen concentration at the outer edge of the tissue as a function of axial position, for example (1) in table I. (I) ———— without axial diffusion, (II) ———— with axial diffusion, (III) — — — — arterial boundary layer solution, (IV) — — — — venous boundary layer solution, (V) ····· composite solution.

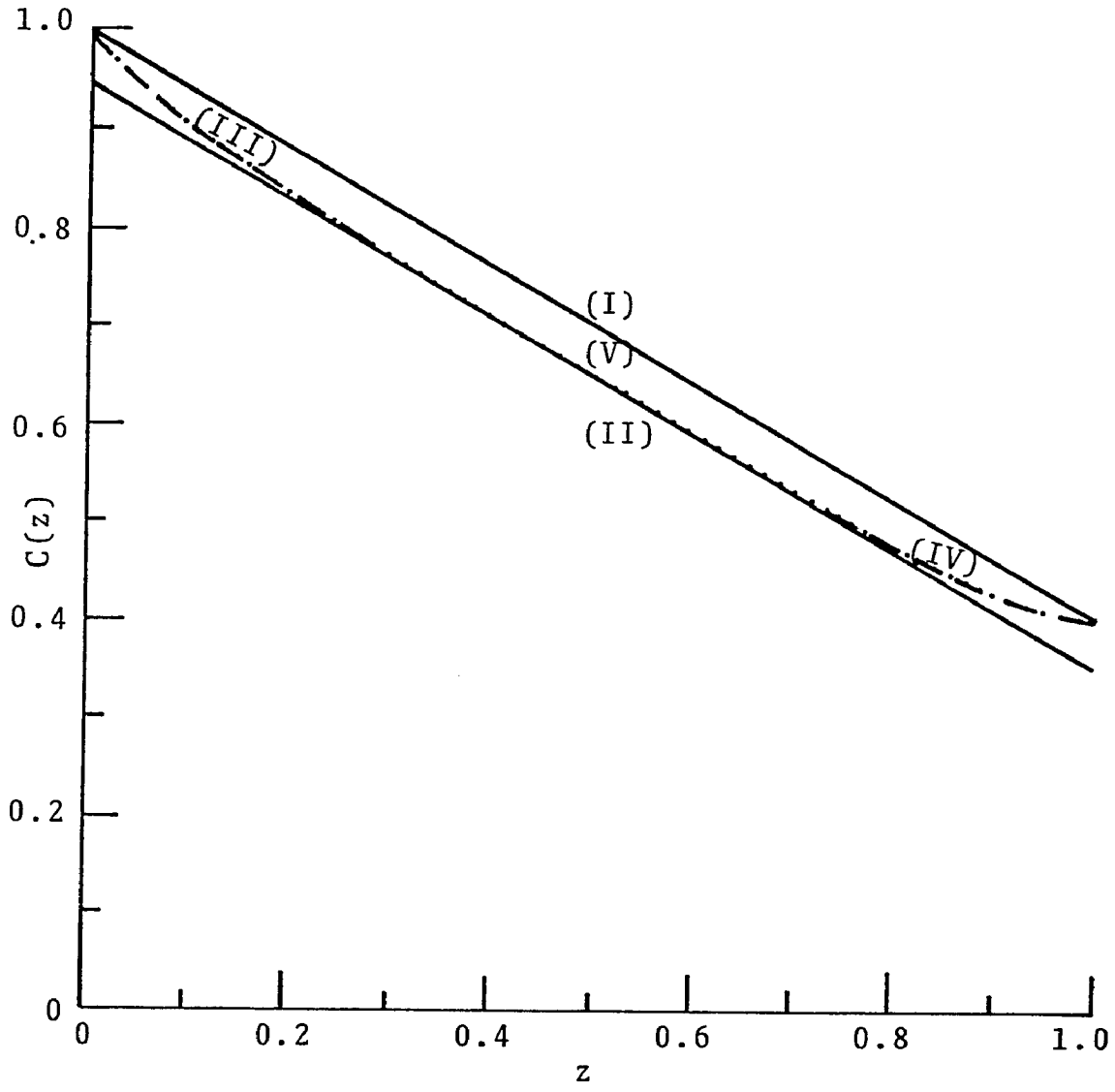

Figure 17. Normalized blood oxygen concentration as a function of distance, for example (2) of table I. (I) ——— without axial diffusion, (II) ——— with axial diffusion, (III) — — — — arterial boundary layer solution, (IV) — — — — venous boundary layer solution, (V) ····· composite solution.

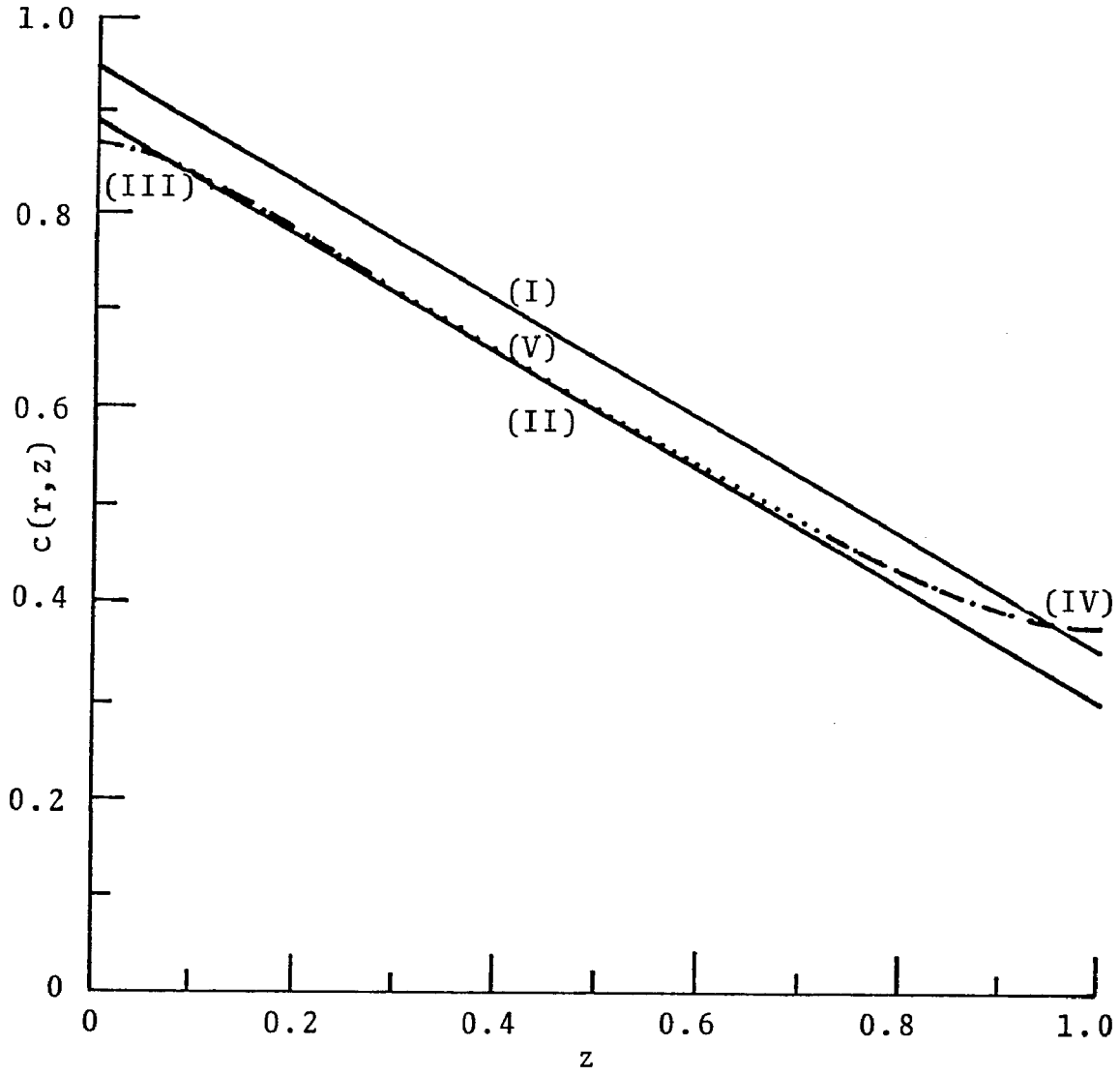

Figure 18. Normalized tissue oxygen concentration midway between the capillary wall and the outer edge of the tissue as a function of axial position, for example (2) in table I. (I) ———— without axial diffusion, (II) ———— with axial diffusion, (III) — — — — arterial boundary layer solution, (IV) — — — — venous boundary layer solution, (V) ····· composite solution.

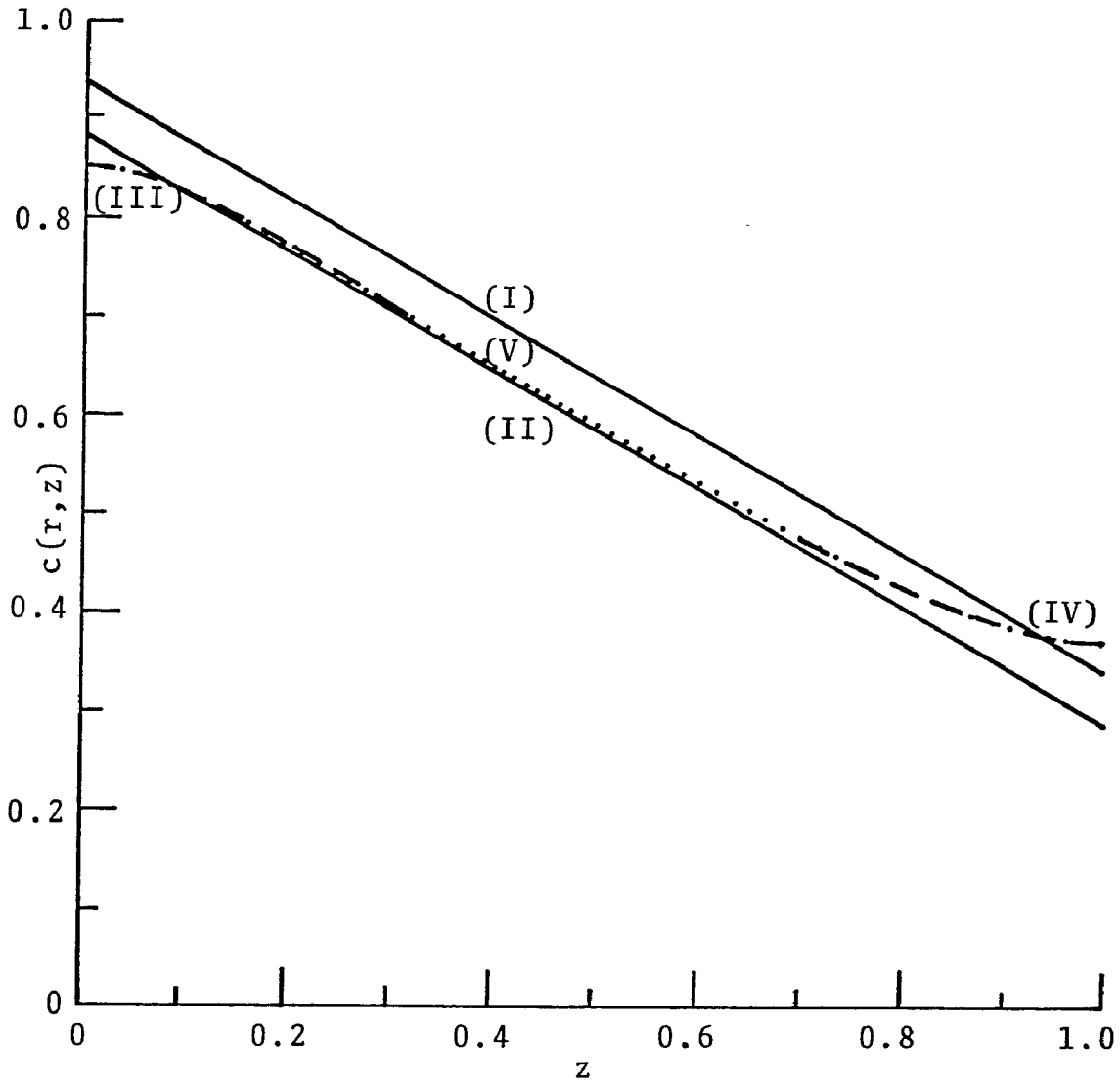

Figure 19. Normalized tissue oxygen concentration at the outer edge of the tissue as a function of axial position, for example (2) in table I. (I) ———— without axial diffusion, (II) ———— with axial diffusion, (III) — — — — arterial boundary layer solution, (IV) — — — — venous boundary layer solution, (V) ····· composite solution.

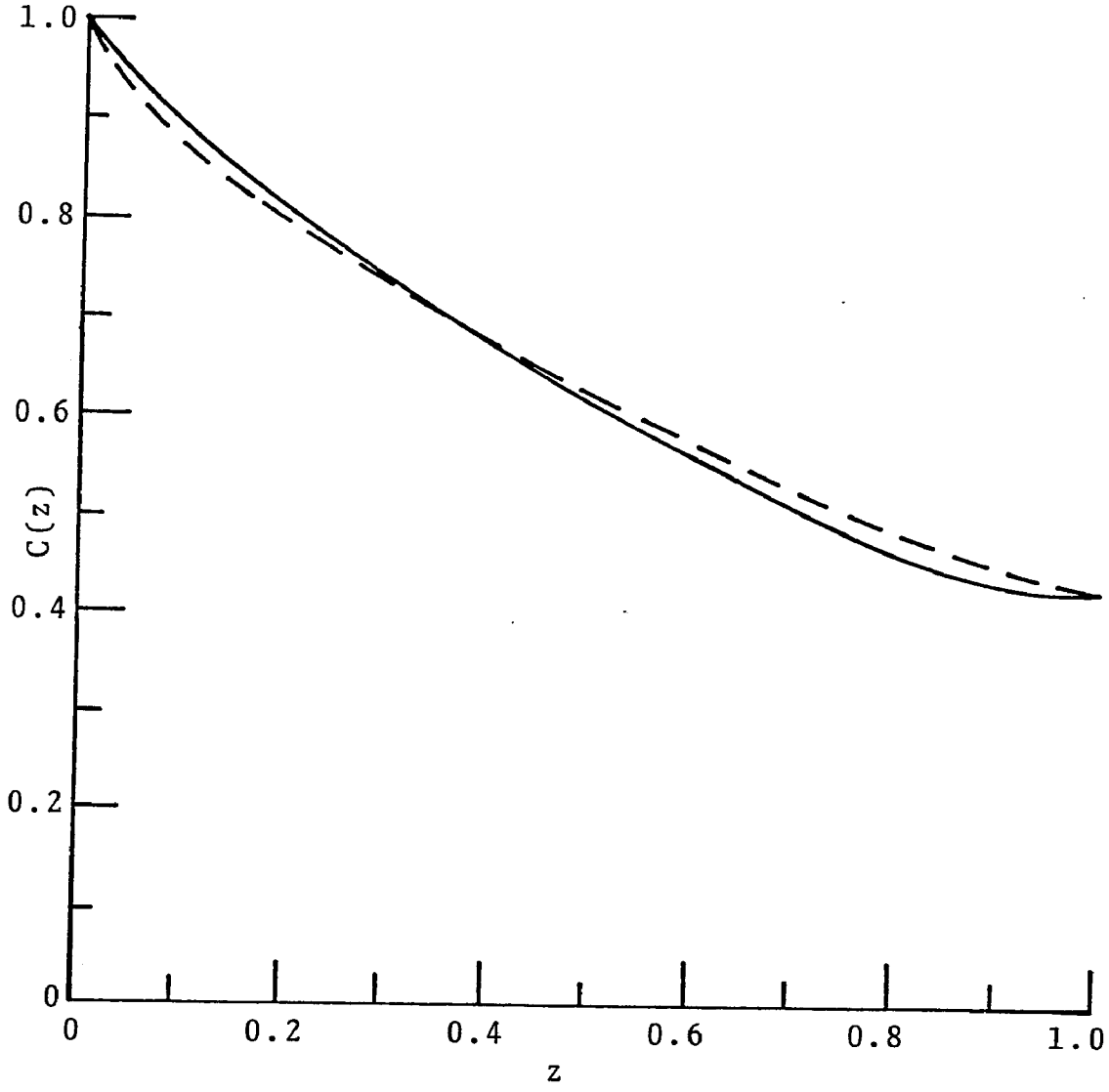

Figure 20. Normalized blood oxygen concentration as a function of distance, for example (1) in table I. ———— composite solution, — — — — exact solution.

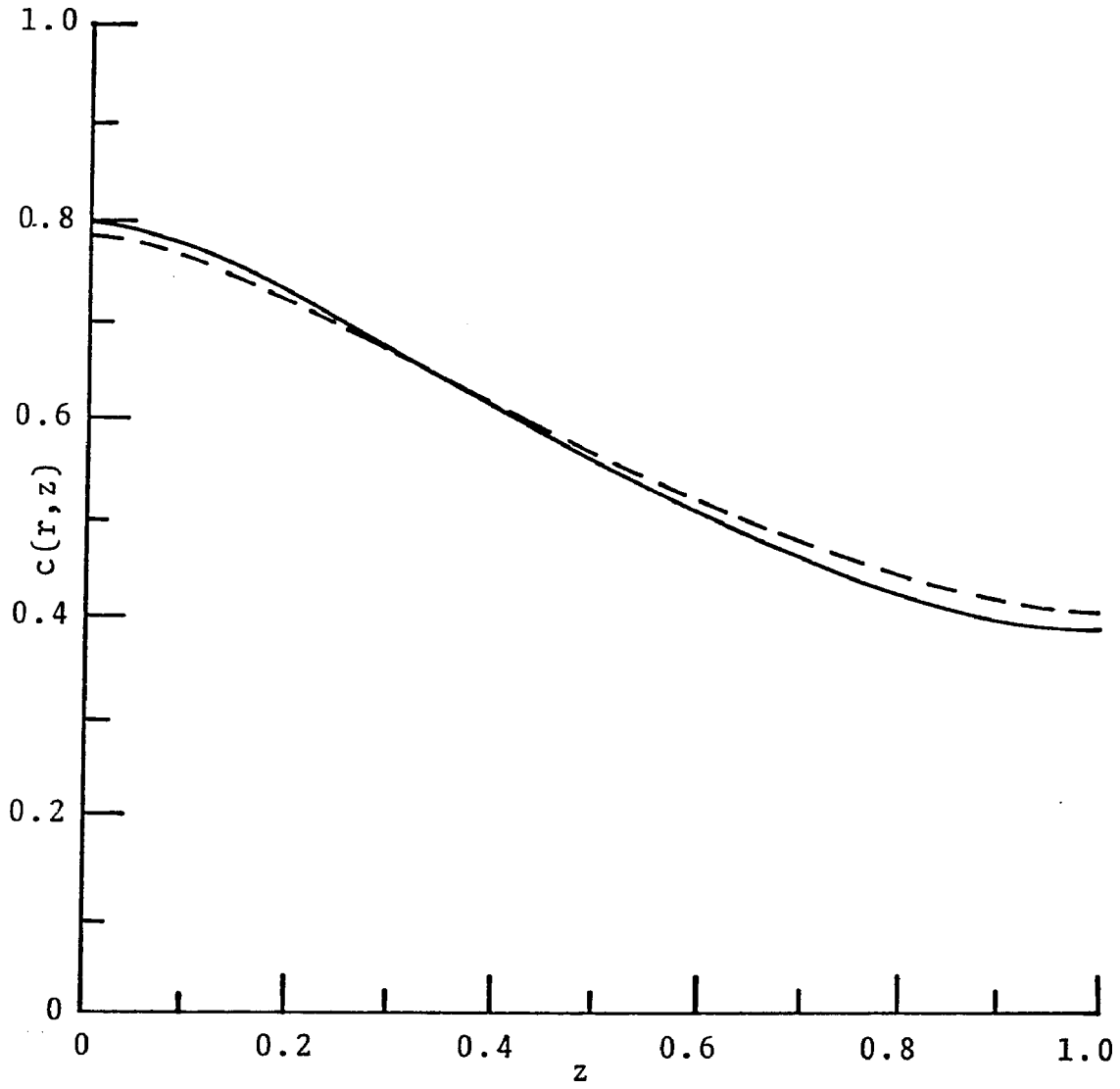

Figure 21. Normalized tissue oxygen concentration midway between the capillary wall and the outer edge of the tissue as a function of axial position, for example (1) in table I. ———— composite solution, — — — exact solution.

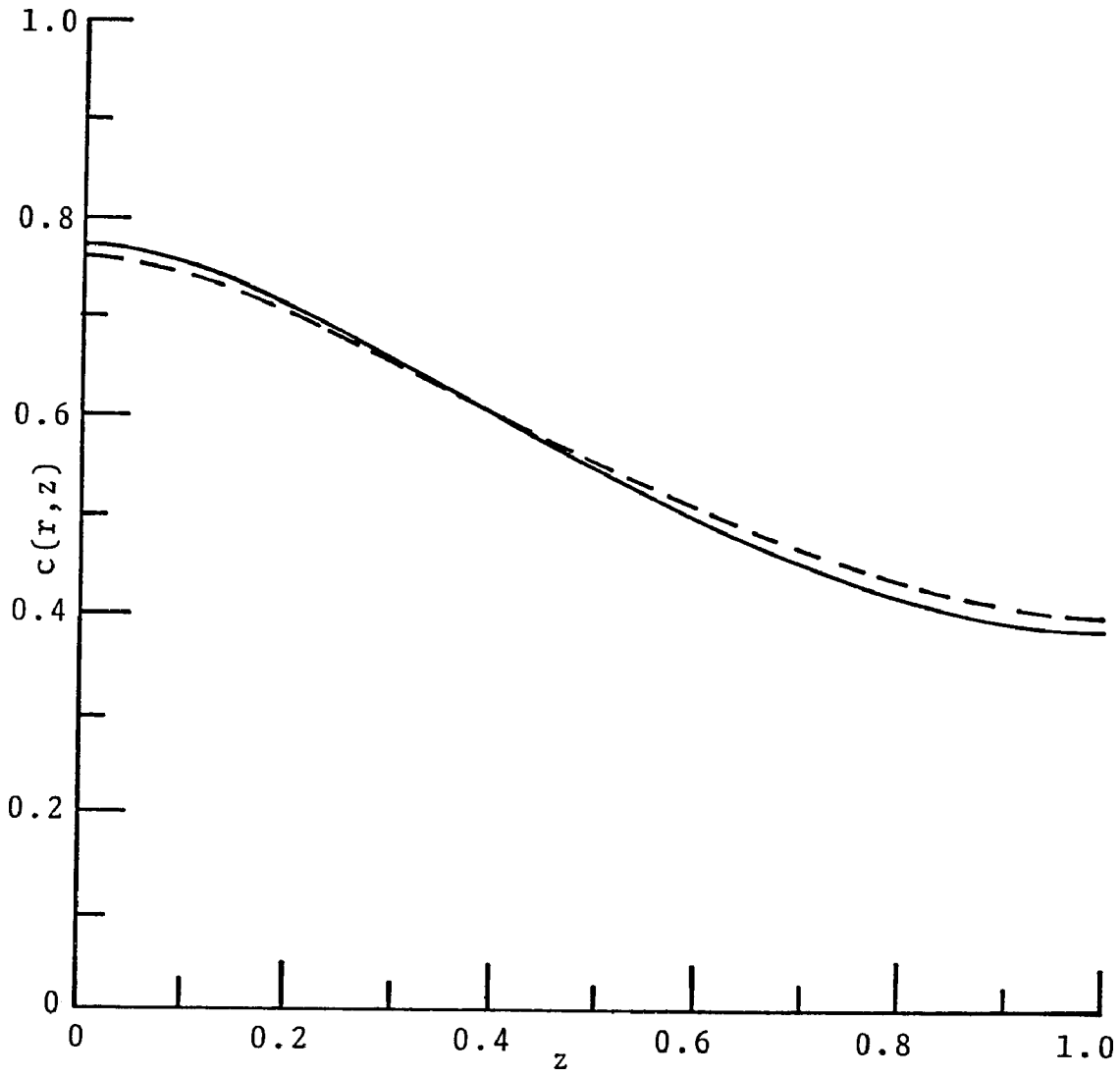

Figure 22. Normalized tissue oxygen concentration at the outer edge of the tissue as a function of axial position, for example (1) in table I. ———— composite solution, — — — — exact solution.

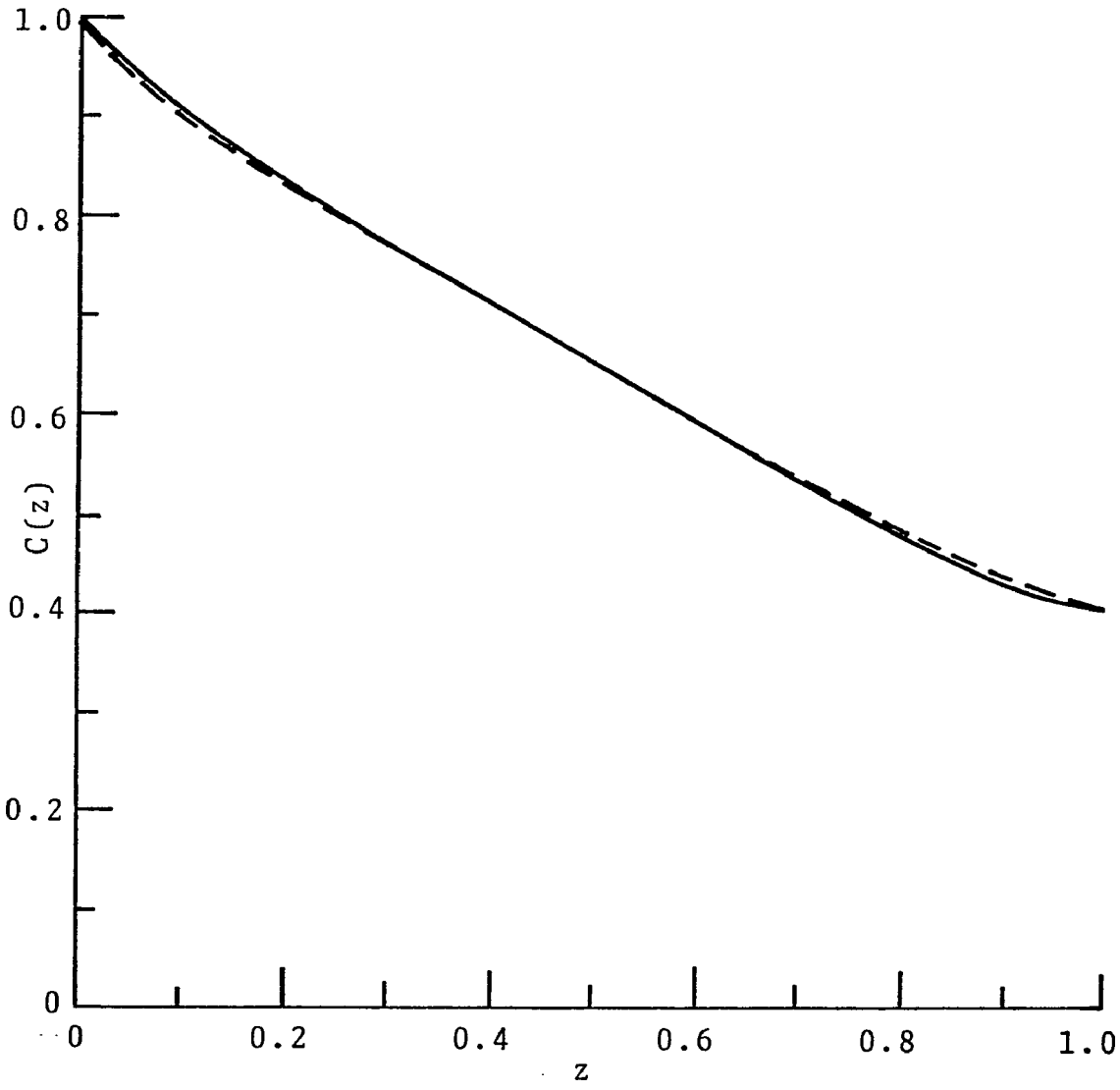

Figure 23. Normalized blood oxygen concentration as a function of distance, for example (2) in table I. ———— composite solution, — — — — exact solution.

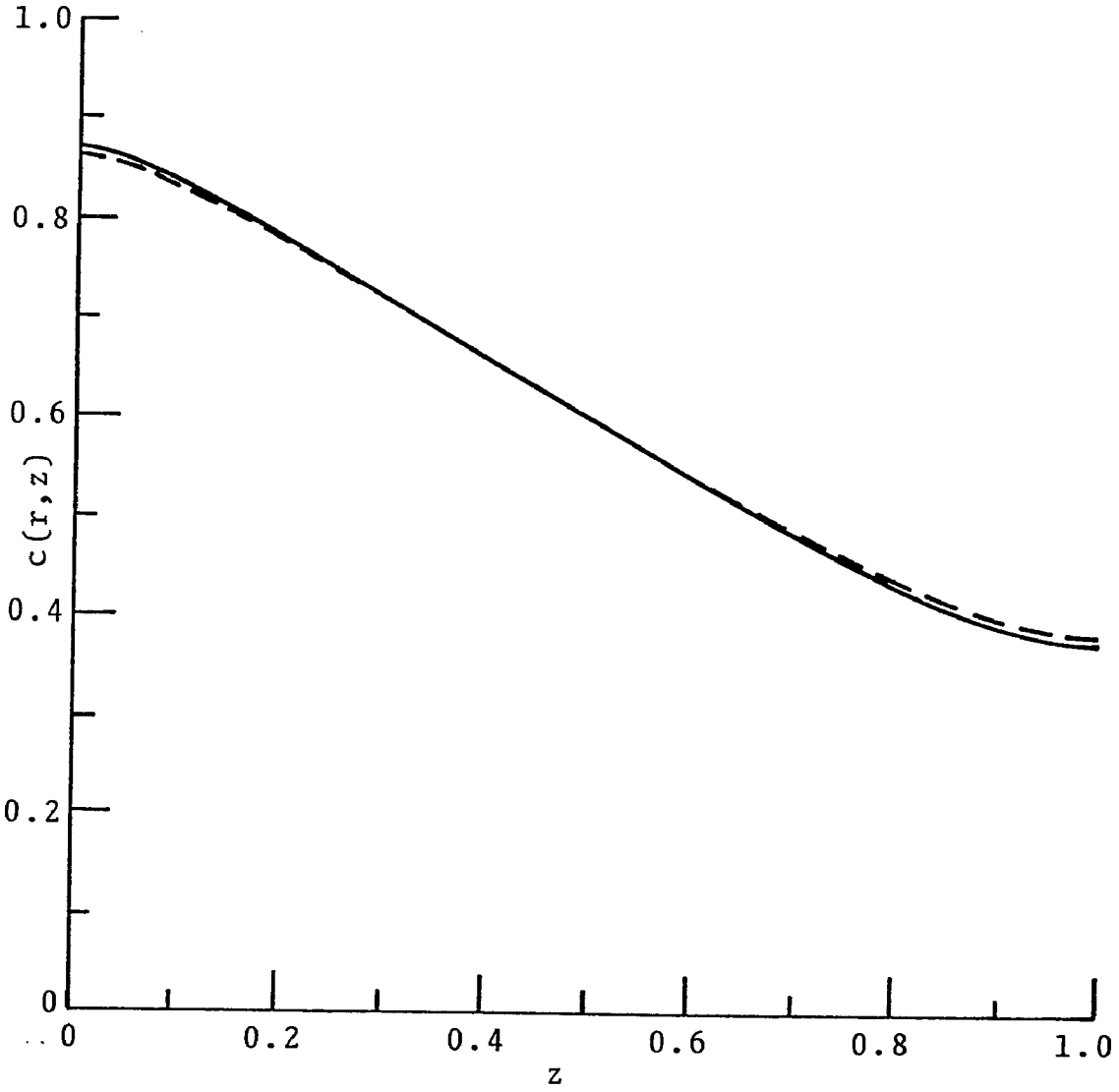

Figure 24. Normalized tissue oxygen concentration midway between the capillary wall and the outer edge of the tissue as a function of axial position, for example (2) in table I. ———— composite solution, — — — — exact solution.

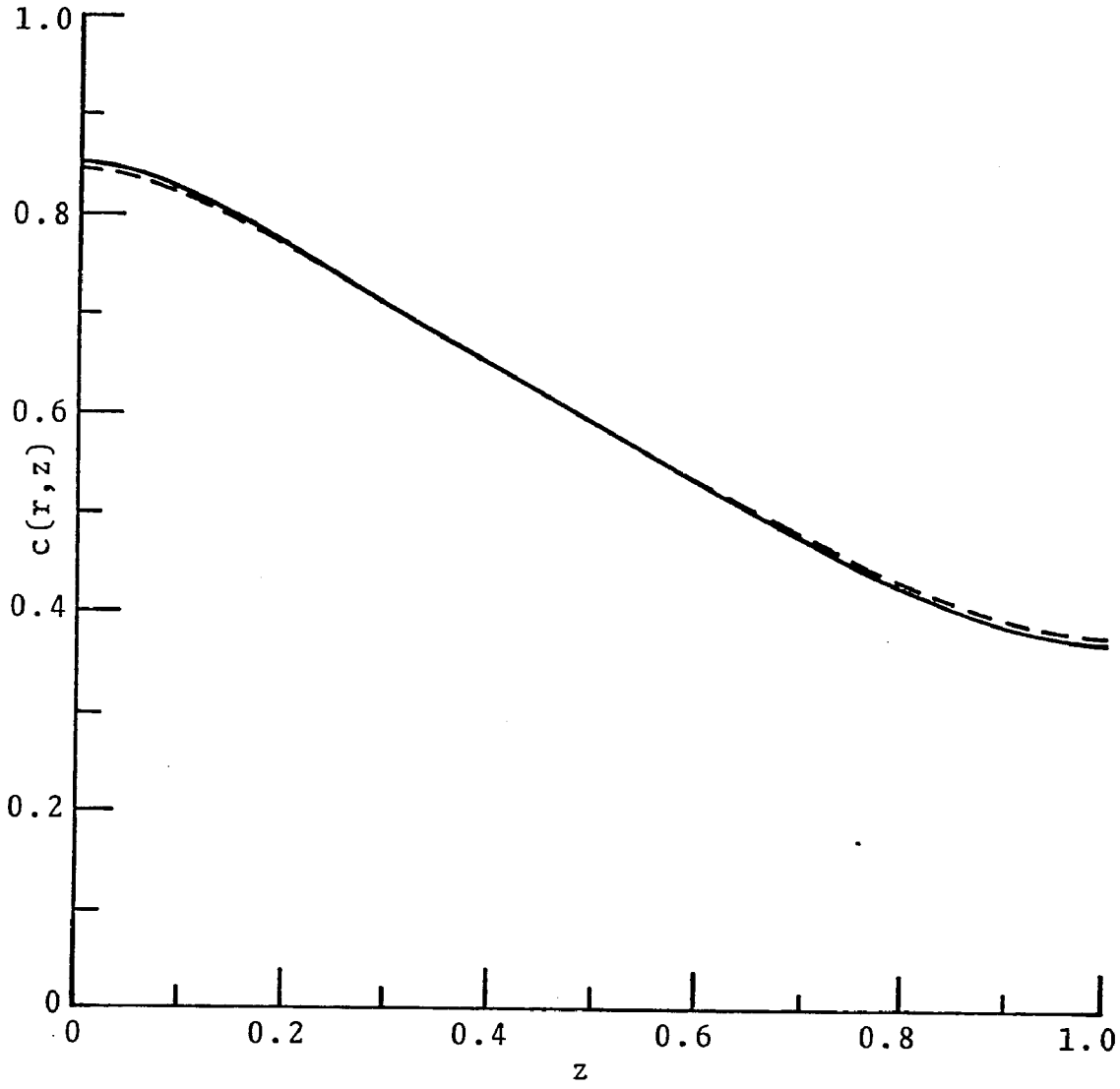

Figure 25. Normalized tissue oxygen concentration at the outer edge of the tissue as a function of axial position, for example (2) in table I. ———— composite solution, — — — — exact solution.

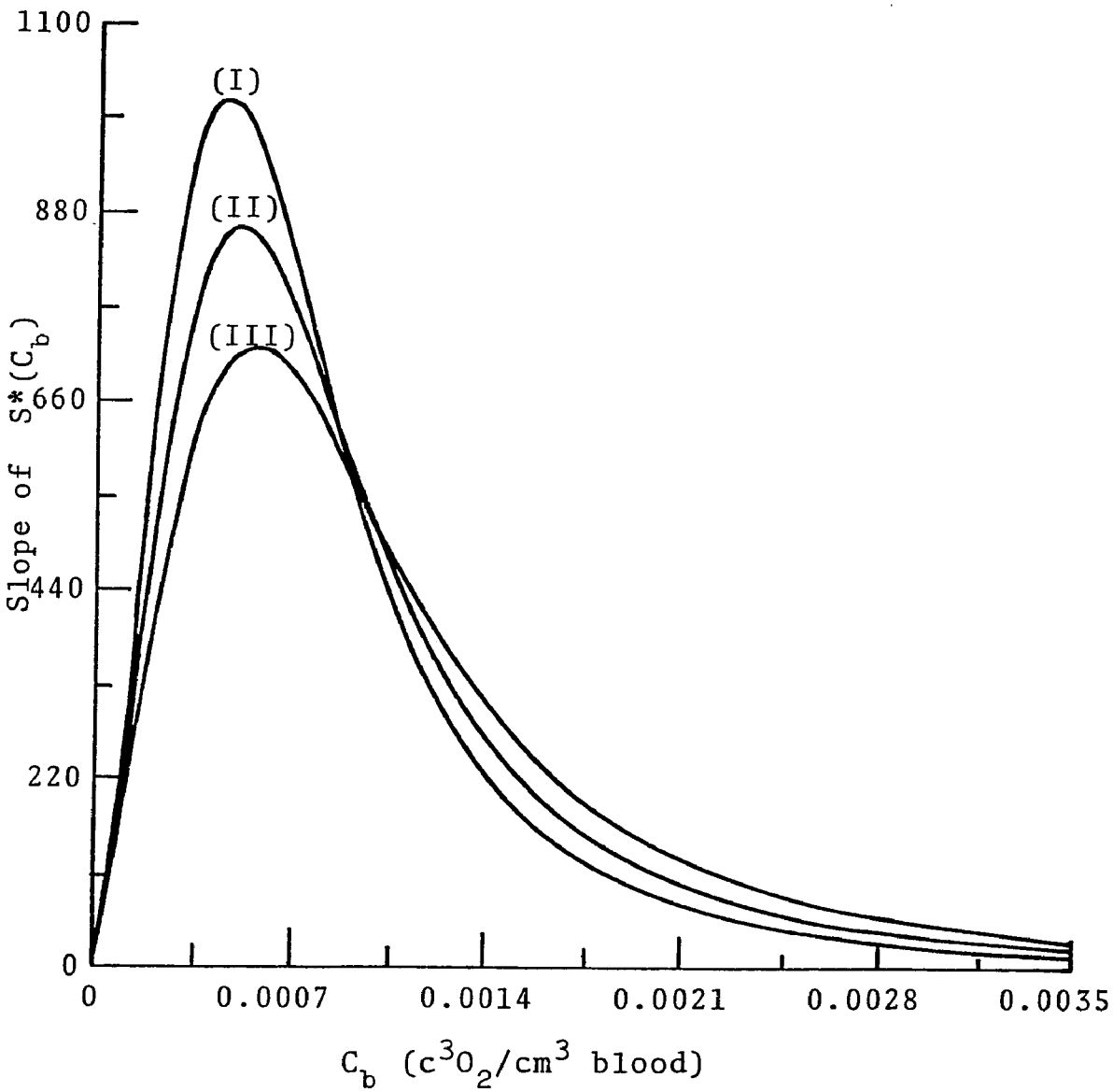

Figure 26. Slope of oxyhemoglobin dissociation curves as a function of blood oxygen concentration for various $S^*(C_b)$ which are shown in figure 2.

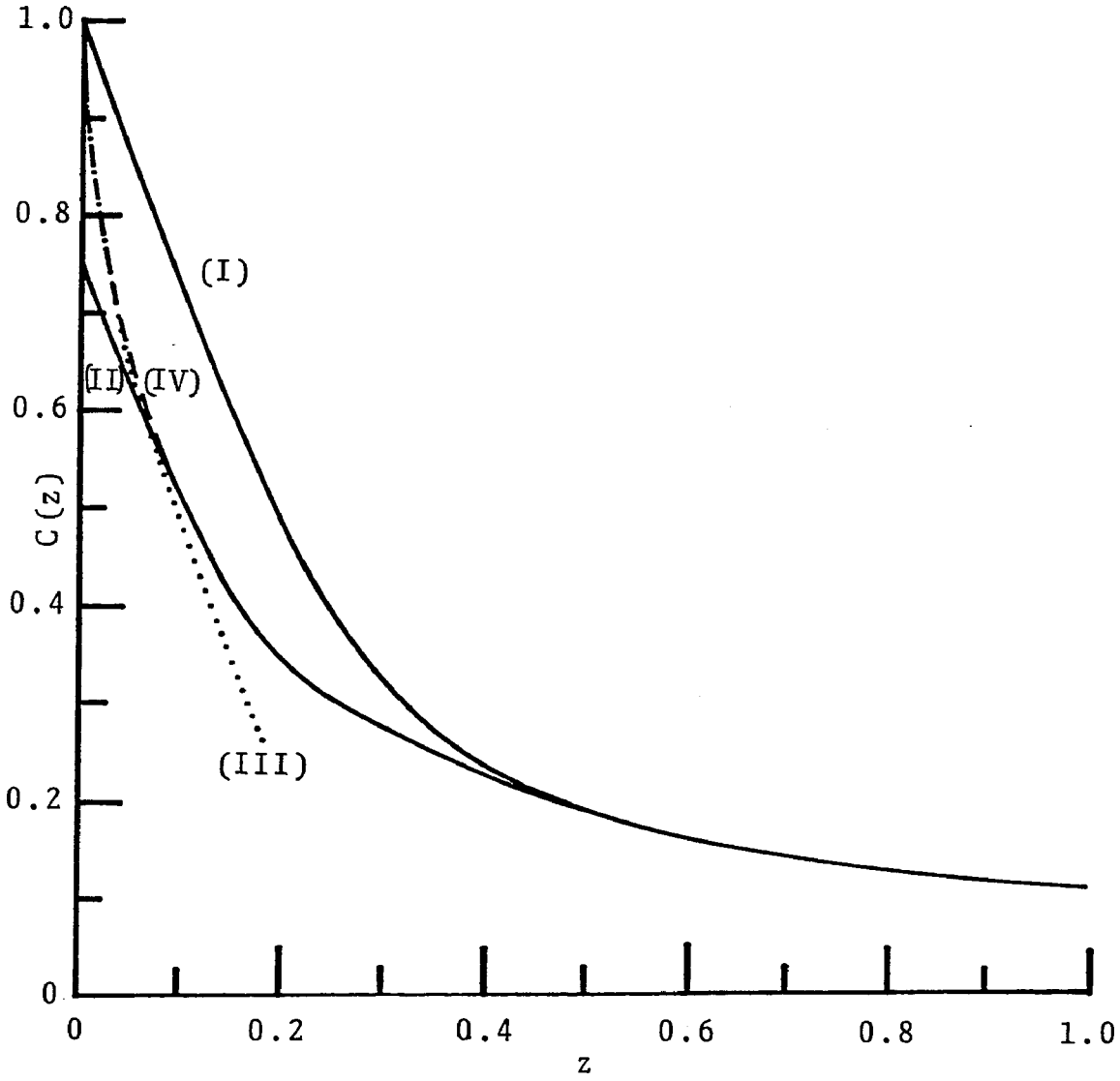

Figure 27. Normalized blood oxygen concentration as a function of axial position z , for the 1st set of data in table III. (I) ———— without axial diffusion, (II) ———— with axial diffusion, (III) ····· boundary layer solution, (IV) — — — — — composite solution.

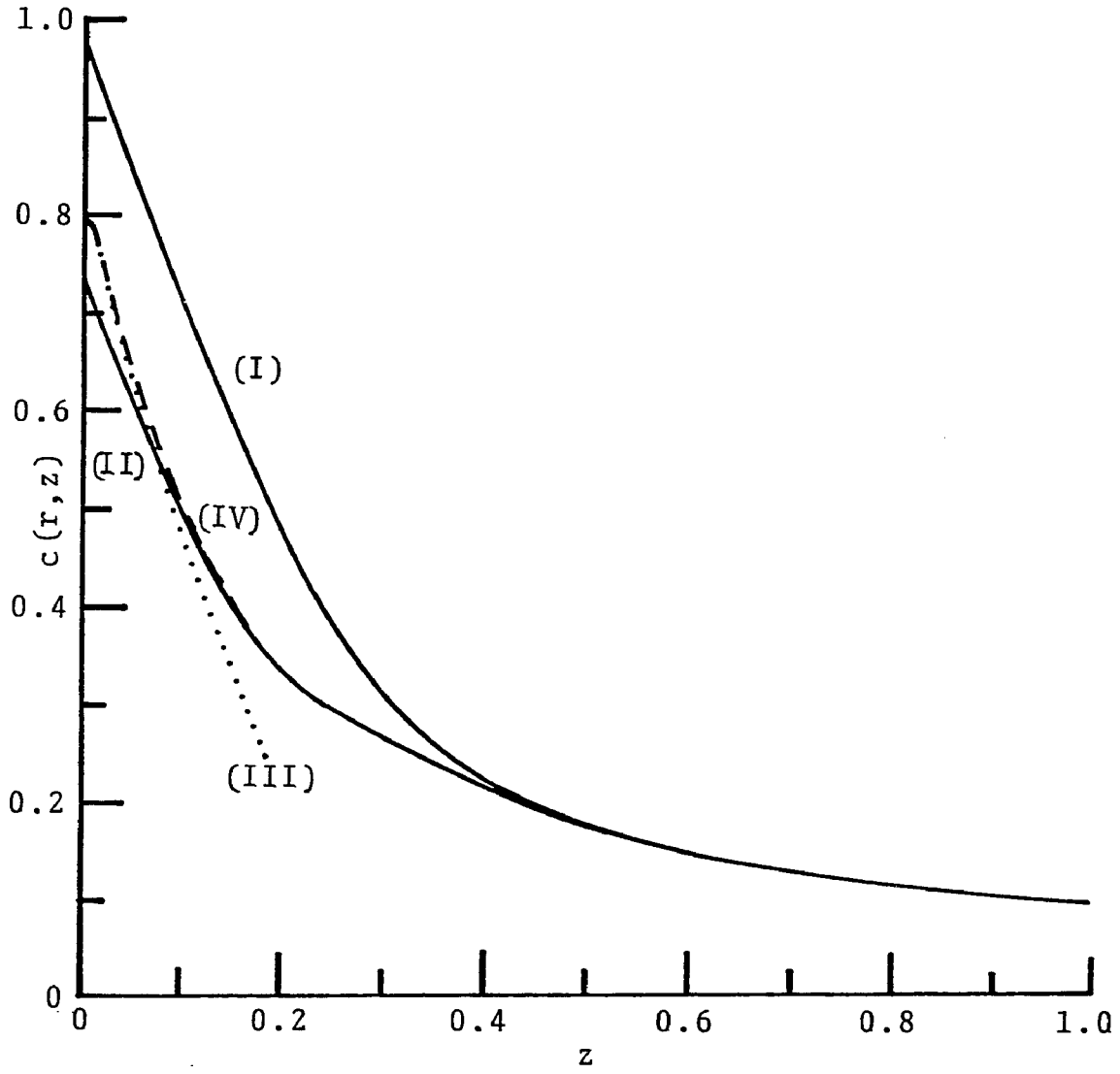

Figure 28. Normalized tissue oxygen concentration midway between the capillary wall and the outer edge of the tissue as a function of axial position z , for the 1st set of data in table III. (I) ———— without axial diffusion, (II) ———— with axial diffusion, (III)····· boundary layer solution, (IV) — — — — — composite solution.

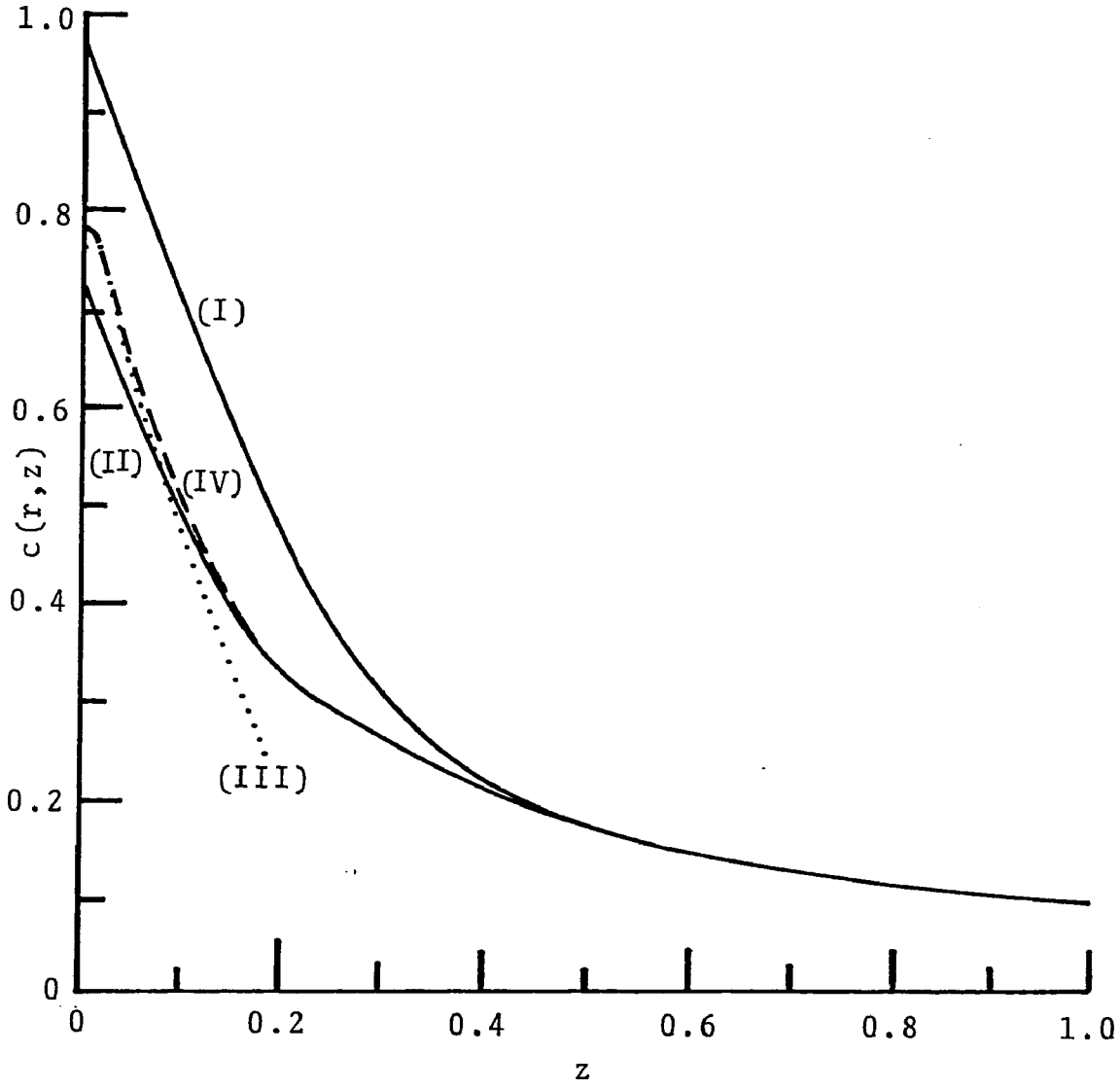

Figure 29. Normalized tissue oxygen concentration at the outer edge of the tissue as a function of axial position z , for the 1st set of data in table III. (I) ———— without axial diffusion, (II) ———— with axial diffusion, (III) ····· boundary layer solution, (IV) — — — — composite solution.

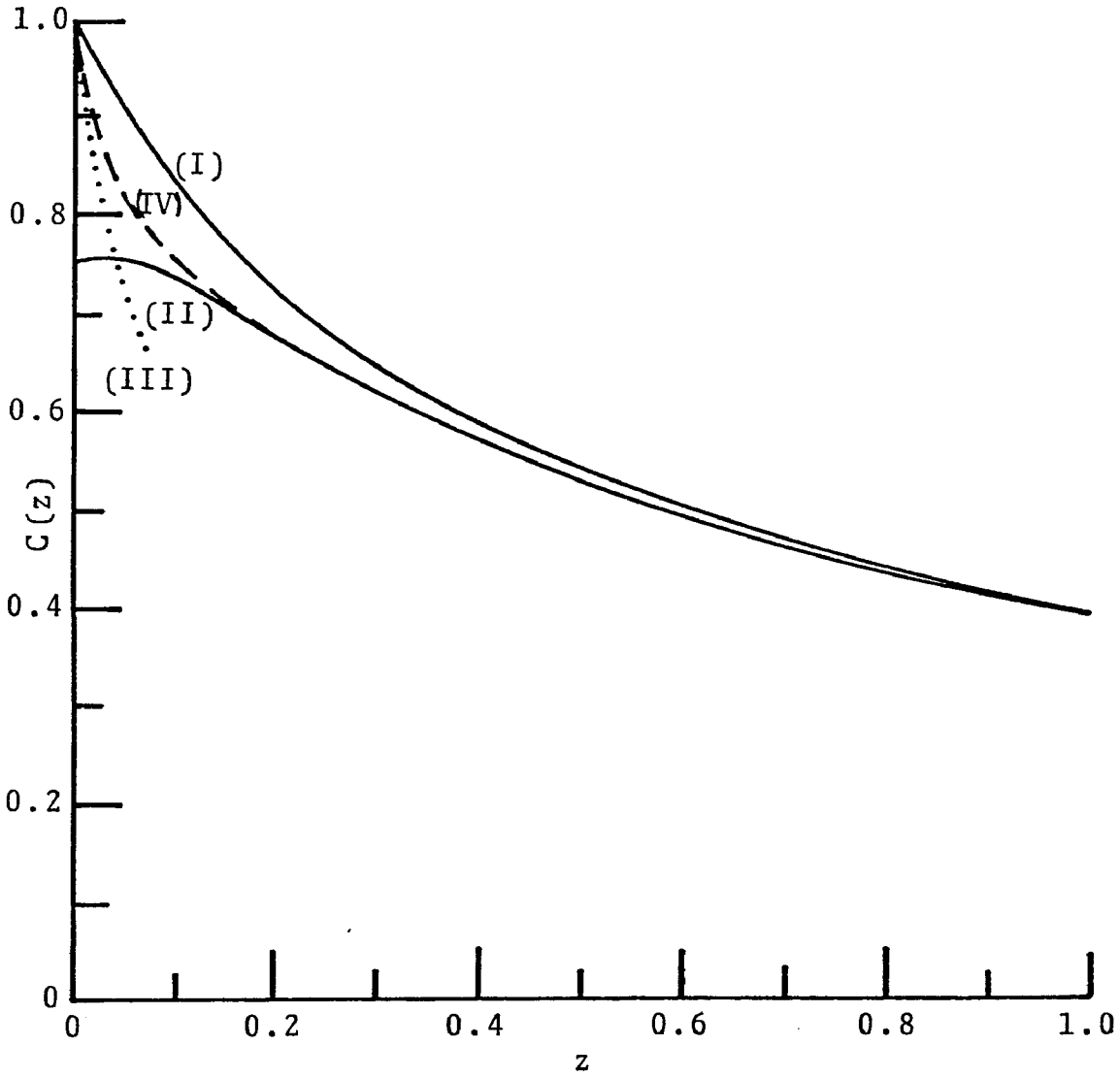

Figure 30. Normalized blood oxygen concentration as a function of axial position z , for the 2nd set of data in table III. (I) ———— without axial diffusion, (II) ———— with axial diffusion, (III) ····· boundary layer solution, (IV) — — — — composite solution.

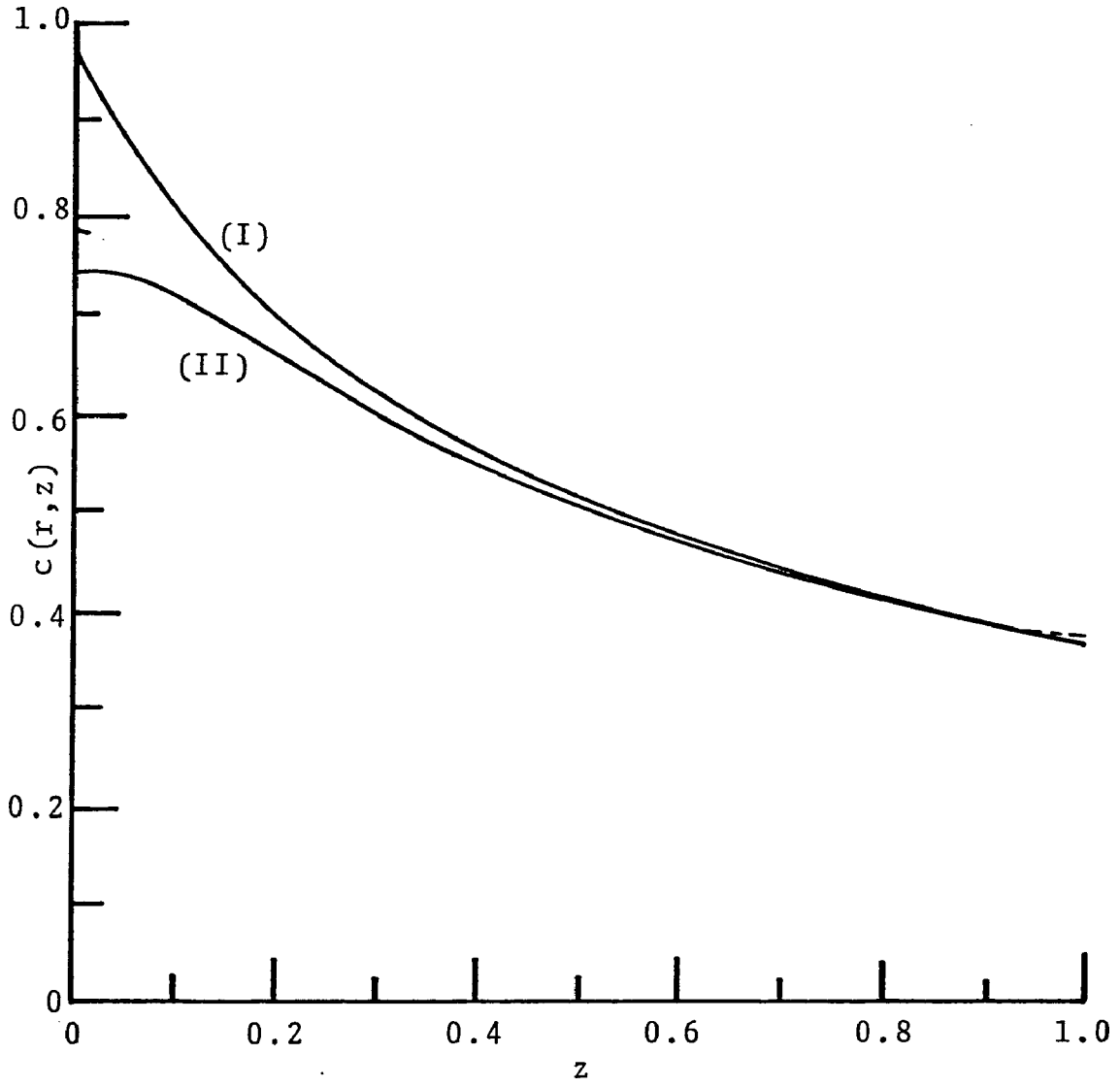

Figure 31. Normalized tissue oxygen concentration midway between the capillary wall and the outer edge of the tissue as a function of axial position z , for the 2nd set of data in table III. (I) ———— without axial diffusion, (II) ———— with axial diffusion, — — — — — boundary layer solution.

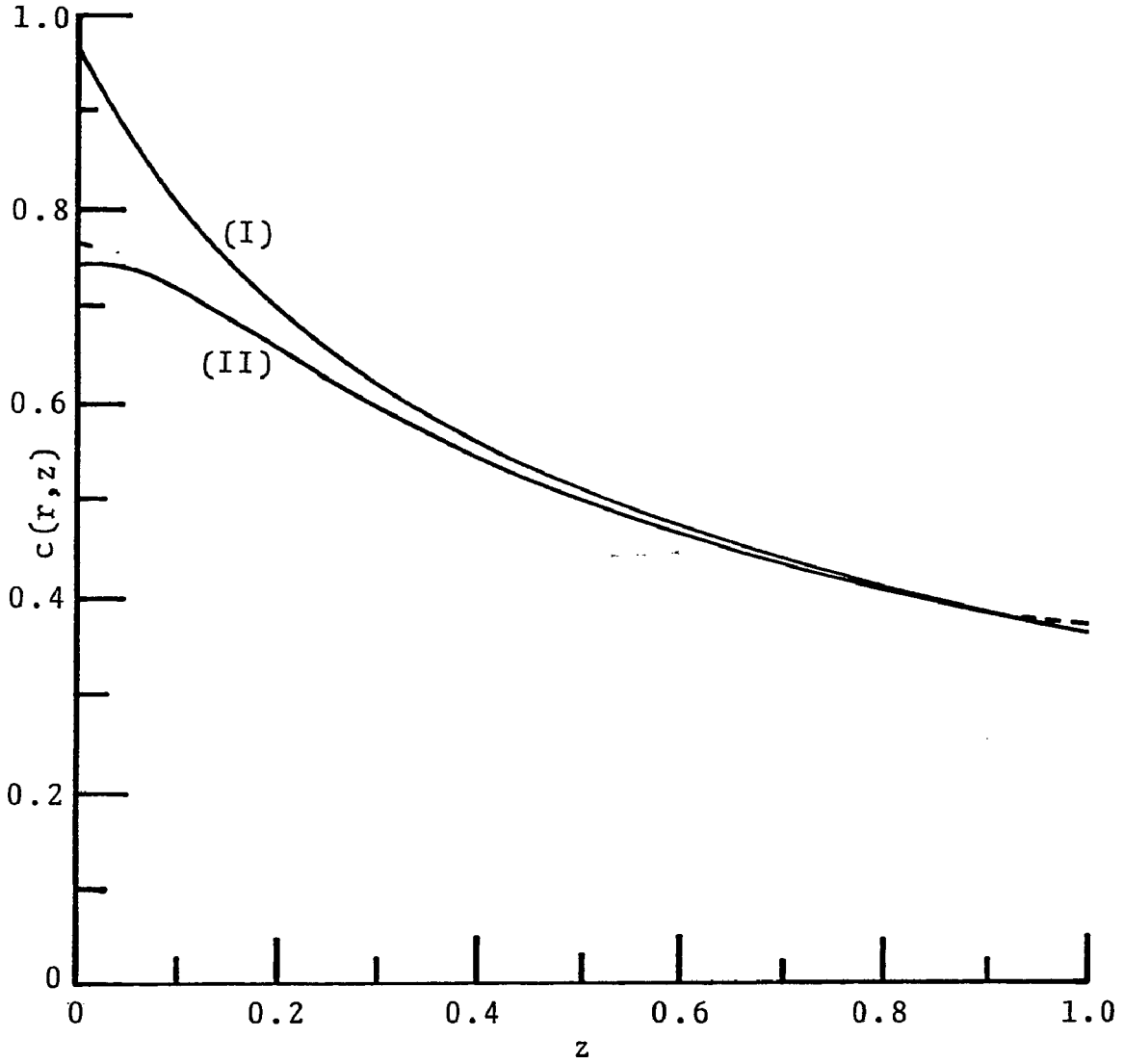

Figure 32. Normalized tissue oxygen concentration at the outer edge of the tissue as a function of axial position z , for the 2nd set of data in table III. (I) ———— without axial diffusion, (II) ———— with axial diffusion, — — — — boundary layer solution.

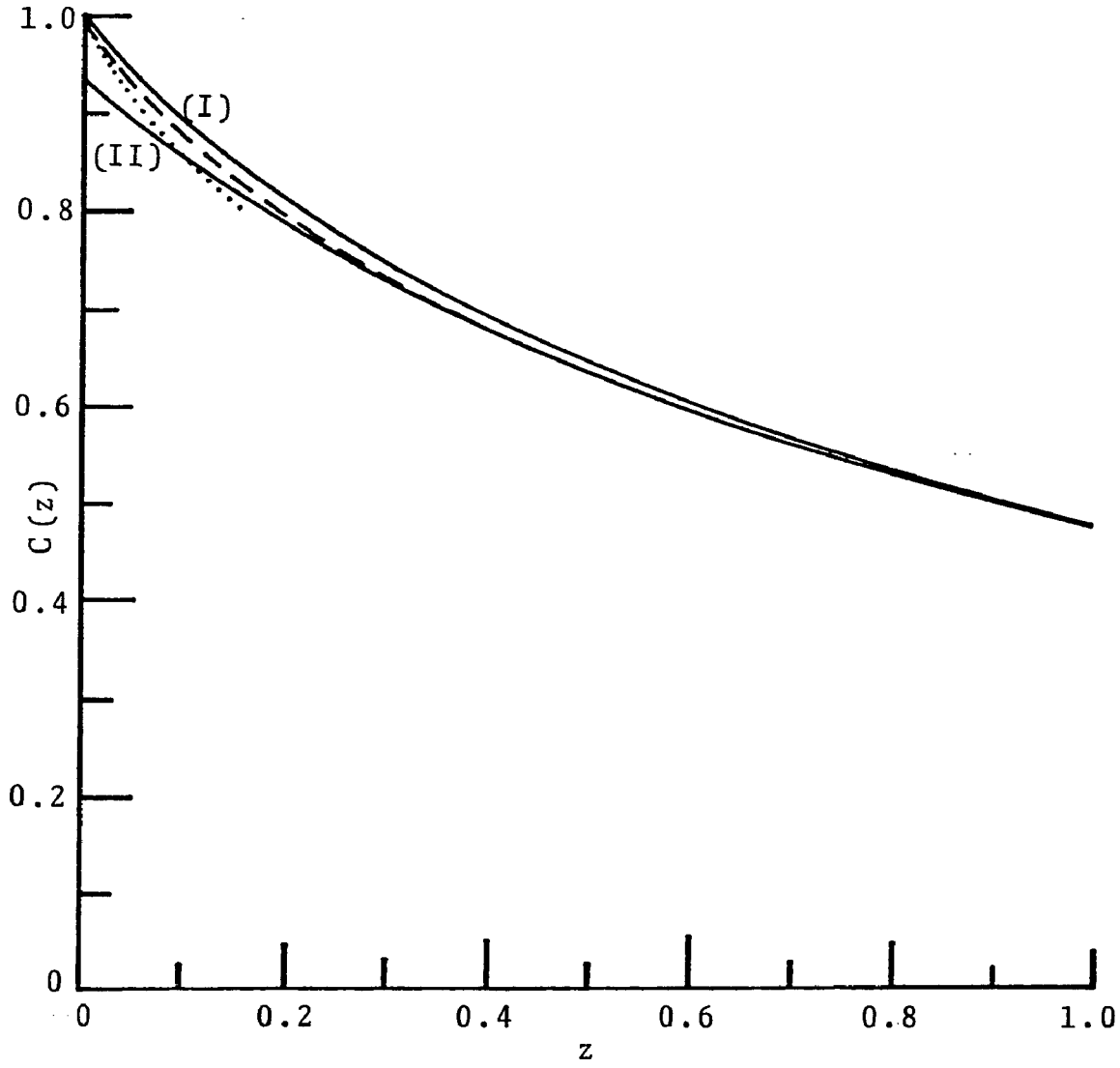

Figure 33. Normalized blood oxygen concentration as a function of axial position z , for the 3rd set of data in table III. (I) ———— without axial diffusion, (II) ———— with axial diffusion, · · · · · · · · boundary layer solution, — — — — composite solution.

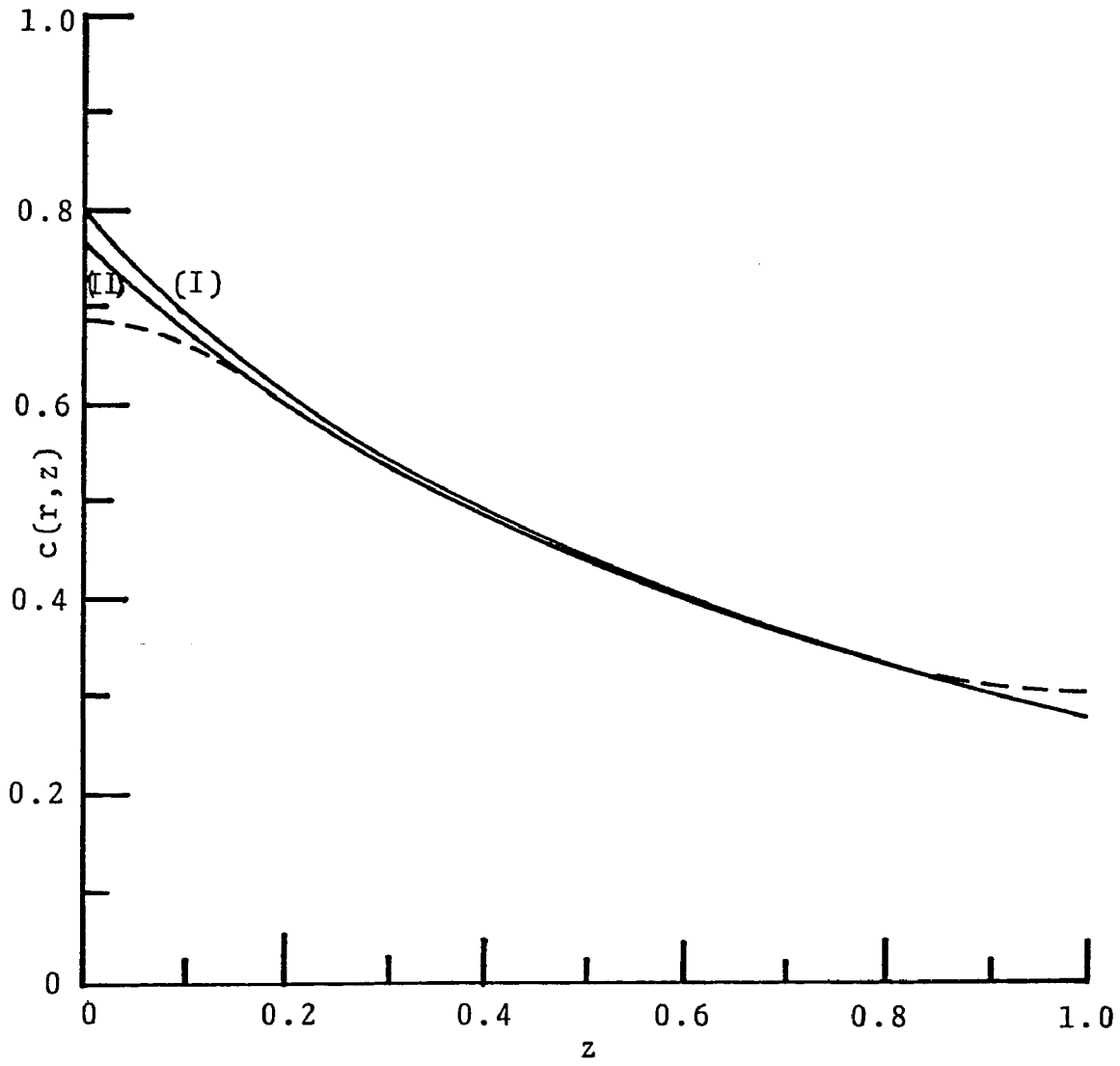

Figure 34. Normalized tissue oxygen concentration midway between the capillary wall and the outer edge of the tissue as a function of axial position z , for the 3rd set of data in table III. (I) ———— without axial diffusion, (II) ———— with axial diffusion, — — — — — boundary layer solution.

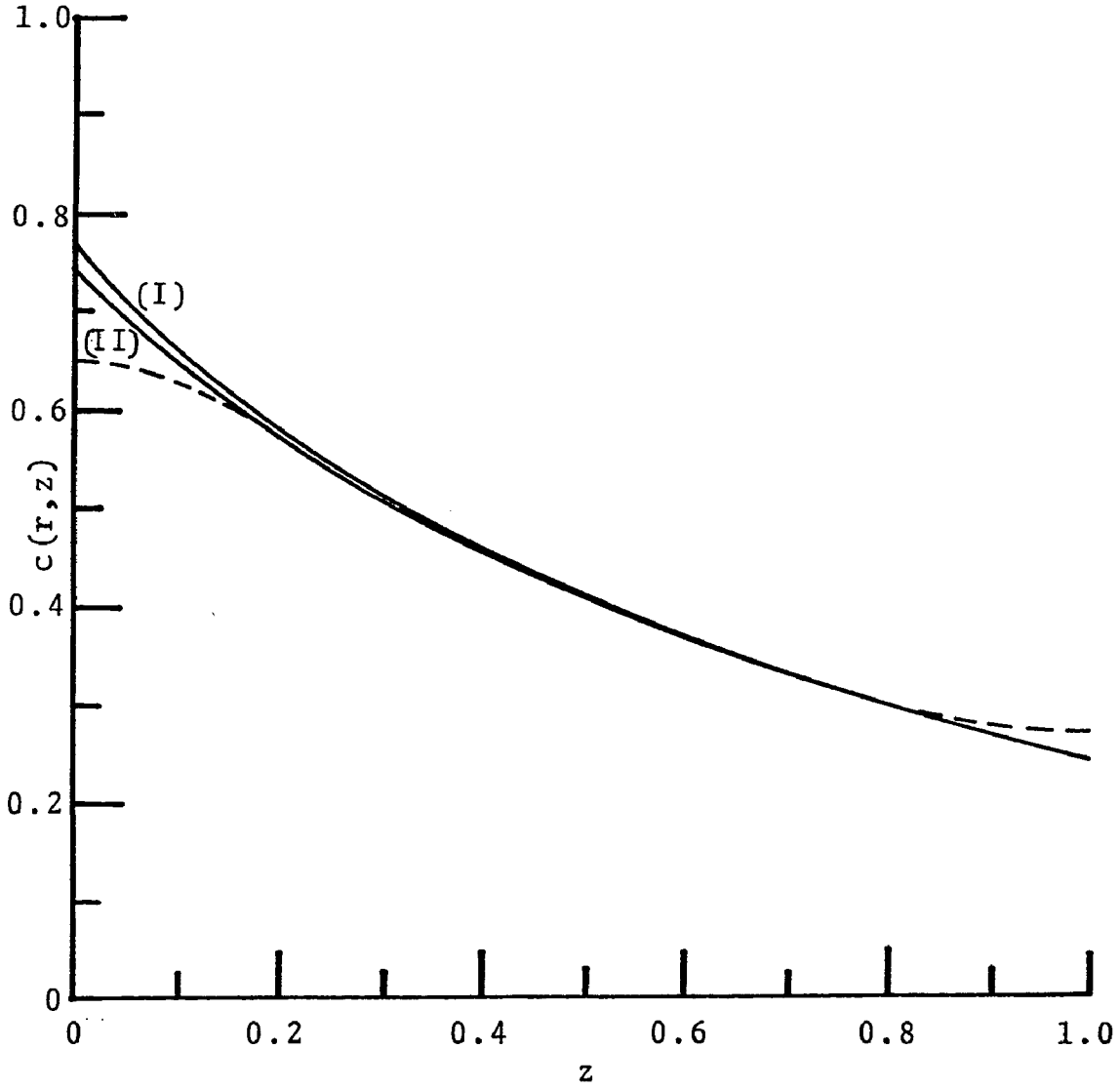

Figure 35. Normalized tissue oxygen concentration at the outer edge of the tissue as a function of axial position z , for the 3rd set of data in table III. (I) ———— without axial diffusion, (II) ———— with axial diffusion, — — — — boundary layer solution.

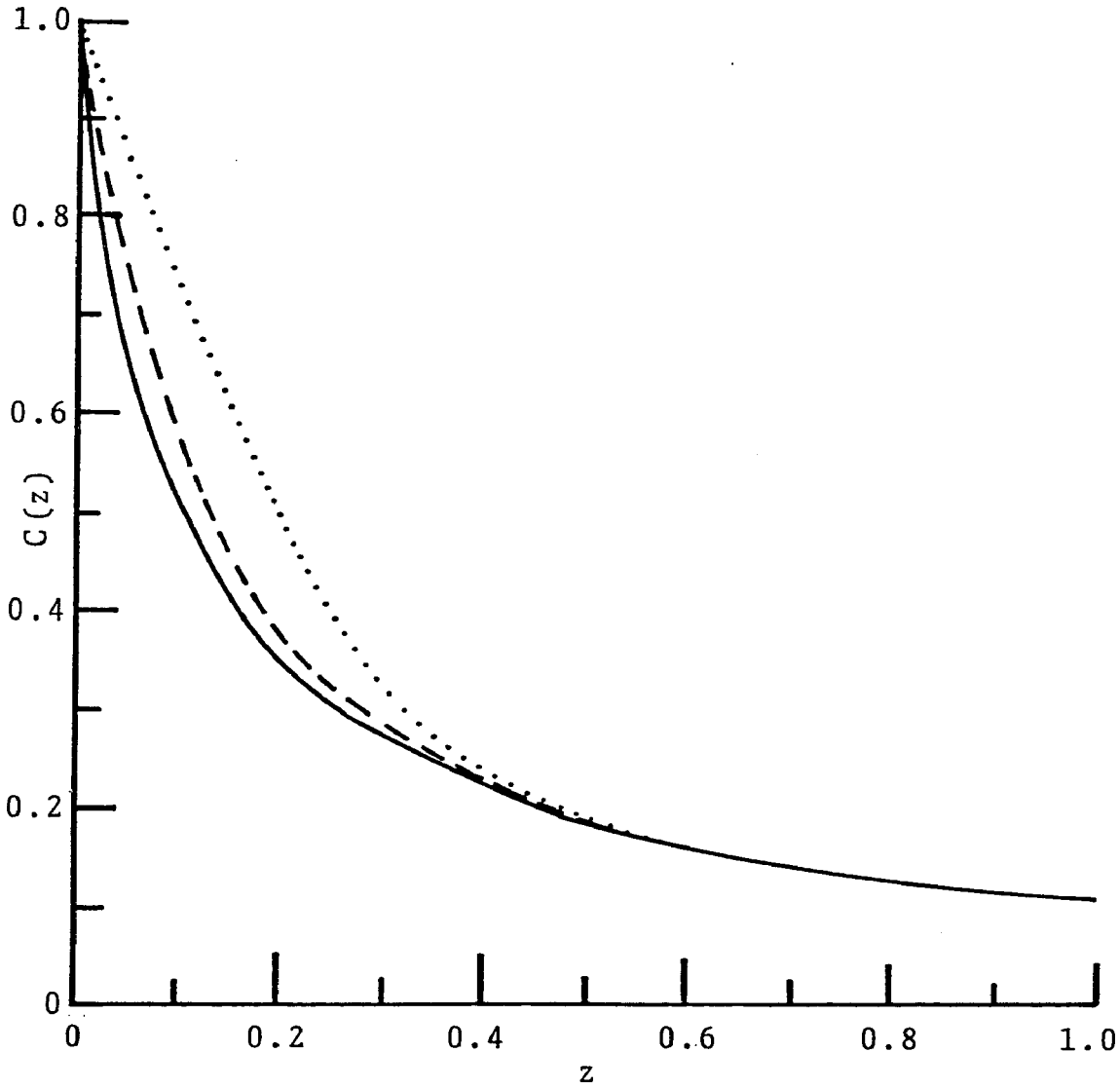

Figure 36. Normalized blood oxygen concentration as a function of axial position z , for the 1st set of data in table III. ····· without axial diffusion, — — — — exact solution, ———— composite solution.

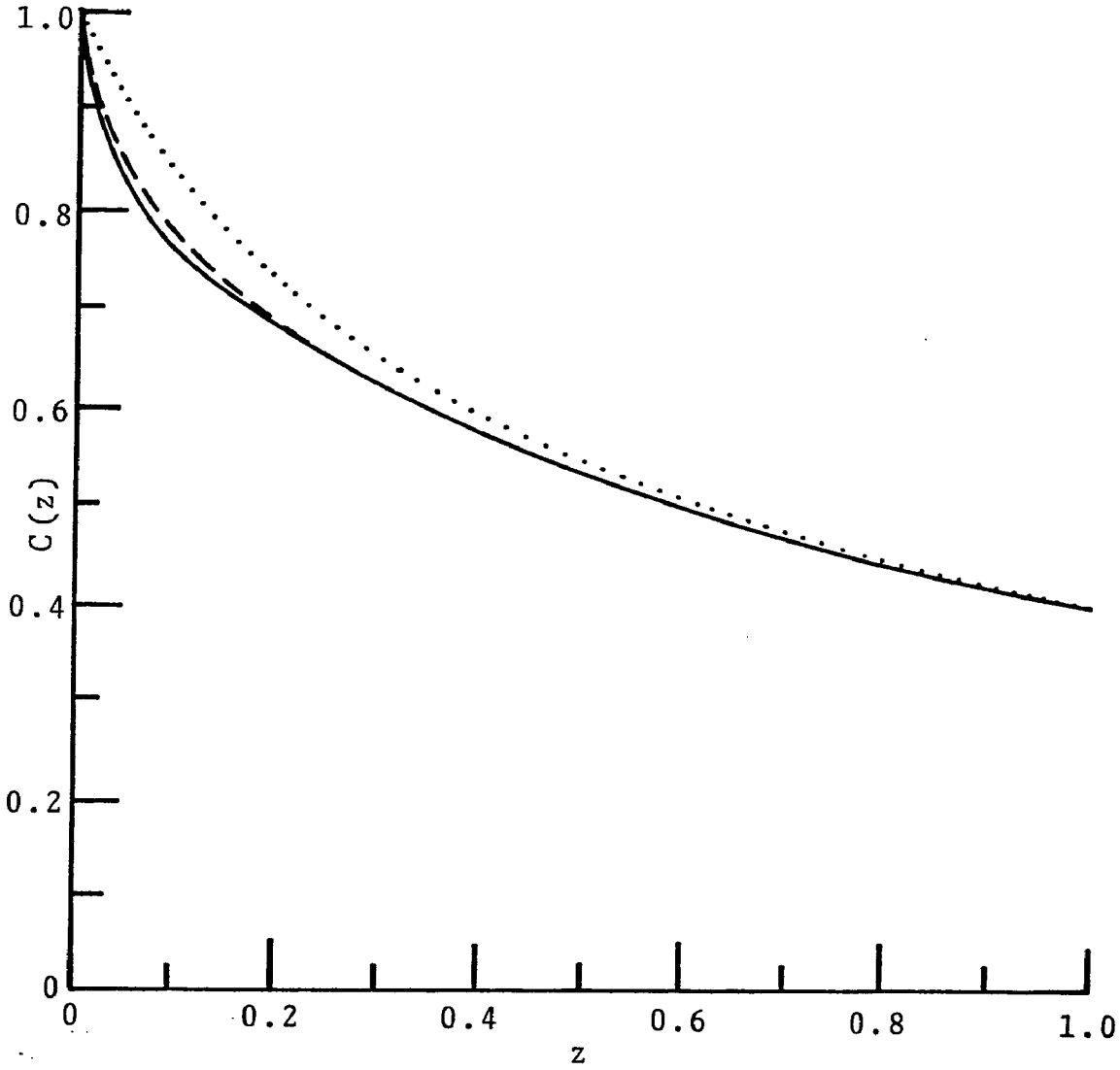

Figure 37. Normalized blood oxygen concentration as a function of axial position z , for the 2nd set of data in table III. ····· without axial diffusion, — — — — exact solution, ———— composite solution.

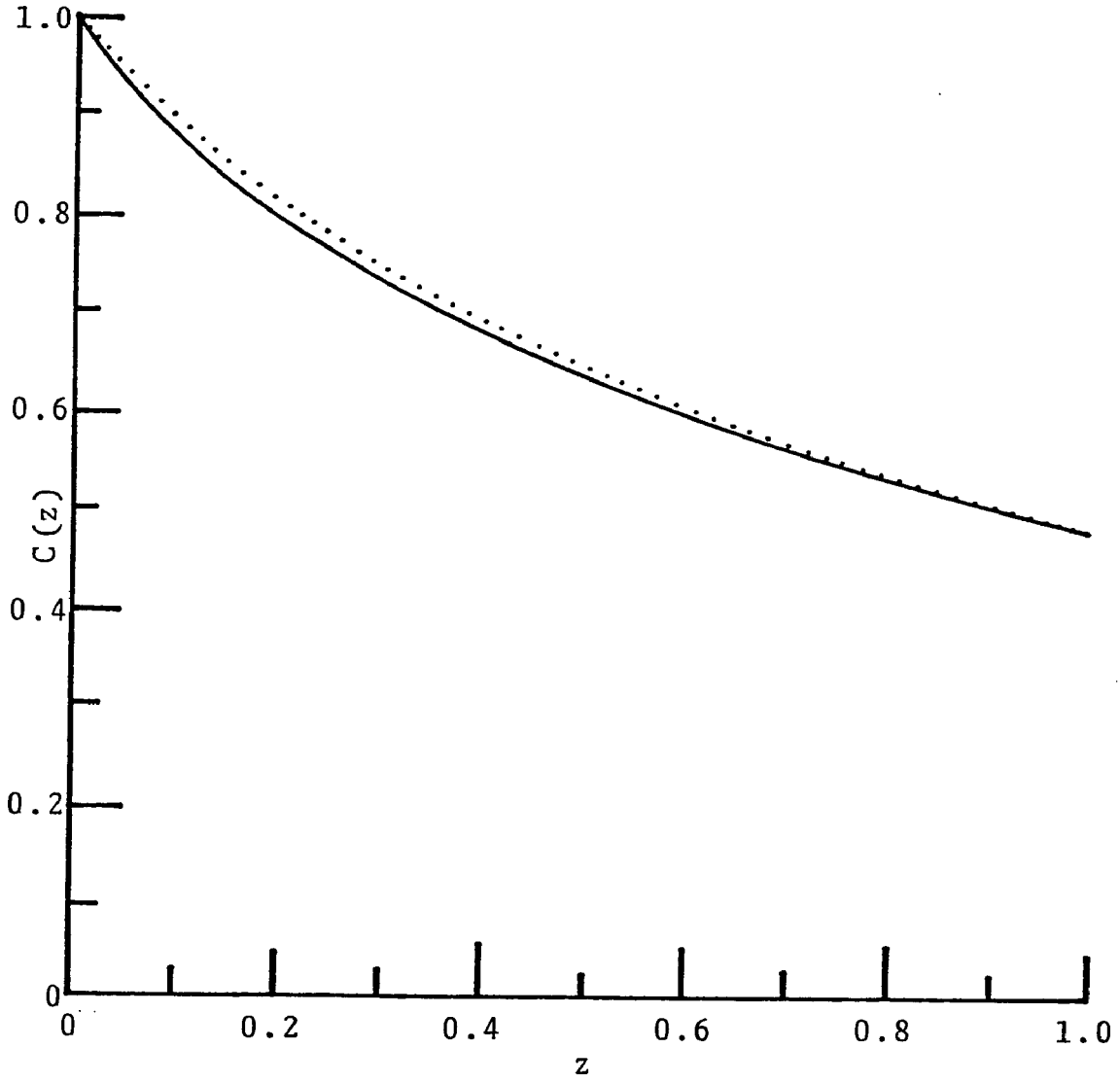

Figure 38. Normalized blood oxygen concentration as a function of axial position z , for the 3rd set of data in table III. ····· without axial diffusion, ———— exact solution and composite solution.

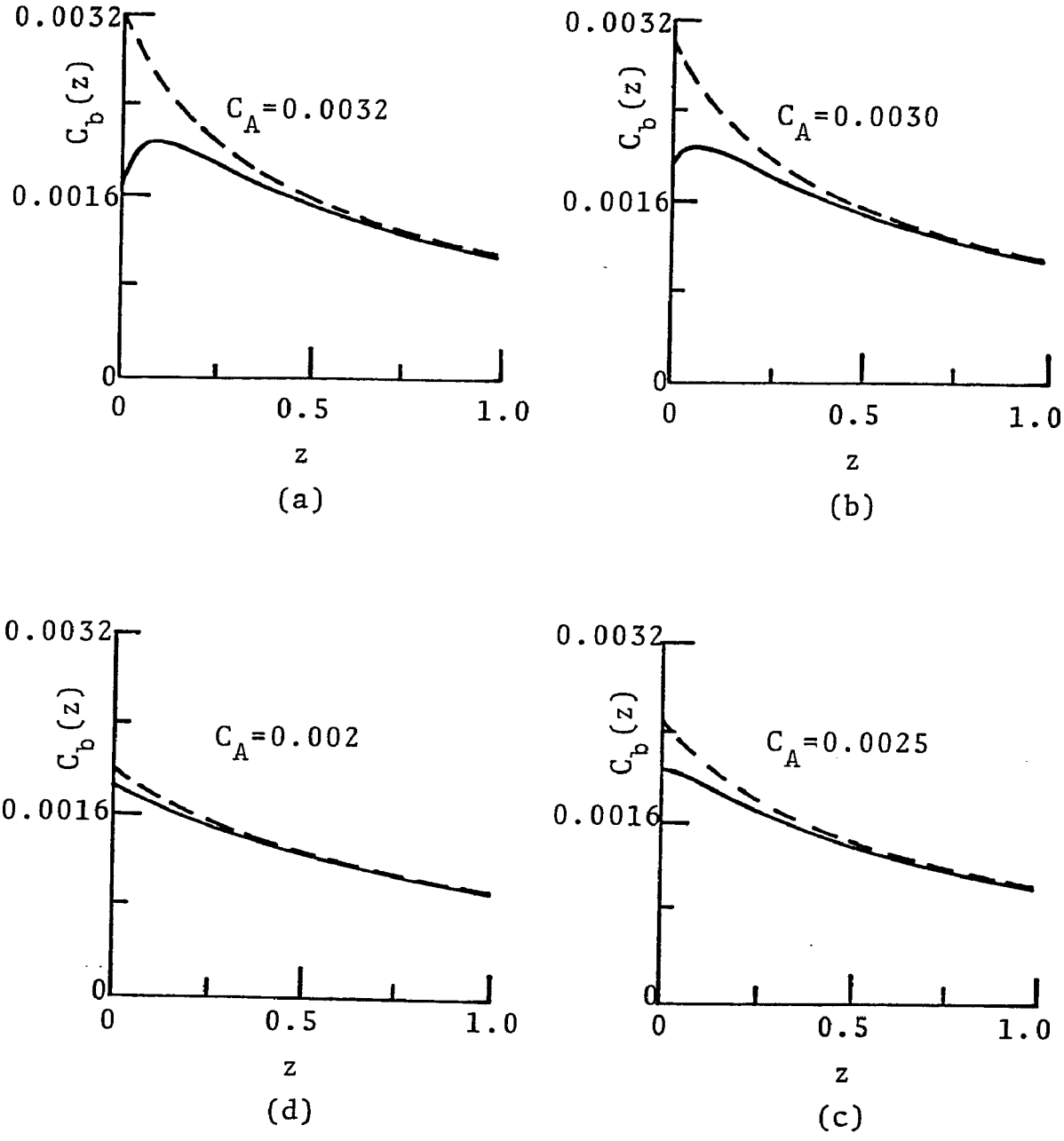

Figure 39. Blood oxygen concentration, C_b (cm^3O_2/cm^3 blood), as a function of axial position, for the values in the 3rd set of data of table III and various values of arterial oxygen concentration, C_A, in cm^3O_2/cm^3 blood. ———— with axial diffusion, — — — — without axial diffusion.

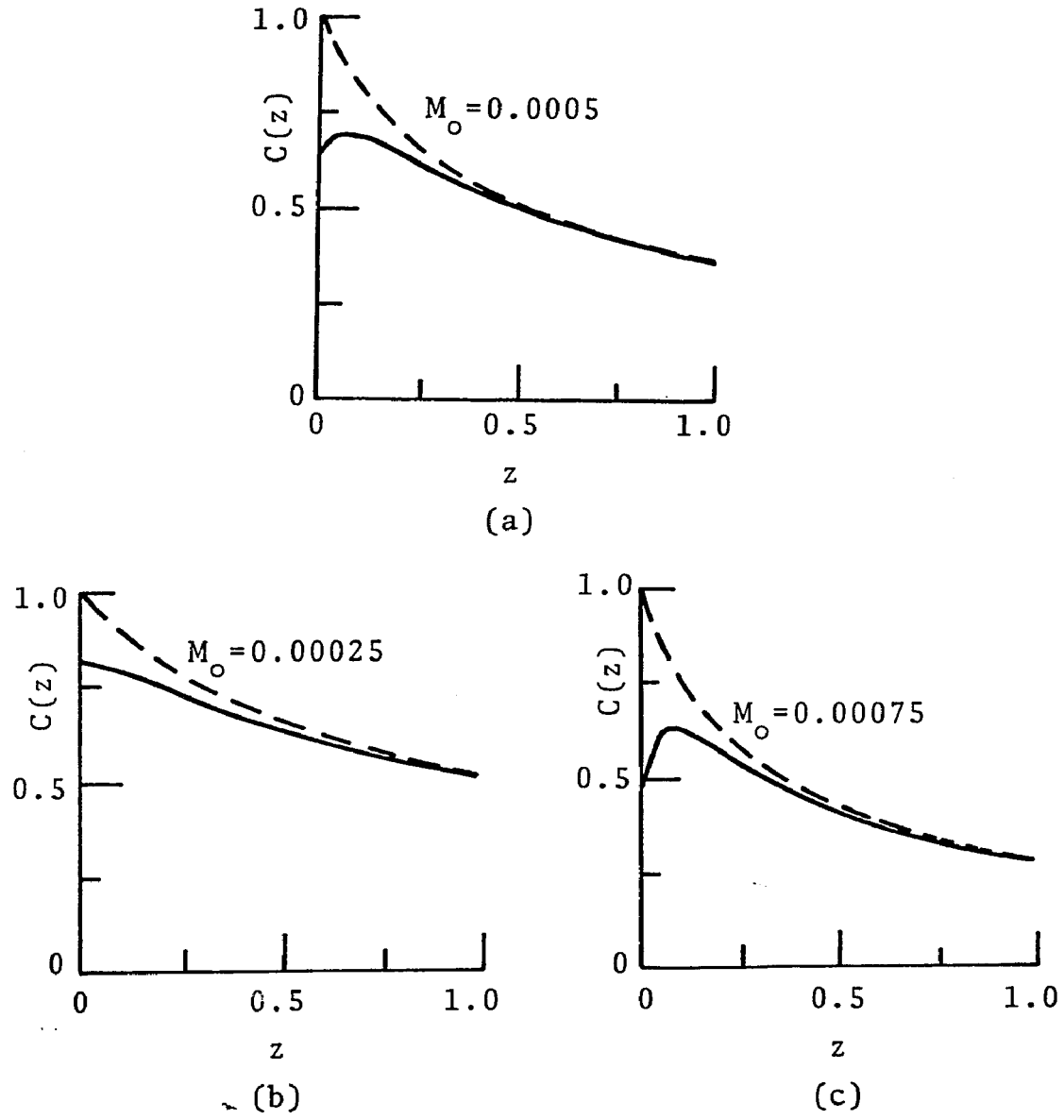

Figure 40. Normalized blood oxygen concentration as a function of axial position, for C_A=0.003 cm^3O_2/cm^3 blood, the values in the 3rd set of data of table III with various values of tissue oxygen consumption rate, M_o, in cm^3O_2/cm^3 tissue-sec. ———— with axial diffusion, — — — — without axial diffusion.

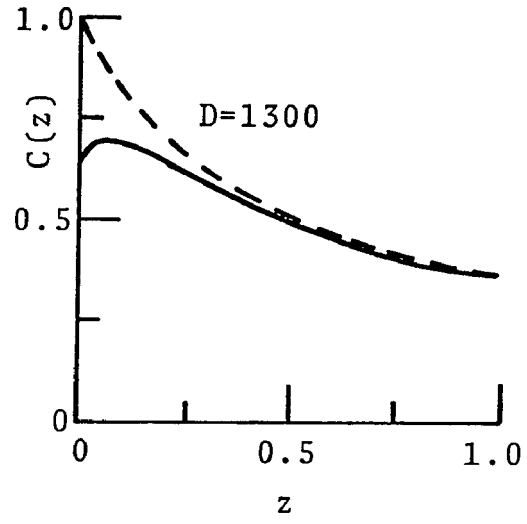

(a)

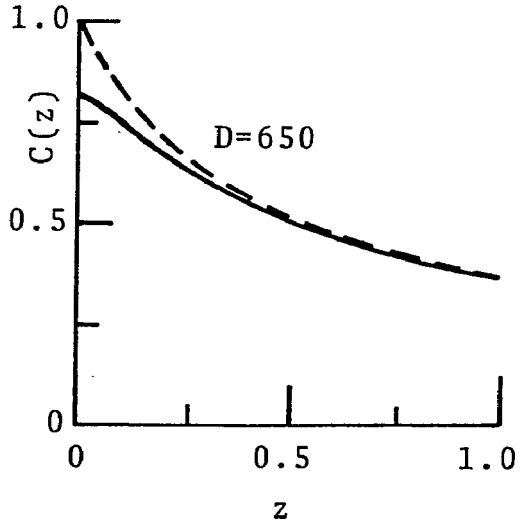

(b)

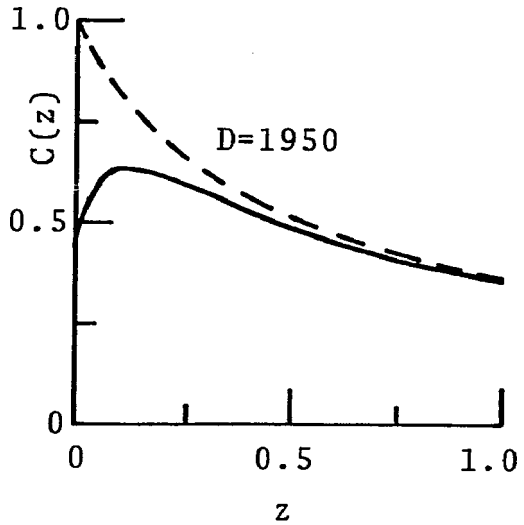

(c)

Figure 41. Normalized blood oxygen concentration as a function of axial position, for C_A=0.003 cm^3O_2/cm^3 blood, the values in the 3rd set of data of table III with various values of tissue oxygen diffusivity, $D=D_r=D_z$, in $\mu m^2/sec$. ———— with axial diffusion, — — — — without axial diffusion.

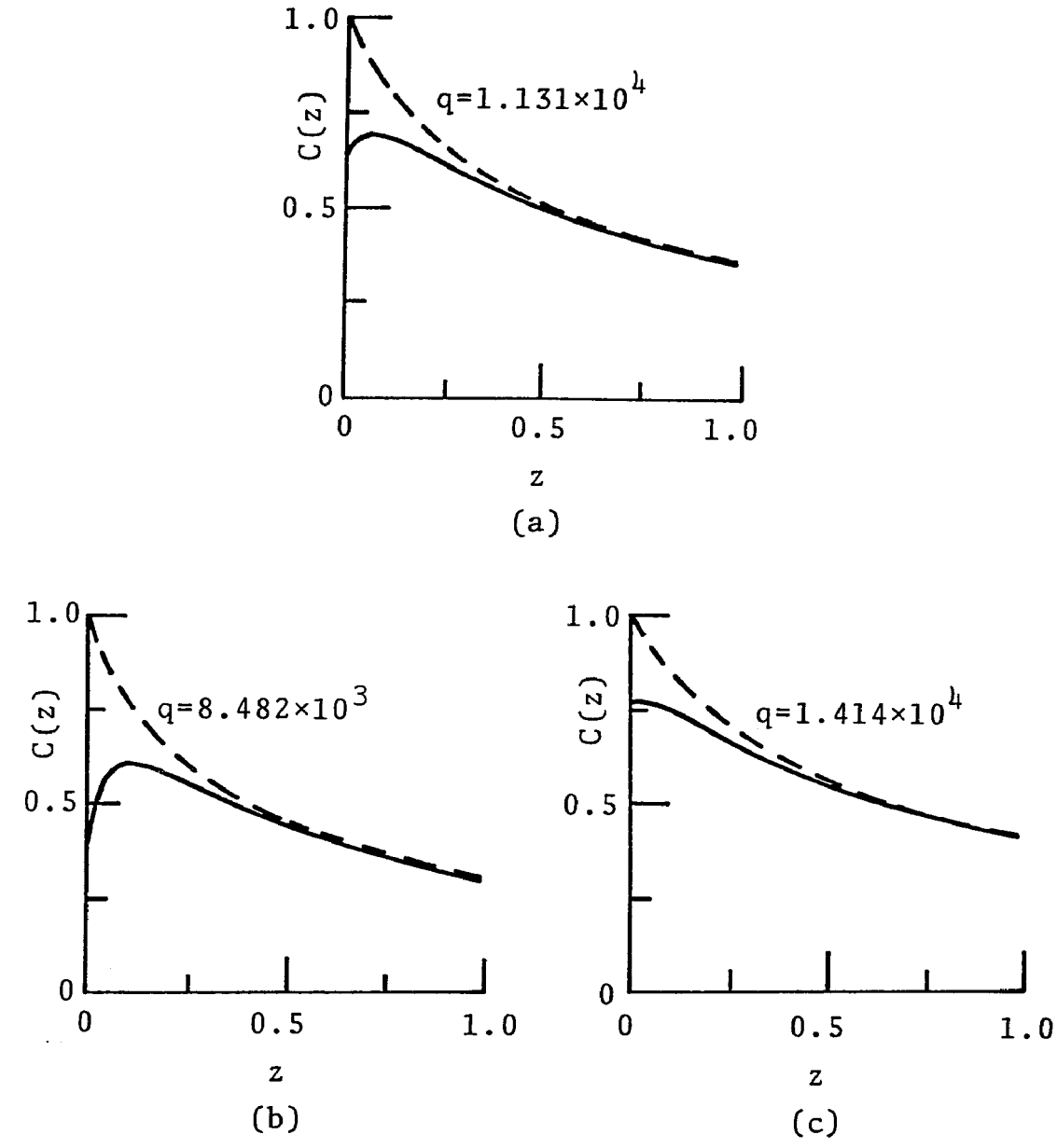

Figure 42. Normalized blood oxygen concentration as a function of axial position, for C_A=0.003 cm^3O_2/cm^3 blood, the values in the 3rd set of data of table III with various values of volume blood flow rate, q , in $\mu m^3/sec$. ———— with axial diffusion, — — — — — without axial diffusion.

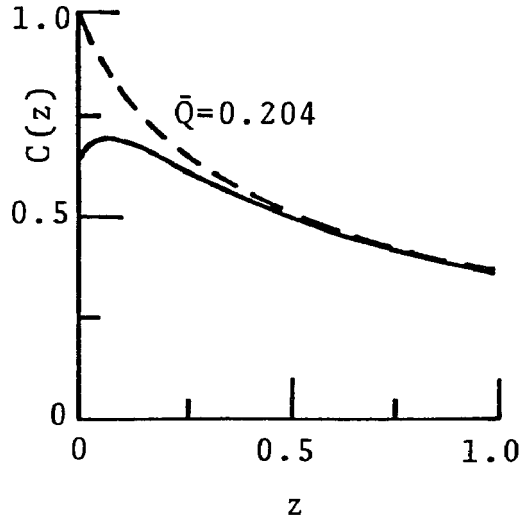

(a)

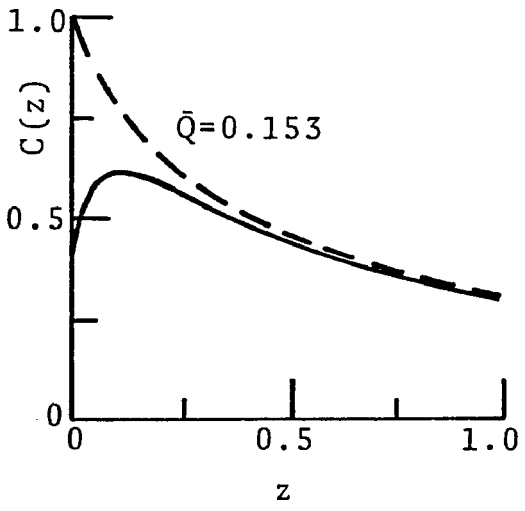

(b)

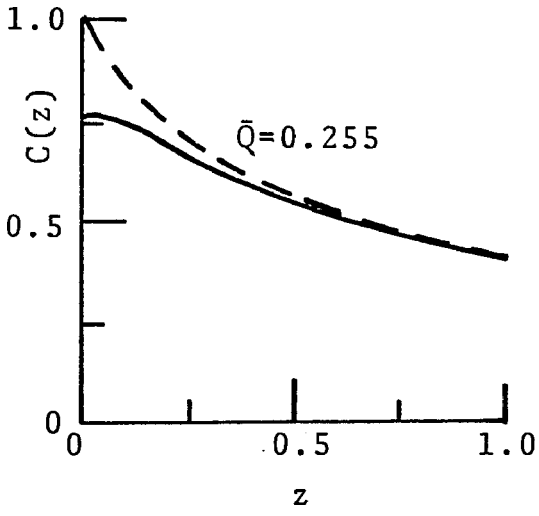

(c)

Figure 43. Normalized blood oxygen concentration as a function of axial position, for C_A=0.003 cm^3O_2/cm^3 blood, the values in the 3rd set of data of table III with various values of blood oxygen capacity, $\bar{Q}$, in cm^3O_2/cm^3 blood. ———— with axial diffusion, — — — — without axial diffusion.

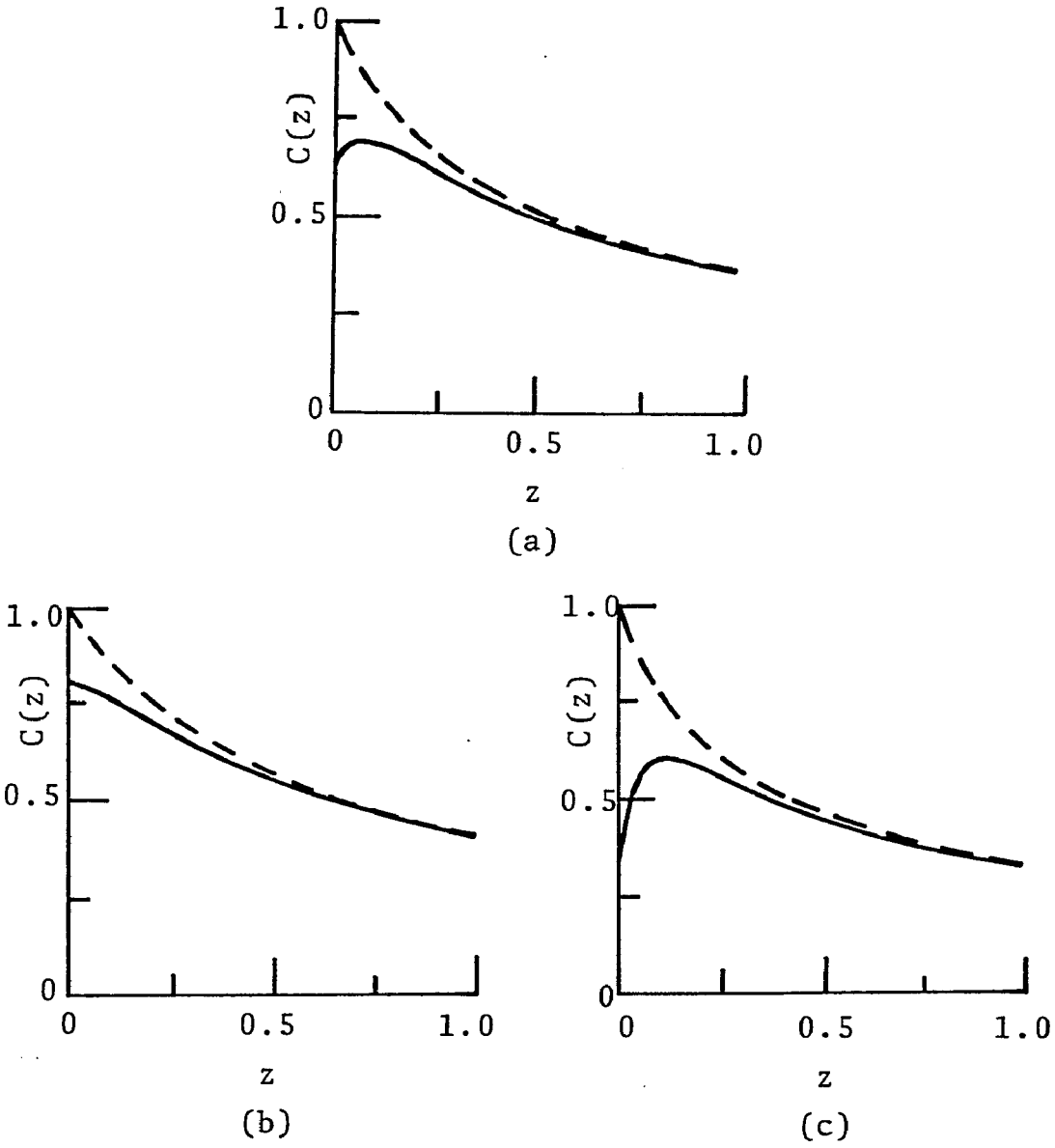

Figure 44. Normalized blood oxygen concentration as a function of axial position, for C_A=0.003 cm^3O_2/cm^3 blood, the values in the 3rd set of data of table III, and various oxyhemoglobin dissociation curves shown in figure 2. (a) Curve (II), (b) Curve (III), (c) Curve (I). ——— with axial diffusion, — — — — without axial diffusion.

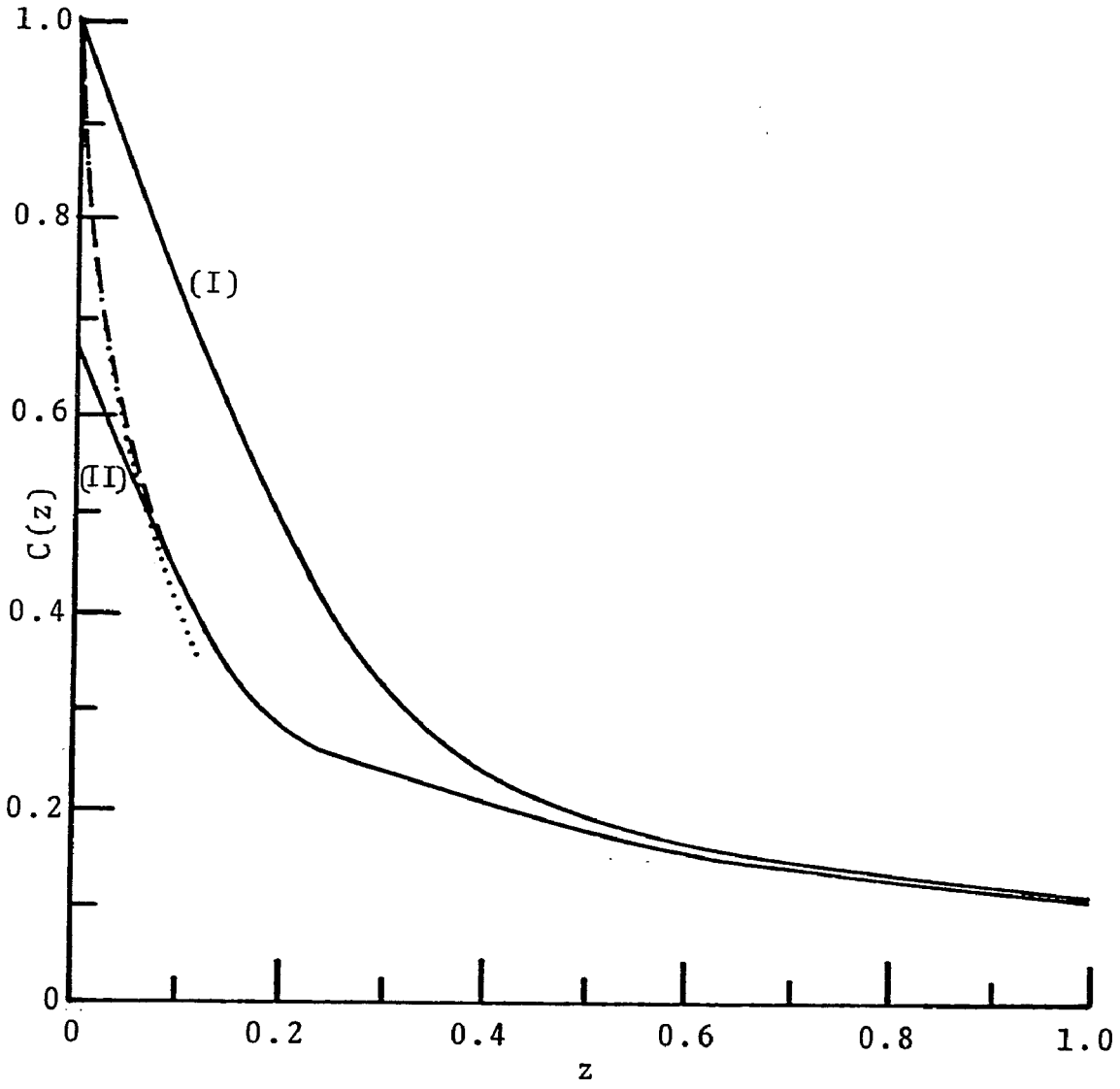

Figure 45. Normalized blood oxygen concentration as a function of axial position, for the outflux Krogh model with $f_1=f_2=0.03M_oL$, and the 1st set of data in table III. (I) ——— without axial diffusion, (II) ——— with axial diffusion, ····· boundary layer solution, — — — — composite solution.

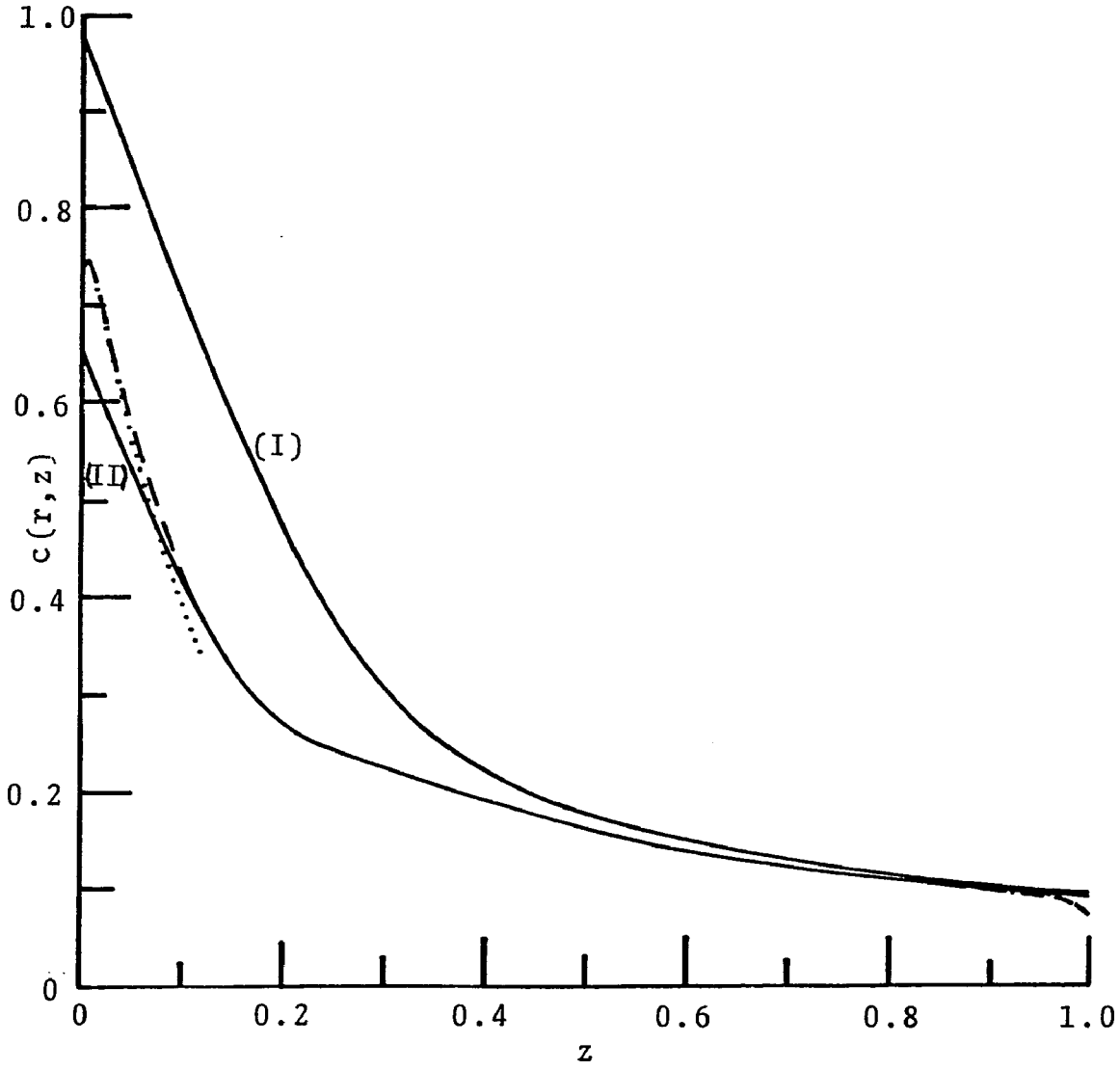

Figure 46. Normalized tissue oxygen concentration midway between the capillary wall and the outer edge of the tissue as a function of axial position, for the outflux Krogh model with $f_1=f_2=0.03M_oL$, and the 1st set of data in table III. (I) ——— without axial diffusion, (II) ——— with axial diffusion, ····· boundary layer solution, — — — — composite solution.

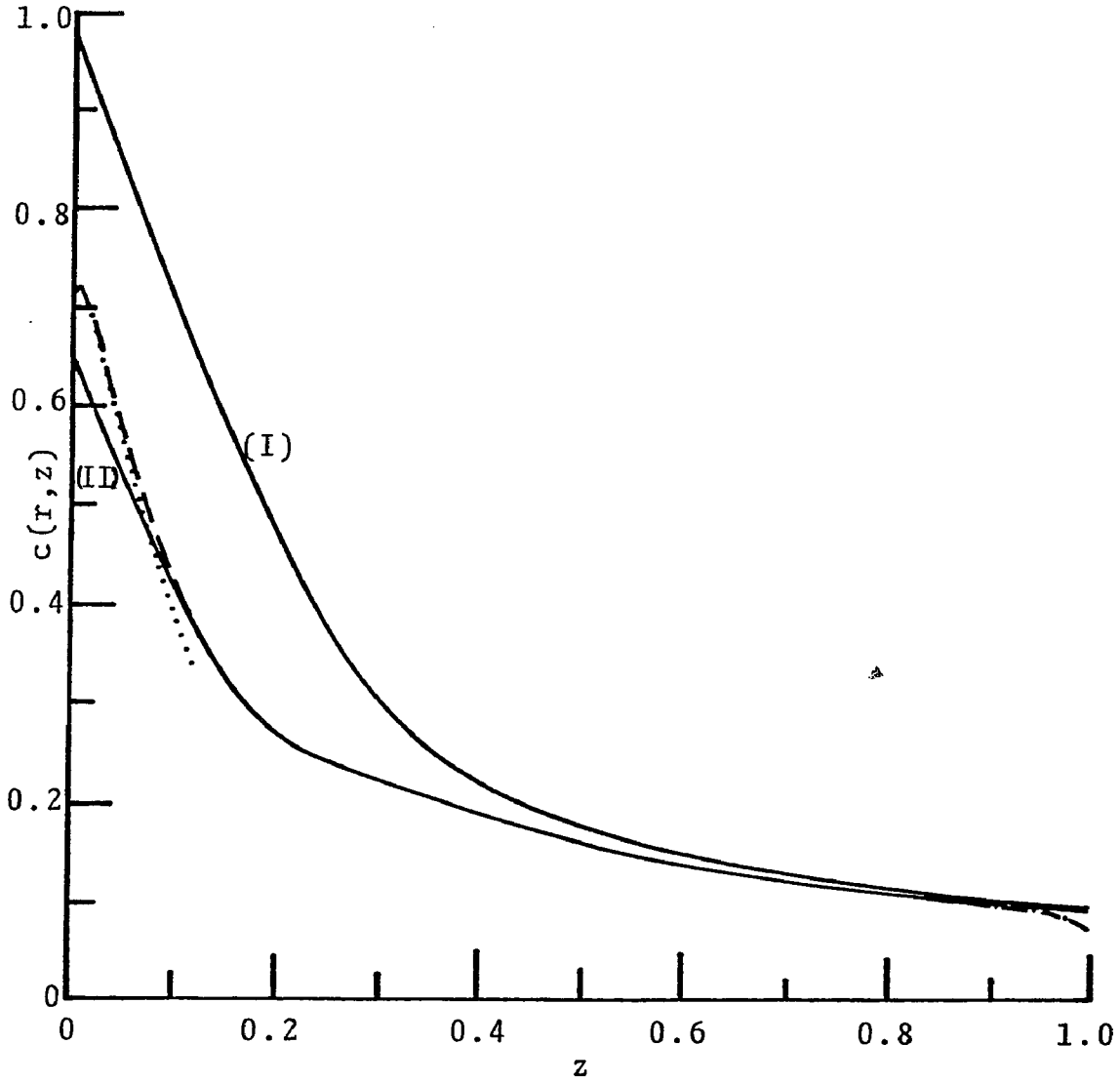

Figure 47. Normalized tissue oxygen concentration at the outer edge of the tissue as a function of axial position, for the outflux Krogh model with $f_1=f_2=0.03M_oL$, and the 1st set of data in table III. (I) ———— without axial diffusion, (II) ———— with axial diffusion, ····· boundary layer solution, — — — — composite solution.

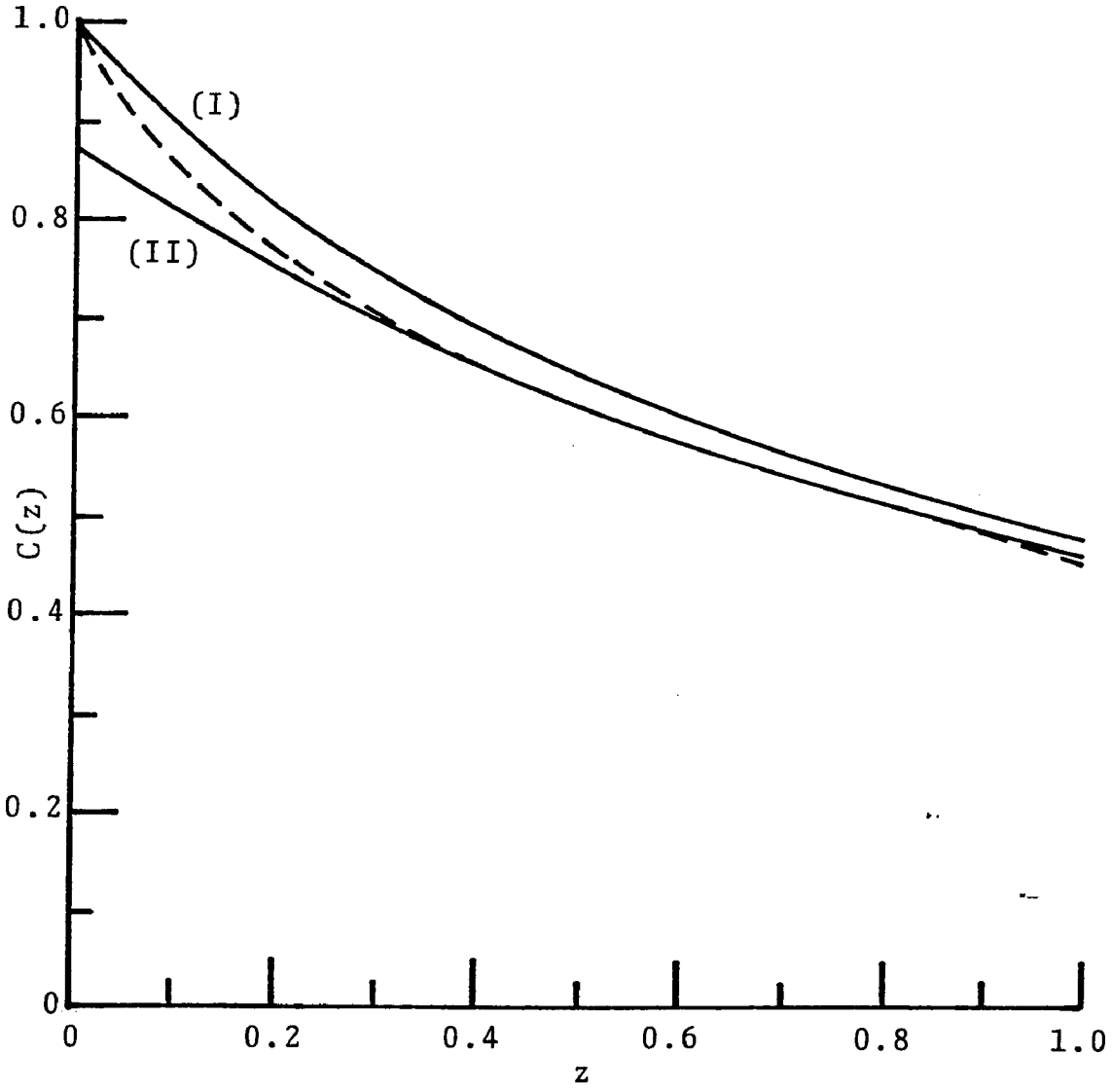

Figure 48. Normalized blood oxygen concentration as a function of axial position, for the outflux Krogh model with $f_1=f_2=0.05M_oL$, and the 3rd set of data in table III. (I) ——— without axial diffusion, (II) ——— with axial diffusion, — — — — composite solution.

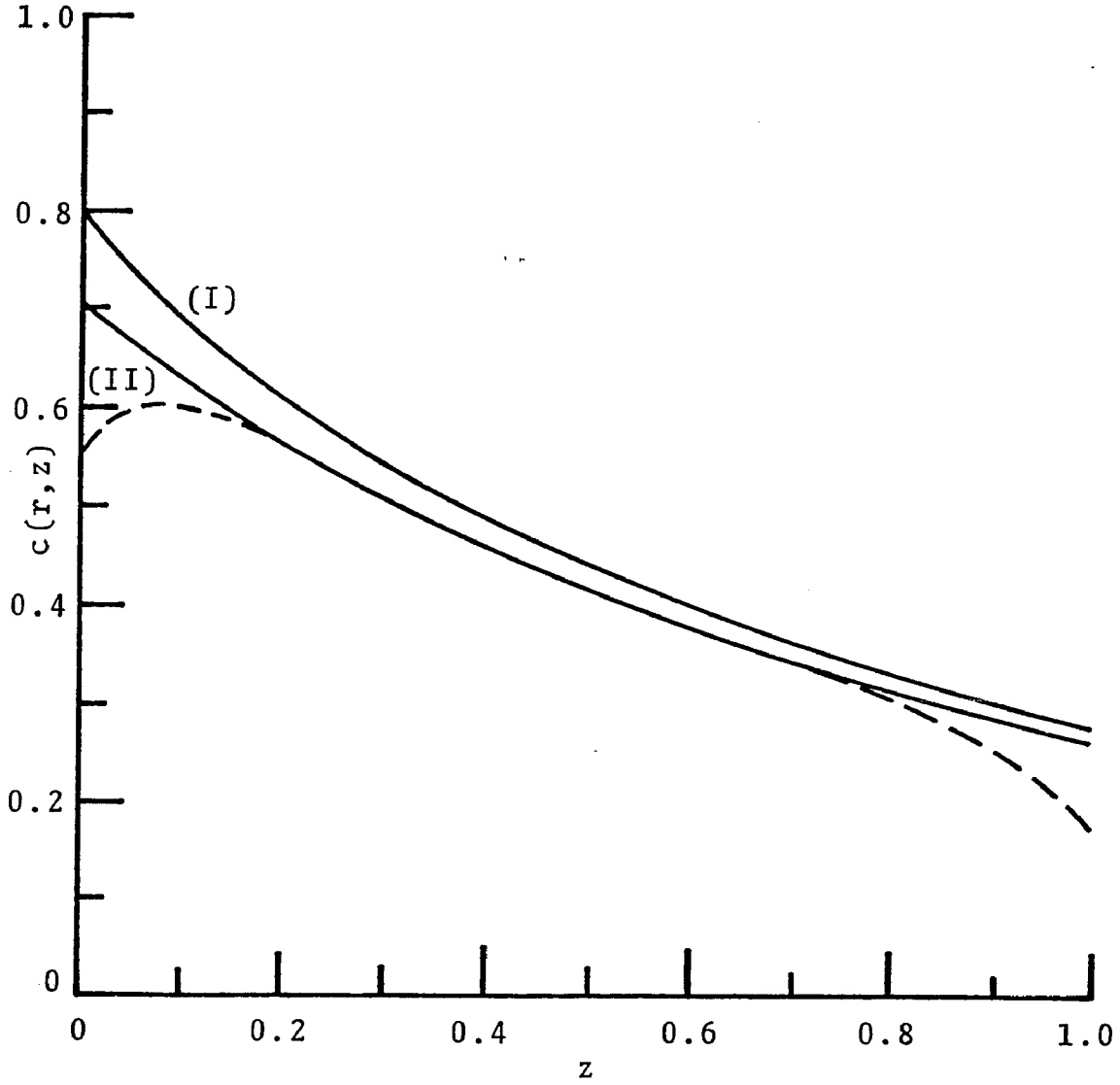

Figure 49. Normalized tissue oxygen concentration midway between the capillary wall and the outer edge of the tissue as a function of axial position, for the outflux Krogh model with $f_1=f_2=0.05M_oL$, and the 3rd set of data in table III. (I) ———— without axial diffusion, (II) ———— with axial diffusion, — — — — composite solution.

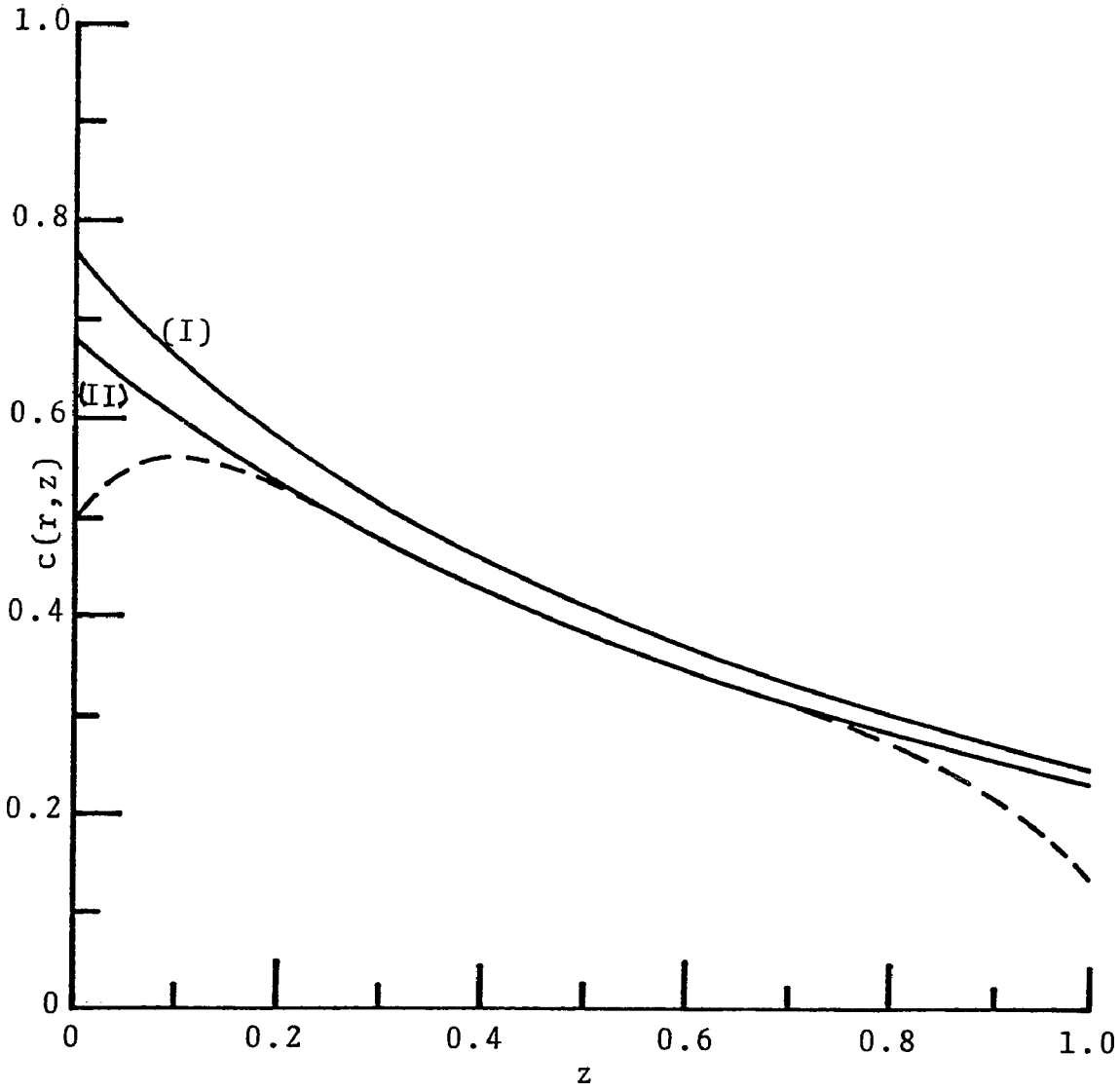

Figure 50. Normalized tissue oxygen concentration at the outer edge of the tissue as a function of axial position, for the outflux Krogh model with $f_1=f_2=0.05M_oL$, and the 3rd set of data in table III. (I) ——— without axial diffusion, (II) ——— with axial diffusion, — — — — composite solution.

REFERENCES

Apelblat, A., A. Katzir-Katchalsky, and A. Silberberg (1974). A mathematical analysis of capillary-tissue fluid exchange. Biorheology 11: 1.

Artigue, R. S., and W. A. Hyman (1976). Effect of myoglobin on oxygen and lactic acid transport in skeletal muscle subjected to ischemia. Annals of Biomedical Engineering 4: 128.

Block, I. (1943). Some theoretical conditions concerning the interchange of metabolites between capillaries and tissue. Bull. Math. Biophys. 5: 1.

Blum, J. J. (1960). Concentration profiles in and around capillaries. Am. J. Physiol. 198: 991.

Bruley, D. F., and H. I. Bicher, eds. (1973). Oxygen Transport to Tissue. In Advances in Experimental Medicine and Biology, Vol. 37B. Plenum Press, New York-London.

Bugliarello, G., and G. C. Hsau (1970). A mathematical model of the flow in the axial plasmatic gaps of the smaller vessels. Biorheology 7: 5.

Carslaw, H. S., and J. C. Jaeger (1959). Conduction of Heat in Solids, 2nd ed. Oxford University Press.

Cole, J. J. (1968). Perturbation Methods in Applied Mathematics. Blaisdell Publishing Co., Waltham, MA-Toronto-London.

Crank, J. (1975). The Mathematics of Diffusion, 2nd ed., 1st ed. 1964. Claredon Press, Oxford.

Crone, C., and N. A. Lassen, eds. (1970). Capillary Permeability. Academic Press, New York.

Davis, E. J., D. O. Cooney, and R. Chang (1974). Mass transfer between capillary blood and tissues. Ch. E. J. 7: 213.

Duling, B. R., and R. Berne (1970). Longitudinal gradients in periarteriolar oxygen tension. Circ. Res. 27: 669.

Duling, B. R., and R. N. Pittman (1975). Oxygen tension: dependent or independent variable in local control of blood flow? Federation Proc. 34: 2012.

Fletcher, J. E. (1973). A mathematical model of the unsteady transport of oxygen to tissue in the microcirculation. In Advances in Experimental Medicine and Biology, Vol. 37B, Bruley and Bicher, eds. Plenum Press, New York-London.

Fletcher, J. E. (1975). A model describing the unsteady transport of substrate to tissue from the microcirculation. SIAM J. Appl. Math. 29(3): 449.

Fletcher, J. E. (1976). Some model results on hemoglobin kinetics and its relationship to oxygen transport in blood. In Advances in Experimental Medicine and Biology, Vol. 75, Grote, Reneau and Thews, eds. Plenum Press, New York-London.

Forster, R. E. (1964). Factors affecting the rate of exchange of O_2 between blood and tissues. In Oxygen in the Animal Organism, Dickens and Neil, eds. Pergamon, New York.

Gross, J. F., and J. Aroesty (1972). Mathematical model of capillary flow: A critical review. Biorheology 9: 225.

Grote, J., D. D. Reneau, and G. Thews, eds. (1976). Oxygen Transport to Tissue - II. In Advances in Experimental Medicine and Biology, Vol. 75. Plenum Press, New York-London.

Guilbeau, E. J., D. D. Reneau, and M. H. Knisely (1973). A detailed quantitative analysis of O_2 transport in the human placenta during steady- and unsteady-state conditions. Advance in Chemistry series, 118.

Guyton, A. C. (1976). Textbook of Medical Physiology, 5th ed. W. B. Saunders, Co., Philadelphia.

Hill, A. V. (1928). The diffusion of oxygen and lactic acid through tissues. Proc. Roy. Soc. B 104: 39.

Hyman, W. A. (1973). A simplified model of the oxygen supply function of capillary blood flow. In Advances in Experimental Medicine and Biology, Vol. 37B. Bruley and Bicher, eds. Plenum Press, New York-London.

Hyman, W. A., D. J. Grounds, and P. H. Newell, Jr. (1975). Oxygen tension in a capillary-tissue system subject to periodic occlusion. Microvasc. Res. 9: 49.

Hyman, W. A., and R. S. Artigue (1977). Oxygen and lactic acid transport in skeletal muscle: effect of reactive hyperemia. Annals of Biomedical Engineering 5: 260.

Kantorovich, L. V., and V. I. Krylon (1958). Approximate Methods of Higher Analysis, translated from the Russian by C. D. Benster. Interscience, New York.

Keller, K. H., and S. K. Friedlander (1966). Investigation of steady state oxygen transport in hemoglobin solution. Chemical Engineering Progress Symposium Series 66.

Kety, S. S. (1957). Determinants of tissue oxygen tension. Fed. Proc. 16: 666.

Knisely, M. H., D. D. Reneau, and D. F. Bruley (1969). The development and use of equations for predicting the limits on the rates of oxygen supply to the cells of living tissues and organs. Angiol. Suppl. 20: 1.

Krogh, A. (1919). The number and distribution of capillaries in muscle with calculations of oxygen head necessary for supplying the tissue. J. Physiol. 52: 409.

Krogh, A. (1930). Anatomy and Physiology of Capillaries. New Haven: Yale University Press, 2nd ed. (1st ed. 1922).

Lambertsen, C. J. (1974). Transport of oxygen and carbon dioxide by the blood. In Medical Physiology, Vol. 2, Mountcastle, ed. The C. V. Mosby Co., St. Louis.

Landis, E. M., and J. R. Pappenheimer (1963). Exchange of substrates through the capillary walls. Handbook of Physiology, Sec. 2, Vol. 2: Circulation, Hamilton and Dow, eds. Amer. Physiol. Soc., Washington, D.C.

Leonard, E. F., and S. B. Jorgensen (1974). The analysis of convection and diffusion in capillary beds. Ann. Rev. Biophys. Bioeng. 1974: 293.

Lightfoot, E. N., Jr. (1973). Simplifying the description of tissue oxygenation. In Advances in Experimental Medicine and Biology, Vol. 37B. Bruley and Bicher, eds. Plenum Press, New York-London.

Lightfoot, E. N., Jr. (1974). Transport Phenomena in Living System. Wiley, New York.

Lih, M. M. (1975). Transport Phenomena in Medicine and Biology. John Wiley & Sons, New York, London, Sydney, Toronto.

Middleman, S. (1972). Transport Phenomena in the Cardiovascular System. Wiley-Interscience, New York.

Mikhlin, S. G. (1964). Integral Equations, translated from the Russian by A. H. Armstrong. Pergamon Press, New York.

Opitz, E., and M. Schneider (1950). The oxygen supply of the brain and the mechanism of deficiency effects. Ergeb. Physiol. Biol. Chem. Expt. Pharmakol. 46: 126.

Prothero, J., and A. C. Burton (1961). The physics of blood flow in capillaries. Biophys. J. 1: 565.

Reisdrof, D. L. (1975). Oxygen distribution in cat gracilis muscle. M.S. Thesis, The University of Arizona.

Reneau, D. D., D. F. Bruley, and M. H. Knisely (1967). A mathematical simulation of oxygen release, diffusion and consumption in the capillaries and tissue of the human brain. In Chemical Engineering in Medicine and Biology, D. Hershey, ed. Plenum Press, New York.

Reneau, D. D., D. F. Bruley, and M. H. Knisely (1969). A digital simulation of transient oxygen transport in capillary-tissue systems. AICHE J. 15: 916.

Reneau, D. D., D. F. Bruley, and M. H. Knisely (1970). A computer simulation for prediction of oxygen limitations in cerebral gray matter. JAAMI 4: 211.

Reneau, D. D., and L. L. Lafitte (1973). Calculation of concentration profiles of excess acid in human brain tissue during conditions of partial anoxia. In Advances in Experimental Medicine and Biology, Vol. 37B. Bruley and Bicher, eds. Plenum Press, New York-London.

Reneau, D. D., E. J. Guilbeau, and J. M. Cameron (1974). A theoretical analysis of the dynamics of oxygen transport and exchange in the placental-fetal system. Microvasc. Res. 8: 346.

Reneau, D. D., E. J. Guilbeau, and R. E. Null (1977). Oxygen dynamics in brain. Microvasc. Res. 13: 357.

Roughton, F. J. W. (1964). Transport of oxygen and carbon dioxide. In Handbook of Physiology, Vol. 1. Fenn and Rahn, eds. The Williams & Wilkins Co., Baltimore.

Saaty, T. L., and J. Bram (1964). Nonlinear Mathematics. McGraw-Hill, New York.

Saaty, T. L. (1967). Modern Nonlinear Equations. McGraw-Hill, New York.

Salathé, E. P., and P. R. Beaudet (1978). The anoxic curve for oxygen transport to tissue during hypoxia. Microvasc. Res. 15: 357.

Sejrsen, P., and K. H. Tonneson (1972). Shunting by diffusion in inert gas in skeletal muscle. Acta Physical Scand. 86: 82.

Spaeth, E. E. (1970). The oxygenation of blood in artificial membrane devices. In Blood Oxygenation. Hershey, ed. Plenum Press, New York.

Staub, N., J. Bishop, and R. Forster (1961). Velocity of O_2 uptake by human red blood cells. J. Appl. Physiol. 16(2): 51.

Stewart, R. R., and C. A. Morrazzi (1973). Oxygen transport in the human brain - Analytical solutions. In Advances in Experimental Medicine and Biology, Vol. 37B. Bruley and Bicher, eds. Plenum Press, New York-London.

Thews, G. (1960). Oxygen diffusion in the brain. A contribution to the question of the oxygen supply of the organ. Pflugers Archiv. 271: 197.

Van Dyke, M. (1975). Perturbation Methods in Fluid Mechanics. Annotated ed., 1st ed., 1964. Parabolic Press, Stanford, CA.

Watson, G. N. (1952). A Treatise on the Theory of Bessel Functions, 2nd ed. Cambridge University Press, Cambridge.

APPENDIX A

A brief description of Blum's analysis will be given here, and it will be shown why his solution is wrong. For simplicity, Blum's analysis will be discussed only for $D_r = D_z$, and the notation of the present paper will be used. Blum obtained a general solution to eqn. (4.13) of the form

$$c(r,z) = \frac{Mr^2}{4} + y_1 + y_2 \ell n\, r + y_3 z + \sum_{n=1}^{\infty} F_n(r) G_n(z), \quad (A.1)$$

where

$$F_n(r) = e_n J_o(\mu_n r) + f_n Y_o(\mu_n r) , \quad (A.2)$$

$$G_n(z) = g_n \cosh(\mu_n z) + h_n \sinh(\mu_n z) , \quad (A.3)$$

and e_n, f_n, g_n, h_n are constants. The appearance of the Bessel functions J_o and Y_o, instead of the modified Bessel functions I_o and K_o, and of the hyperbolic functions sinh and cosh, instead of the trigonometric function sin and cos, distinguish Blum's solution from the present solution. It results from using the opposite sign for the separation constant when solving eqn. (4.13) by separation of variables, and the choice made by Blum was incorrect for this problem.

Blum satisfied the boundary condition, eqn. (4.14), by setting $y_2 = -\frac{M}{2}$, $e_n = Y_o(\mu_n R)$, $f_n = -J_o(\mu_n R)$

and determining μ_n , $n=1,2,3,\ldots$, from the eigenvalue equation

$$Y_o(\mu R)J_1(\mu) - J_o(\mu R)Y_1(\mu) = 0 \ . \qquad (A.4)$$

The choice of e_n , f_n results in $c(R,z) = \frac{MR^2}{4} + y_1 - \frac{M}{2} \ln R + y_3 z$, so that the tissue concentration is a linear function of z at the capillary wall. The boundary conditions, eqn. (4.15) and (4.16), were satisfied by Blum by choosing $g_n = \frac{h_n(1-\cosh \mu_n)}{\sinh \mu_n}$ and determining h_n from

$$\sum_{n=1}^{\infty} h_n \mu_n F_n(r) = y_3 \ . \qquad (A.5)$$

The tissue concentration, $c(r,z)$, is now completely determined, and the capillary concentration $C(z)$ is determined uniquely by eqn. (4.18) and boundary condition eqn. (4.19). No use has been made of eqn. (4.17) in obtaining these solutions, and there is no way that it can now be satisfied. In fact, substituting the solutions for $C(z)$ and $c(r,z)$ into eqn. (4.17) shows that it is not satisfied.

APPENDIX B

In this appendix, the orthogonality relation for the eigenfunctions $\Psi_n(r)$, as well as certain properties of these functions used in the text, will be derived. By using the method of separation of variables in eqns. (5.62)-(5.66), the eigenfunctions $\Psi_n(r)$, $n=1,2,3,\ldots$, satisfy the ordinary differential equation

$$\frac{1}{r}\frac{d}{dr}\, r\, \frac{d\Psi_n(r)}{dr} + \lambda_n^2 \Psi_n(r) = 0 , \quad R \leq r \leq 1 , \tag{B.1}$$

$$\left.\frac{d\Psi_n(r)}{dr}\right|_{r=1} = 0 , \quad \Psi_n(R) = 0 , \tag{B.2}$$

where eigenvalues λ_n, $n=1,2,3,\ldots$, are the roots of eqn. (5.69).

If α_m and α_n are two different eigenvalues, we have

$$\frac{1}{r}\frac{d}{dr}\, r\, \frac{d\Psi_m(r)}{dr} + \alpha_m^2 \Psi_m(r) = 0 , \tag{B.3}$$

and

$$\frac{1}{r}\frac{d}{dr}\, r\, \frac{d\Psi_n(r)}{dr} + \alpha_n^2 \Psi_n(r) = 0 . \tag{B.4}$$

Multiplying eqn. (B.3) by $\Psi_n(r)$ and eqn. (B.4) by $\Psi_m(r)$ and subtracting, we get

$$(\alpha_m^2-\alpha_n^2) r \Psi_m(r)\Psi_n(r) = \Psi_m(r)\frac{d}{dr}\left(r\frac{d\Psi_n(r)}{dr}\right) - \Psi_n(r)\frac{d}{dr}\left(r\frac{d\Psi_m(r)}{dr}\right) .$$

Integrating both sides of this with respect to r from

R to 1 , and applying boundary conditions, eqn. (B.2), we have

$$(\alpha_m^2-\alpha_n^2)\int_R^1 r\Psi_m(r)\Psi_n(r)dr = 0 . \qquad (B.5)$$

Since $\alpha_m \neq \alpha_n$, and $\alpha_m>0$, $\alpha_n>0$. From eqn. (B.5), we have proved eqn. (5.85).

Multiplying eqn. (B.1) by $2\frac{d\Psi_n(r)}{dr}$, we find that

$$\frac{d}{dr}\left[r^2\left(\frac{d\Psi_n(r)}{dr}\right)^2\right] + \lambda_n^2 r^2 \frac{d\Psi_n^2(r)}{dr} = 0 .$$

Integrating this with respect to r from R to 1 , and using integration by parts, yields

$$\int_R^1 r\Psi_n^2(r)dr = \frac{1}{2\lambda_n^2} r^2\left[\frac{d\Psi_n(r)}{dr}\right]^2\Bigg|_R^1 + \frac{1}{2} r^2\Psi_n^2(r)\Bigg|_R^1 . \qquad (B.6)$$

Applying boundary conditions, eqn. (B.2), and eqn. (5.71) to eqn. (B.6), this gives eqn. (5.86).

The integration, $\int_R^1 r\Psi_n(r)dr$, n=1,2,3,... , can be calculated by directly using the definition of $\Psi_n(r)$, eqn. (5.68). We have

$$\int_R^1 r\Psi_n(r)dr = \int_R^1 r[Y_o(\lambda_n R)J_o(\lambda_n r)-J_o(\lambda_n R)Y_o(\lambda_n r)]dr . \qquad (B.7)$$

Since

$$\int_R^1 \zeta J_o(\zeta)d\zeta = \zeta J_1(\zeta) = -\zeta\frac{dJ_o(\zeta)}{d\zeta} ,$$

and

$$\int_R^1 \zeta Y_o(\zeta)d\zeta = \zeta Y_1(\zeta) = -\zeta \frac{dY_o(\zeta)}{d\zeta} ,$$

which can be found in textbooks of Bessel functions, eqn. (B.7) becomes

$$\int_R^1 r\Psi_n(r)dr = \frac{1}{\lambda_n^2}\left[rY_o(\lambda_n R) \frac{dJ_o(\lambda_n r)}{dr} - rJ_o(\lambda_n R) \frac{dY_o(\lambda_n r)}{dr}\right]\Bigg|_R^1$$

$$= \frac{1}{\lambda_n^2}\left(r \frac{d\Psi_n(r)}{dr}\right)\Bigg|_R^1 . \qquad \text{(B.8)}$$

Applying boundary condition, eqn. $(B.2)_1$, and eqn. (5.71) to eqn. (B.8), this completes the calculation of eqn. (5.89).

Résumé

Tseng-Chan Wang
4 West Fourth Street
Center for the Application of Mathematics
Bethlehem, PA 18015
Phone: (215) 691-7000, ext. 622

Professional Objective	Research and development of mathematical modeling in Biomedical Science.
Education	Ph.D., expected in October 1978, Lehigh University Major: Applied Mathematics Dissertation: Mathematical Studies of Oxygen Transport to Tissue
	M.S., October 1975, Lehigh University Major: Applied Mathematics Thesis: A Relativistic Nonlocal Thoery of Electromagnetic Interactions with Matter
	B.S., July 1971, National Chung-Hsing University, Taiwan, R.O.C. Major: Applied Mathematics
Experience	
1974-1978	Center for the Application of Mathematics, Lehigh University, Bethlehem, PA. Fellow Performed research work on Continuum Mechanics, Biomedical Engineering and Mathematical Modeling. Also have experience in computer modeling of physical systems.
Spring Semester & Summer 1976	Department of Physiology, The University of Arizona, Tucson, AZ. Unclassified Student Studied physiology for engineers and performed research work on microvascular system and physiological transport phenomena.
1972-1974	Department of Applied Mathematics, National Chung-Hsing University, Taiwan, R.O.C. Teaching Assistant Performed teaching work on Linear Algebra, Complex Variables and Numerical Analysis.

1971-1972	Chinese Military Police School, Taiwan, R.O.C. ROTC Teacher Performed teaching work on Algebra and Analytic Geometry.
Academic Honors	C. Kemble Baldwin Fellow, Ford Foundation Fellow, Chinese Culture and Science Scholar, Former Vice President Cheng of the Republic of China Scholar.
Personal	Single 5'7" 140 lbs. 30 years old
References	Furnished upon request.